EFFECTS OF SUBSTRATE STIFFNESS ON PHOSPHORYLATION OF ENDOTHELIAL NITRIC OXIDE SYNTHASE AND NITRIC OXIDE BIOAVAILABILITY

FOROUGH ATAOLLAHI

DISSERTATION SUBMITTED IN FULFILMENT OF THE REQUIREMENTS FOR THE DEGREE OF MASTER OF ENGINEERING SCIENCE

INSTITUTE OF GRADUATE STUDIES
FACULTY OF ENGINEERING
UNIVERSITY OF MALAYA
KUALA LUMPUR

2015

This thesis is dedicated to my parents, my husband, my sisters, and my brothers

for their endless love, support and encouragement

UNIVERSITY MALAYA

ORIGINAL LITERARY WORK DECLARATION

Name of candidate: Forough Ataollahi (**I.C/Passport No**:

Registration/Metric No: KGA120031

Name of Degree: Master of Engineering Science

Title of dissertation: Effects of Substrate Stiffness on Phosphorylation of Endothelial Nitric Oxide Synthase and Nitric Oxide Bioavailability

Field of study: Biomedical Engineering

I do solemnly and sincerely declare that:

(1) I am the sole author/writer of this work.
(2) This work is original.
(3) Any use of any work in which copyright exists was done by way of fair dealing and for permitted purposes and any excerpt or extract from or reference to or reproduction of any copyright work has been disclosed expressly and sufficiently and the title of the work and its authorship have been acknowledged in this work.
(4) I do not have any actual knowledge nor I do I ought reasonably to know that the making of this work constitutes an infringement of any copyright work.
(5) I hereby assign all and every rights in the copyright to this work to the university of Malaya (UM), who henceforth shall be owner of the copyright in this work and that any reproduction or use in any form or by any means whatsoever is prohibited without the written consent of UM having been first had and obtained.
(6) I am fully aware that if in the course of making this work I have infringed any copyright whether intentionally or otherwise, I may be subject to legal action or any other action as may be determined by UM.

Candidature signature **Date**

Subscribed and solemnly declared before,

Witness's Signature **Date:**

Name:
Designation:

ABSTRACT

Blood vessels are exposed to mechanical loading (pulse) approximately 75 times per minute. Mechanical loading triggers nitric oxide (NO) production, which is an essential mediator in blood vessel tone regulation. However, disorders, such as aging and atherosclerosis, affect NO produced in each pulse because of blood vessel stiffness. The mechanisms involved in reducing NO production in stiff blood vessels are not fully understood, because the mechanical environment in blood vessels is a complex system consisting of shear stress, tensile loading, and pressure that each of those involves specific mechanisms. This study aims to determine the effect of substrate stiffness on endothelial NO synthase (eNOS) phosphorylation and NO production under tensile loading.

Bovine aortic endothelial cells were isolated through incorporation of a new method in conventional enzymatic digestion, and were characterized by CD.31, Von Willbrand Factor, 1,1'-dioctadecyl-1,3,3,3',3'-tetramethylindocarbocyanine perchlorate acetylated LDL, and angiogenesis behavior. Then, cells were seeded on the substrates with different stiffness. Substrates were prepared through mixing polydimethylsiloxane (PDMS) gel with 5 wt% and 10 wt% alumina (Al_2O_3), and were characterized by mechanical, structural, and morphological analysis. Approximately 10% of the strains with 1 Hz frequency were applied on the cells seeded on the substrates for 3 h. NO production was then measured in the culture medium, and the intensity of eNOS phosphorylated at $Serin^{1177}$ was detected in cell lysate through enzyme-linked immunosorbent assay (ELISA) kits.

The incorporation of filter paper in conventional enzymatic digestion enhanced the purity of isolated endothelial cells to approximately 90%. Membrane characterization showed that Al_2O_3 particles were distributed properly in the PDMS base and did not

affect the surface roughness. Moreover, adding Al_2O_3 to the PDMS base increased membrane stiffness. The Young's modulus of the membranes was 0.331, 0.592, and 1.076 MPa for pure PDMS, PDMS/5% Al_2O_3, and PDMS/10% Al_2O_3, respectively. The stretch loading results showed that 10% stretch of cells seeded on compliant substrates (pure PDMS) with 1 Hz frequency and 3 h duration enhanced the fleuroscnce intensity of p-eNOS at $Serin^{1177}$ to 1.6 and increased NO bioavailability to 600 μg/ml. However, p-eNOS intensity was 1.07 and 1.06 in PDMS/5% Al_2O_3 and PDMS/10% Al_2O_3, respectively, which were significantly less than the pure PDMS. Moreover, NO concentration in response to tensile loading decreased three times in cells seeded on PDMS/5% Al_2O_3 compared with those in pure PDMS, and was undetectable in PDMS/10% Al_2O_3.

This study presented the findings related to the phosphorylation of eNOS and NO production in response to tensile loading. In addition, this study showed that tensile loading elevated eNOS phosphorylation and NO production dependent on substrate stiffness.

Keywords: bovine aortic endothelial cells, polydimethylsiloxan, alumina, stretch, endothelial nitric oxide synthase, nitric oxide.

ABSTRAK

Saluran darah terdedah kepada bebanan mekanikal (nadi) dengan anggaran 75 kali seminit. Pembebanan mekanik mengaktifkan pengeluaran nitric oksida (NO), yang merupakan agen pengantara dalam pengawalan nada saluran darah. Walau bagaimanapun, gangguan seperti penuaan dan aterosklerosis boleh menjejaskan penghasilan NO dalam setiap nadi, disebabkan oleh kekakuan saluran darah. Mekanisme yang terlibat dalam pengeluaran penghasilan NO dalam kekakuan saluran darah belum dapat dipahami sepenuhnya, disebabkan persekitaran mekanikal di dalam saluran darah yang mempunyai sistem yang sangat kompleks, yang terdiri daripada tegasan ricih, bebanan tegangan dan tekanan yang terlibat di dalam setiap mekanisme yang spesifik. kajian ini bertujuan untuk menentukan kesan kekakuan substrat keatas endothelial NO sintase (eNOS) pemfosforilan dan pengeluaran NO di bawah pembebanan tegangan.

Sel-sel "*Bovine aortic endohtelial*" diasingkan melalui penyatuan kaidah baru dalam penghadaman enzim konvensional, dan dikategorikan sebagai CD.31, Von Willbrand Factor, 1,1'-dioctadecyl-1,3,3,3',3'-tetramethylindocarbocyanine perchlorate acetylated LDL, dan angiogenesis. Seterusnya sel-sel akan disemai pada substrat dengan kekakuan yang berbeza. Substrat disediakan melalui pencampuran gel polydimethylsiloxane (PDMS) dengan 5 wt% dan 10wt% alumina (AL_2O_3), dan dikategorikan sebagai mekanikal, struktur, dan analisis morfologi. Kira-kira 10% daripada terikan dengan frekuensi 1 Hz akan dikenakan ke atas taburan sel-sel dalam subtract selama tiga jam. Pengeluaran NO kemudiannya akan ditentukan melalui medium kultur, dan keamatan eNOS phosphorylated pada Serin^{1177}dikesan dalam lysate sel melalui enzim-linked immunosorbent assay (ELISA) kits.

Penyatuan kertas penapis dalam penghadaman enzim konvensional akan meningkatkan pengasingan ketulenan sel endothelial sebanyak kira-kira 90%. Ciri-ciri membrane menunjukkan partikel AL_2O_3 diagihkan secara wajar di dalam PDMS base dan tidak meninggalkan kesan permukaan kasar. Selain daripada itu, penambahan AL_2O_3 kepada PDMS base meningkatkan kekakuan mebran. Modulus Young membran, adalah 0.331, 0.592, dan 1.076 MPa untuk PDMS tulen, PDMS/5% AL_2O_3, dan PDMS/10% Al_2O_3. Keputusan regangan muatan menunjukkan bahawa regangan 10% daripada benih-benih semaian dalam subtrat yang mematuhi (PDMS tulen) dengan 1 Hz frekuensi dan tempah masa 3jam meningkatkan keamatan pendarfluor keatas p-eNOS di serine^{1177} kepada 1.6 danpenambahan NO bioavailabilibity kepada 600 μg/ml. Walau bagaimanapun, intensiti p-eNOS masing-masing adalah 1.07 dan 1.06 untuk PDMS/5% Al_2O_3 dan PDMS/10% Al_2O_3, dimana kurang signifikan daripada PDMS tulen. Selanjutnya, kepekatan NO sebagai tindak balas kepada pembebanan tegangan menurun tiga kali dalam sel-sel semaian pada PDMS/5% Al_2O_3 berbanding PDMS tulen, dan tidak dapat dikesan pada PDMS/10% Al_2O_3.

Kajian ini membentangkan penemuan yang berkaitan dengan pemfosforilan eNOS dan pengeluaran NO sebagai tindak balas kepada pembebanan tegangan. Disamping itu, kajian ini menunjuk kanba hawa pembebanan tegangan meningkatkan eNOS pemfosforilan manakala pengeluaran NO bergantung kepada ketegangan substrat.pembebanan tegangan meningkatkan eNOS pemfosforilan manakala pengeluaran NO bergantung kepada ketegangan substrat.

Kata kunci: sel-sel endothelai bovine aortic, polydimethylsiloxan, alumina, ketegangan, endothelial nitric oksida sintase, nitric oksida.

ACKNOWLEDGMENT

I would like to thank the following people for their contributions to this thesis:

First and foremost I would like to express my deep gratefulness to my supervisors Professor Ir. Dr. Noor Azuan Abu Osman and Professor Ir. Dr. Wan Abu Bakar Wan Abas who provide me the powerful opportunity to continue my master's program. I am so thankful for their tireless, kind assistances, supports, critical advices, encouragements and suggestions during the study and preparation of this thesis. Also, I would truly appreciate the guidance of Dr. Belinda Pingguan-Murphy throughout my studies. She provides me with the wonderful opportunity to grow as a researcher.

I would like to express my gratitude towards my friends Ali Moradi, Nafiseh Khalaj, Ali Baradaran, Adel Dalilottojari, and Maryam Majidian for their continuous supports and encouragements.

Last but not least, my honest appreciation goes to Liyana Binti Abu as technician of Tissue engineering laboratory, Mr. Adhli Iskandar Putera Hamzah as technician of Biomaterials laboratory, Ms. Nor Azalianti Noor Wavi as project financial manager, Dr. Lim Fei Tieng from High-Tech company, Malaysia, and all of my colleagues in working office and tissue laboratory who have willing to provide assistances, give advices, and be a friend.

TABLE OF CONTENTS

LIST OF FIGURES

LIST OF TABLES

LIST OF SYMBOLS AND ABBREVIATIONS

Al_2O_3	Alumina	20
AII	Angiotensin II	13
AFM	Atomic Force Microscope	34
BAEC	Bovine Aortic Endothelial Cells	21
BSA	Bovine Serum Albumin	26
CaM	Ca/Calmodulin	9
$CaCl_2$	Calcium chloride	28
DMSO	Dimethyl sulfoxide	26
Dil-Ac-LDL	1,1'-dioctadecyl-1,3,3,3',3'-tetramethylindocarbocyanine perchlorate acetylated LDL	7
DMEM	Dulbecco's Modified Eagle Medium	22
PIP2	Dylinositol Bisphosphate	11
eNOS	Endothelial NOS	1
ET	Endothelin	7
ELISA	Enzyme-linked Immunosorbent Assay	21
EDTA	Ethylenediaminetetraacetic Acid	36
EO	Ethylenoxid	29
ECM	Extra Cellularmatrix	2
FBS	Fetal Bovine Serum	23
FESEM	Field Emission Scanning Electron Microscopy	34
FAD	Flavin Adenine Dinucleotide	9
FMN	Flavin Mononucleotide	9
FTIR	Fourier Transforms Infrared Spectroscopy	33
HBSS	Hank's Balanced Salt Solution	22
Hsp-90	Heat Shock Protein-90	10
HRP	Horseradish Peroxidase	45
HCl	Hydrochloric Acid	29
iNOS	Inducible NOS	9
nNOS	Neuronal NOS	9
NADPH	Nicotinamide Adenine Dinucleotide Phosphate	9
NO	Nitric Oxide	1
NOS	Nitric Oxide Sythase	9

PBE	Phosphate Buffer EDTA	37
PBS	Phosphate Buffered Saline	22
PDK	Phosphatidylinositol Dependent Kinases	11
p-eNOS	Phosphorylated-eNOS	21
PI3K	Phosphosinositide-3-kinase	2
PECAM-1	Platelet Endothelial Cell Adhesion Molecule-1	11
PCL	Polycaprolactone	19
PDMS	Polydimethylsiloxane	19
PGI_2	Prostacyclin	7
PKA	Protein Kinase A	1
ROS	Reactive Oxygen Species	18
Ser	Serin	1
SOD	Superoxide Dismutase	18
BH4	Tetrahydrobiopterin	9
3D	Three Dimension	28
TEN	Tris/EDTA/Nacl	37
UMMC	University Malaya Medical Center	29
VSMC	Vascular Smooth Muscle Cells	2
XRD	X-Ray Diffraction	32

CHAPTER 1

INTRODUCTION

1. 1. Background

Tissues require constant oxygen and essential nutrients, which are delivered by blood circulation. Hence, blood pulsatile ejection must be converted to a constant flow pattern in the distal circulation (Gnasso et al., 2001). Transferring the pulsatile ventricular ejection into continuous flow, called Windkessel function, is one of the abilities of the vascular tree, particularly the compliant arteries (Dart & Kingwell, 2001; Liao et al., 1999).

Blood vessels consist of three layers, namely, tunica intima, tunica media, and tunica adventitia. Tunica intima is composed of endothelial cell layer and connective tissue layer. The entire cardiovascular system is lined with endothelial cells. At the beginning, endothelial cells have been viewed as inert membranes in the circulatory system. Harvey's description of the circulatory system and studies by Malphigi, Reckingausen, and other researchers have shown the critical role of endothelial cells in physio-pathological processes (Cines et al., 1998).

Beside the endothelial cells role as a barrier, these cells also can secret mediators among which nitric oxide (NO) is the most important. NO can be produced by endothelial Nitric Oxide Synthase (eNOS) under chemical and mechanical stimulations (Fukumura et al., 2001). These stimulators phosphorylate eNOS at different sites, among which Serin^{1177} (Ser^{1177}) is the most important site for NO production. Mechanical stimulations –as the focus of this study- trigger phosphosinositide-3-kinase (PI3K) activation, followed by activation of protein kinase B (called Akt), and protein kinase A (PKA). The mentioned enzymes

phosphorylate eNOS at Ser^{1177} and lead to NO production. NO has profound roles in vasodilatation, platelet aggregation, leukocyte adhesion to endothelial cells, suppression of proliferation and migration of vascular smooth muscle cells (VSMC), and gene regulation related to monocyte adhesion molecules (Rosselli et al., 1998).

However, disorders such as aging and atherosclerosis affect NO production in blood vessels in response to tensile loading (Lakatta & Levy, 2003; Lakatta et al., 2009). Reduction in NO production in these disorders is a consequence of blood vessel stiffness, which is defined as reduction in blood vessel capability to expand and contract in response to pressure changes. Therefore, microenvironment can affect cell responses and functions. Cells can sense the mechanical properties of their environment through receptors attached to extra cellular matrix (ECM). Cells respond to the environment depending on how their receptors transduce mechanical stresses into biochemical signals (Yeung et al., 2005). However, forces imposed from stiff blood vessels to endothelial cells may alter the mechanisms involved in eNOS phosphorylation and NO production in response to tensile loading. The effects of blood vessel stiffness on endothelial cells in dynamic situation have not been well established. This lack of basic mechanistic information must be addressed in further studies. Therefore, this study aims to detect whether or not substrate stiffness can affect eNOS phosphorylation and NO production in dynamic situation.

1. 2. Objectives

This study aims to elucidate the effects of substrate stiffness on eNOS phosphorylation and NO production in dynamic environment. The following objectives were determined to achieve such research aim:

I. To optimize bovine aortic endothelial cell isolation for getting high purity cell population.
II. To prepare substrates with different stiffness and characterize those through mechanical, structural and morphological analysis.
III. To evaluate the effects of substrate stiffness toward endothelial cell response in terms of attachment, proliferation, and morphology to substrate stiffness in static environment.
IV. To develop a dynamic cell culture environment for applying of tensile loading on endothelial cells.

1. 3. Thesis layout

This thesis is divided into six chapters. Chapter 1 is the introduction, in which the background is presented. Chapter 2 provides a critical review of relevant literatures. Chapter 3 presents an overview of experimental techniques employed in the current work. Chapter 4 shows the results, which will also be discussed in chapter 5 as the discussion chapter of this thesis. Finally, Chapter 6 provides the conclusion, future works and limitations.

CHAPTER 2

LITERATURE REVIEW

This chapter gives a comprehensive review of selected literature on topics relevant to endothelial cells and their responses to substrate stiffness in dynamic environment, because stiffness as a common issue in aging and atherosclerosis affects the endothelial cell behavior in respond to blood pulse as dynamic situation.

This chapter starts with the introduction of blood vessel and role of the endothelial cells in blood vessel. It continues with an overview of different theories that were used extensively over the years to enhance the understanding about endothelial cell roles. It was followed by the role of NO as main mediator which affects vascular tone and produces by endothelial cells. Then we reviewed the reduction of NO bioavailability in disorders like aging and atherosclerosis. We also reviewed some of the experimental approaches used to evaluate the effects of stiffness on NO bioavailability in vivo and in vitro. The special focuses were put on investigating the involved mechanisms and the possible causes of reduction in NO bioavailability in respond to substrate stiffness.

2. 1. Blood vessel structure

Blood vessels consist of three layers from the luminal side outwards, namely, tunica intimae, tunica media, and tunica adventitia (Figure 2.1).

Tunica intimae: this layer contains endothelial cell and connective tissue layers. However, a third layer, called sub-connective tissue, which contains collagen, elastin fibrils, smooth muscle cells, and fibroblast cells, can be found in large arteries,

such as aorta. Endothelium is connected to tunica media through basal lamina consisting of collagen type IV, fibronectin, laminin, and proteoglycans.

Tunica media: Smooth muscle cells form this layer, which has been covered through the basal lamina. The relaxation and contraction properties of the vessels are related to this tissue layer. The thickness of tunica media is different between arteries (500 µm) and veins (20 µm to 50 µm).

Tunica adventitia: This layer consists of soft connective tissues, such as collagen type I mixed with elastin, fibroblast cells, nerves, vasa vasorum including arterioles, capillaries, and venules, that all prepare oxygen for thick arteries (Stegemann et al., 2007).

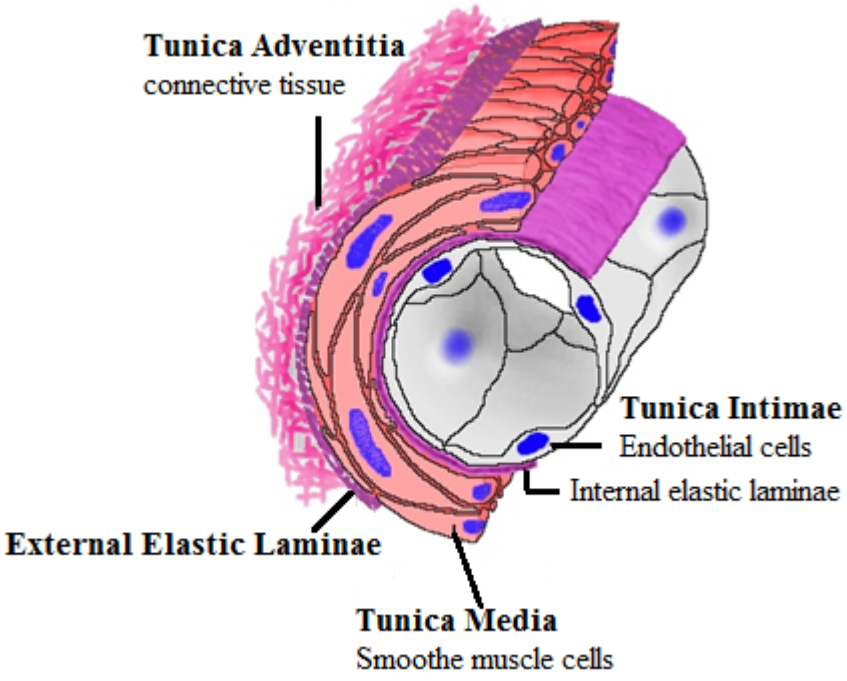

Figure 2.1: Cross section of blood vessel structure consists of the intimae, media, and adventitia layer (Djassemi, 2012)

2. 2. Endothelial cells

Endothelial cells have a critical role in cardiovascular system because they are a source of pleiotropic paracrine and endocrine mediators and act as sensors against physical and chemical stimuli.

However, at the beginning, endothelial cells were considered as inert membrane in blood vessels. William Harvey recognized in 1682 that endothelial cells are far from being an inert layer. Malphigi showed that blood is separated from other tissues through endothelial cells. Meanwhile, Von Reckingausen represented in 1800 that blood vessels are not tunnels between tissues, but lined by cells. Starling proposed in 1896 a law that solidified the role of endothelial cells as selective and static barriers. Finally, studies of blood vessel wall by electron microscope in 1953, physiological evaluations of vessels by Gowan in 1959, and subsequent studies revealed the current view about endothelial cells (Cines et al., 1998).

Endothelial cells are always present in all vessels, and their numbers in an adult person is 1×10^{13} to 6×10^{13}, which has weight of 1 kg and covers 1 m^2 to 7 m^2, whereas the amount of existing connective tissue is dependent on the vessel diameter (Boo et al., 2002).

The life of all tissues depends on blood supply. As long as the inner surface of the blood vessel is lined by endothelial cells, blood supply is dependent on endothelial cell function (Figure 2.2). Endothelial cells have high capacity to adjust themselves in terms of cell number and arrangement to the blood requirements of local tissues. Presence of endothelial cells in the inner surface leads to control of the passage of nutrients into and out of the blood stream. Endothelial cells controls the blood nutrients and cell trafficking, as well as permeability, haemostatic balance,

vasomotor tone, structure and integrity of vessels, proliferation, survival, and immunity (Richards et al., 2010).

The detailed function of endothelial cells was evaluated since techniques involved in endothelial cells isolation and culture in vitro have been developed in 1970 (Cines et al., 1998). These cells are commonly isolated from large elastic mammalian vessels, such as rat (André et al., 1992), porcine (Carrillo et al., 2002) and bovine aorta (Schwartz, 1978), bovine pulmonary artery, and human umbilical cord (Kang et al., 2013). Several techniques, such as physical removal, enzymatic digestion, the outgrowth method, and use of magnetic beads, have been reported in the literature for isolation of endothelial cells (Birdwell et al., 1978; Phillips et al., 1979; Schwartz, 1978; Van Beijnum et al., 2008; Wang et al., 2007). Isolated cells can be identified as endothelial cells by specific markers including CD-31, Von Willebrand factor (factor VIII), 1,1'-dioctadecyl-1,3,3,3',3'-tetramethylindocarbo-cyanine perchlorate acetylated LDL (Dil-Ac-LDL), and angiogenesis as specific behavior of endothelial cells.

Aside from proteins in cytoplasm and surface of endothelial cells, endothelial cells can secrete other proteins as mediators, including endothelin (ET) and platelet-activating factor as vasoconstrictor, and NO, prostacyclin (PGI_2) as vasodilators, where in NO has a crucial role in blood vessel pressure regulation (Cines et al., 1998).

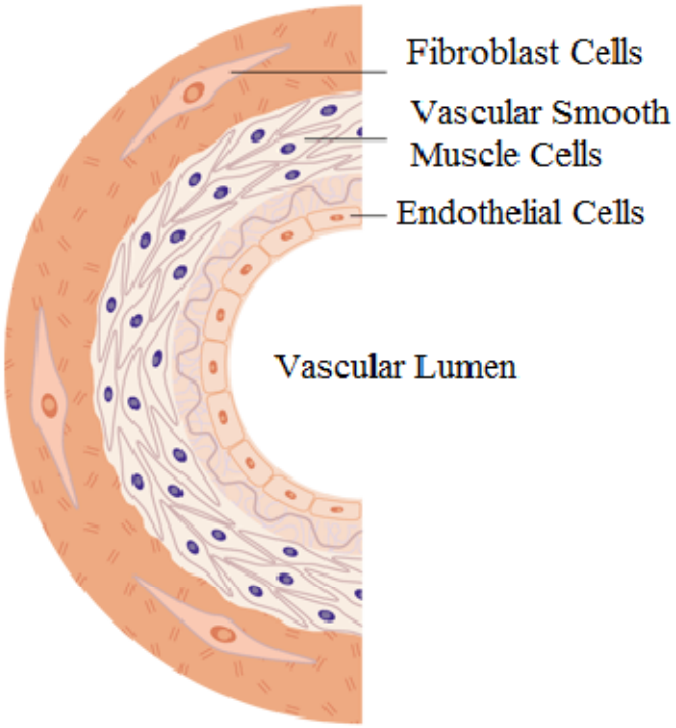

Figure 2.2: Endothelial cells as main constitutive part of the intimae layer (Rodriguez, 2012)

2. 3. Nitric Oxide

Endothelium affects vascular tone and vascular remodeling through transduction of hemodynamic conditions in the smooth muscle layer (Resnick & Gimbrone, 1995). Endothelial cells respond to mechanical forces left by pulsatile perfusion through vasoactive molecules such as NO (Soucy et al., 2006).

NO is the main element in vasodilatation, as well as platelet aggregation, leukocyte adhesion to endothelial cells, suppression of proliferation and migration of VSMC, and gene regulation related to adhesion molecules for monocytes (Dimmeler et al., 1998; Ziegler et al., 1998). NO produced by endothelial cells reacts with the heme group of cytoplasmic guanylatecyclase located in underlying VSMC to induce vasodilatation and ET inhibition as contracting agent (Ziegler et al., 1998). This vital

gas is synthesized through oxidation of L-arginin and oxygen to NO and citrulline by catalytic activity of eNOS (Dimmeler et al., 1998).

2. 4. Nitric Oxide Synthase (NOS)

Three types of NOS in endothelial cells, namely, neuronal nitric oxide synthase (nNOS or NOS-1), inducible nitric oxide synthase (iNOS or NOS-2), eNOS or NOS-3 produce three different kinds of NO (Napoli et al., 2006).

eNOS isoform has profound role in NO production. eNOS is called multi-domain enzyme consisting of oxygenase domain, which has binding sites for heme group, L-arginin, tetrahydrobiopterin (BH4), oxygen and Ca/calmodulin (CaM), and reductase domain consisting of binding sites for nicotinamide-adenine-dinucleotide phosphate (NADPH), flavin adenine dinucleotide (FAD), and flavin mononucleotide (FMN), from which an electron transfer to heme group in oxygenase domain (Figure 2.3) (Dimmeler et al., 1998; Napoli et al., 2006; Ziegler et al., 1998).

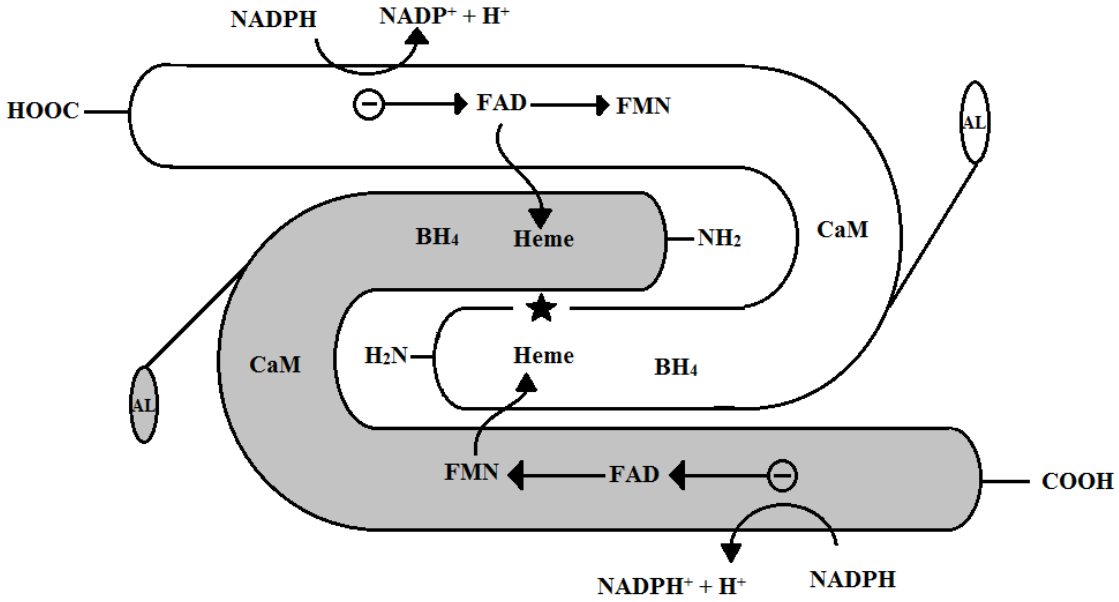

Figure 2.3: Diagram of electron transfer pathway in eNOS structure and interaction between co-factors in NO production process (Fleming & Busse, 1999).

eNOS phosphorylation is a critical regulatory mechanism to control NO bioavailability. To date, the eNOS molecule has at least five phosphorylation sites, namely, Ser^{1177}, Ser^{635}, Ser^{617}, Ser^{116}, and $threonine^{495}$. Ser^{1177}, Ser^{635}, and Ser^{617} are stimulatory sites of eNOS, whereas Ser^{116} and $threonine^{495}$ are inhibitory sites.

These phosphorylation sites can act through chemical and mechanical stimulators. However, phosphorylation sites triggered by mechanical stimulations are Ser^{1177} and Ser^{635} that the former one has profound role in NO production (Boo et al., 2002; Dimmeler et al., 1998; Dudzinski & Michel, 2007).

eNOS protein in basal condition is inactivated by Calveolin-1; however, mechanical stimulations upregulate this protein and remove inhibitions through protein kinases, such as heat shock protein-90 (Hsp-90) and PI3K.

2. 4. 1. Protein kinases involved in eNOS phosphorylation

Calveolin-1:.calveolin-1 is one of the main components of calveolae, a small invagination in plasmalemmal membrane surface of endothelial cells (Farber & Loscalzo, 2004). In basal (un-stimulated) condition, majority of eNOS bind to calveolin at the reductase domain. Connection of eNOS to Caveolin-1 inhibits eNOS activation; however, this inhibition can be overcome by high concentration of Ca/M (Feron & Balligand, 2006).

Heat shock protein-90 (Hsp-90): Hsp-90 has a critical effect in eNOS activation. Stretch and shear stress activate Hsp90 through ATP hydrolysis, and then Hsp90 interacts with eNOS and elevates NO production in two pathways. At the first hand, Hsp90 dissociates the interaction between eNOS and calveolin-1 by CaM, and activates eNOS by phosphorylation of eNOS at Ser^{1177} through recruiting PI3K and

Akt/PKA. On the other hand, eNOS is dephosphorylated at residue Thr^{495} through the calcineurin- dependent pathway (Averna et al., 2008).

Phosphoinositide 3-kinases (PI3Ks): Deformation of endothelial cells in response to physical stimuli transfer stress to the whole of cell structure and leads to activation of platelet endothelial cell adhesion molecule-1 (PECAM-1) and thereby PI3K activation.

This protein produces phosphatidylinositol trisphosphate (PIP3) from phosphate dylinositol bisphosphate (PIP2). PIP3 induces translocation of Akt from cytoplasm to plasma membrane to be phosphorylated by phosphatidylinositol-dependent kinases (PDKs). Therefore, activated Akt can activate eNOS through Ser^{1177} phosphorylation. This phosphorylation elevates the affinity of eNOS to CaM because it removes the inhibitory effect of the auto-inhibitory loop of Ser^{1177} from CaM binding site (Morello et al., 2009).

2. 4. 2. NO production

The main stimulators for eNOS activation and NO production in endothelial cells are Physical stimulation (stretch and shear stress) which are applied on endothelium roughly 75 times/min in normal situation (Fisslthaler et al., 2000).

eNOS activation: eNOS is located under the plasma membrane of endothelial cells and is inhibited through binding with Calveolin 1 in Calveolae. Inactivated eNOS needs to be activated by certain stimulators, either physical or hormonal stimulators. These stimulators increase the concentration CaM in the calvoelae and remove the interaction of eNOS and calveolin 1 through Hsp90. Furthermore, stress distribution across the cell structure and changes in the connection of actin filaments and cytoskeletal proteins lead to conversion of PIP2 to PIP3 through PI3K activation.

Activated PIP3 transfers inactive kinase Akt to the cell plasma membrane to be phosphorylated by PDKs. The simultaneous connection of CaM and Hsp90 with activated Akt induces eNOS phosphorylation at Ser^{1177}. eNOS can then be used in the NO production process (Figure 2.4).

NO production: The oxygenase domain of eNOS produces electrons by reducing NADPH. The produced electrons are transferred to the reductase domain by flexible protein strand located between the oxygenase and reductase domains. The electrons released from NADPH are transferred to the oxygenase domain and convert ferric heme to ferrous, which actively binds to oxygen. Binding of oxygen and L-arginin produces NO, in which BH4 is a necessary conversion cofactor.

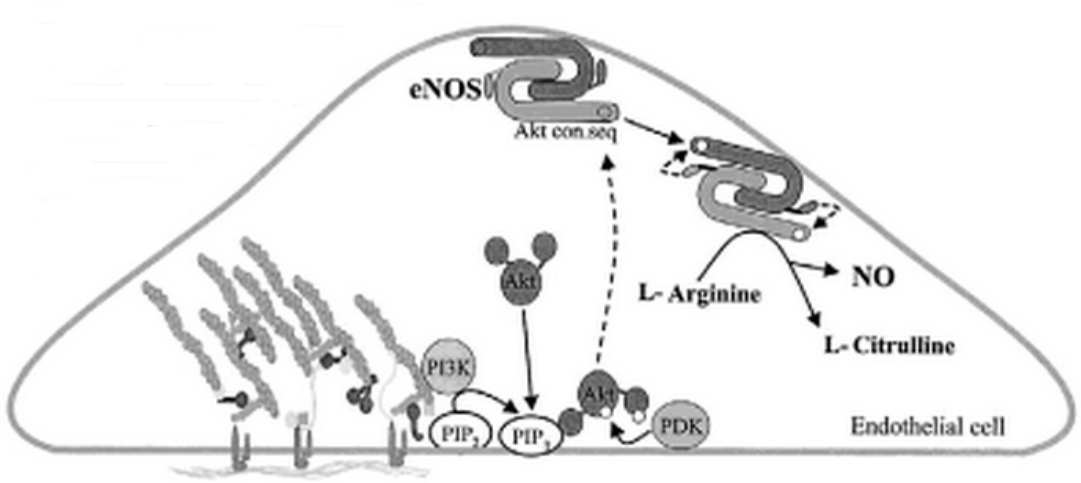

Figure 2.4: Proposed model of eNOS phosphorylation by Akt/PKB in response to mechanical stimulation (Ignarro, 2000).

2. 5. Endothelial dysfunction

Endothelial dysfunction is a disorder in which impaired NO signaling reduces endothelial-derived vasorelaxation and induces vasoconstriction (Cai & Harrison, 2000). Disorders such as aging and atherosclerosis, in which arterial stiffness is a critical issue reduce NO production and induce endothelial dysfunction (Soucy et al.,

2006). Elevation in systolic blood pressure, a slight depletion in diastolic blood pressure, and consequently, a widened pulse pressure are consequences of arterial stiffness (Mancia et al., 2013; Steppan et al., 2011; Stewart et al., 2003). Systolic hypertension and widened pulse pressure as surrogate indicators of stiffness can induce adverse consequences in elder hypertensive patients including myocardial infarction, heart failure, stroke, dementia, and renal disease (Kals et al., 2006).

Increased vascular stiffness can be justified by structural alterations and cellular dysfunctions as precursors in aging and atherosclerosis.

2. 5. 1. Aging

Structural changes: From the structural point of view, collagen and elastin are the determining elements in vascular wall stability and compliance (Wilkinson et al., 2002; Zieman et al., 2005). However, enhanced arterial pressure and stretch in large elastic arteries, especially near bifurcations, influence the structural matrix protein through excessive collagen proliferation and fractured elastin (Lee & Park, 2013). Excessive collagen proliferation, as well as, weakness in the elastin array, accompanies a high tendency toward mineralization by calcium and phosphorous that leads to aging-deprived stiffness (Park & Lakatta, 2012).

Cellular dysfunction: The effects of cellular dysfunction on arterial stiffness are related to endothelial cells and VSMC tone (Lakatta & Levy, 2003). VSMC tone can be regulated through mechano-stimulations (e.g., stretch caused by calcium signaling) and by paracrine mediators (e.g., NO, Angiotensin II (AII), and ET) (Park & Lakatta, 2012).

eNOS inhibition, a decline in NO expression, and NO scavenging by superoxides can reduce NO bioavailability. Aside from the aforementioned reasons, decline in Akt-mediated eNOS phosphorylation also inhibits eNOS activity during aging (Figure 2.5). Impaired NO bioavailability induces severe reduction in pulse-mediated vasodilation, which has positive feedback on NO reduction (Zieman et al., 2005).

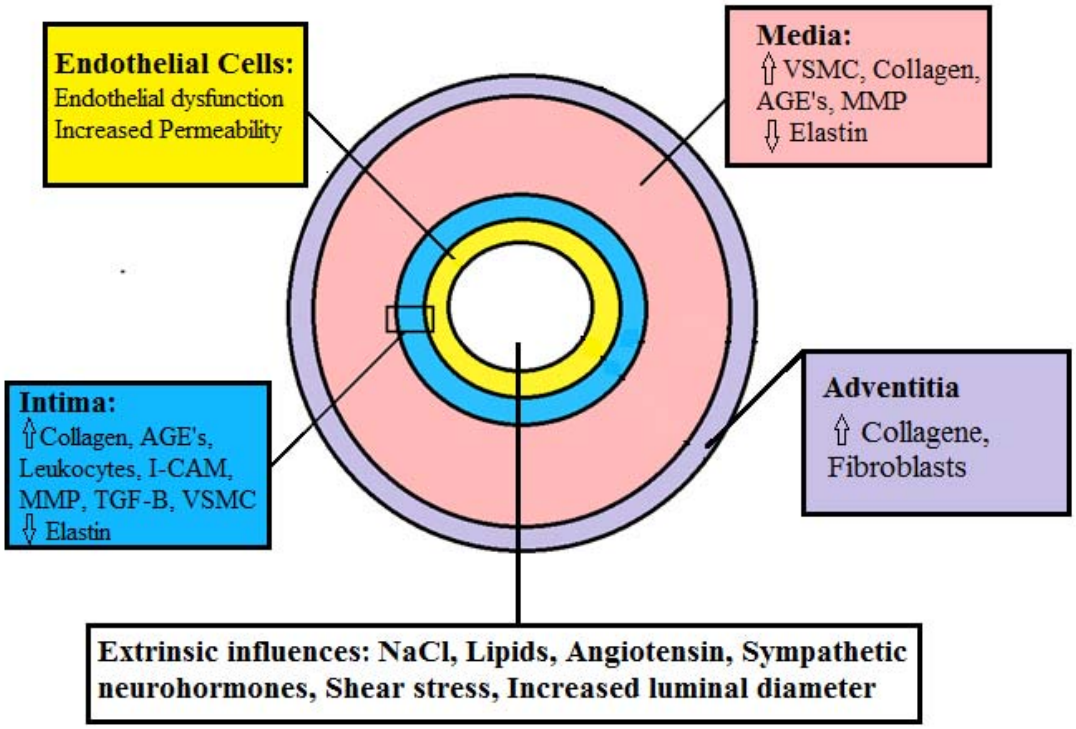

Figure 2.5: Cellular and structural mechanisms involved in arterial stiffness as a result of aging (Zieman et al., 2005).

2. 5. 2. Atherosclerosis

Atherosclerosis, created through the amalgamation of arteriosclerosis and atheromatosis, is a general term that covers the biological diversity of the arterial wall processes (Zhao et al., 1995). Arteriosclerosis refers to media thickness, whereas

atheromathosis (atherosclerotic lesion) defines an inflammatory endothelial disorder (Hamilton et al., 2007).

Structural changes: The pro-inflammatory agents stimulate endothelial cells to express adhesion molecules to attract monocyte and lymphocyte. Interaction between monocytes and endothelial cells increases infiltration of macrophages. Macrophages matured from monocytes increase scavenger receptor expression and turn macrophages into foam cells attached to the endothelial cells. This stage is characterized as the early stage of atherosclerosis (Dao et al., 2005).

Advanced stages of atherosclerosis are defined with appearance of fibrous tissue. VSMC activity and overproduction of extracellular matrix such as collagen lead to fibrous formation phase. VSMC migration from media to tunica intimae layer leads to platelet attachment (Libby, 2002). Intra plaque neovascularization favors the chance of hemorrhage within the plaque, and hence thrombin activation (Figure 2.6) (Oemar et al., 1998).

Endothelial cells dysfunction: The net results of atherosclerosis ranges from tunica media thickening to increased stiffness leading to endothelial dysfunction (Hamilton et al., 2007). Many studies have found that low expression of eNOS and low production of NO, NO scavenging, hypercholesterolemia, and atherosclerosis diminish endothelial cell relaxation (Figure 2.6) (Harrison, 1997; Oemar et al., 1998).

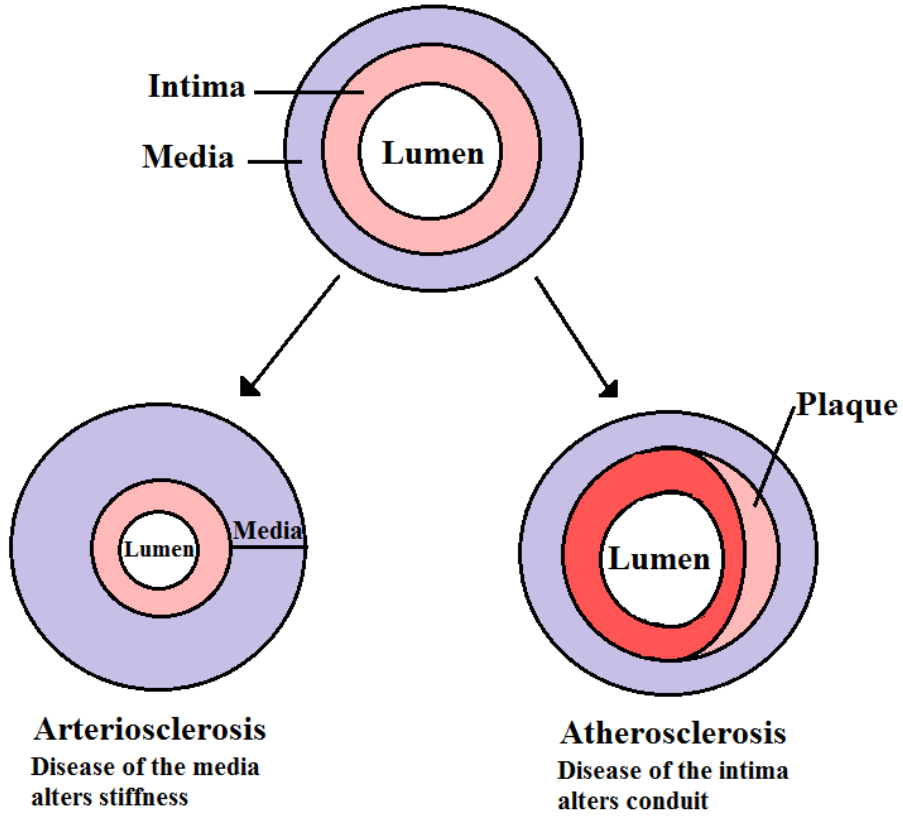

Figure 2.6: Intimae and media involvement in atherosclerosis through plaque formation in intimae and increase in thickness in media layer (Mookadam et al., 2010).

2. 6. Effects of stiffness on endothelial cell behavior

In the body, blood vessel stiffness from structural point of view is related to wall thickness enhancement and wall resistance to expansion and contraction. Consequently, wall strain and CaM releasing declined, which consequently decreased eNOS phosphorylation and NO production.

In the cellular concept, cells impose forces on their environment as ECM; however, ECM applies forces such as gravity, tissue-specific interactions, mechanical forces, and ECM stiffness to cells. Cells can sense the outer environment by integrin receptors, which are connected to the cell cytoskeleton by F-actin or α-actinin. Cells

have the ability to convert mechanical cascades into complicated intracellular signaling inputs which induce cell responses appropriately.

Mechanical stimulators like stretch stimulate at least one of these three proteins to active cellular response. Endothelial cells respond to mechanical stimuli to regulate vessel biology. Stretch sensed by these proteins can be converted to intracellular signals through different mechanism, namely, enzyme activation by stretch, opening ion channels, signal transferring through cytoskeleton, and cells contacts together (Figure 2.7).

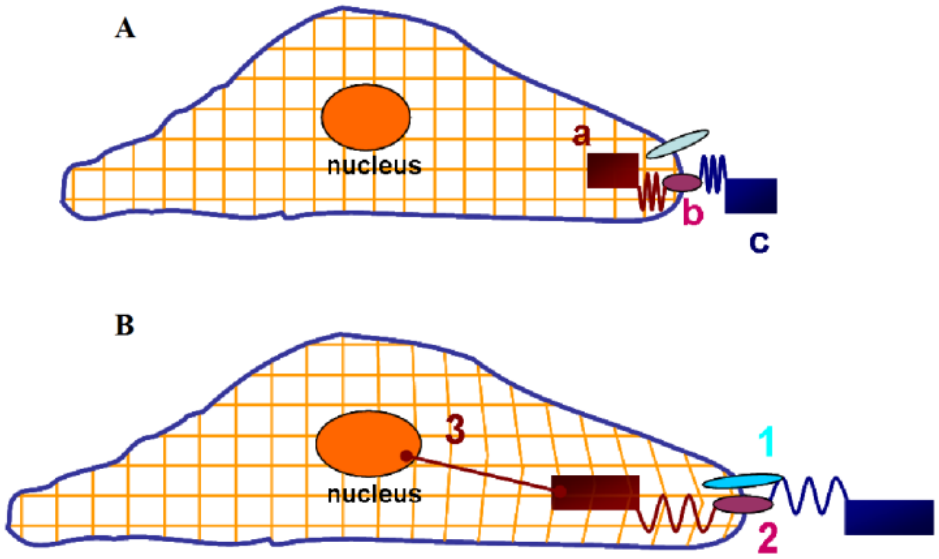

Figure 2.7: Diagram of cell-substrate interaction: A) Resting state of cells, a) Linker protein to cytoskeleton b) Integrin receptors as a liker between ECM and cells c) ECM
B) Stretched position of cell and transferring intracellular signals to nucleus (Vogel, 2006).

The converted signals are transferred to the nucleus which induces different behavior in cells, such as, inducing conformational changes in the protein production and protein forms (Vogel, 2006).

In terms of protein production, strain can regulate expression of eNOS gene, change mRNA level through alteration in mRNA transcription or RNA degeneration, and finally control eNOS protein stability (Awolesi et al., 1995), While alterations in protein form as a result of strain is related to protein phosphorylation (Takeda et al., 2006). For example, strain can activate PI3K and Akt, and induce eNOS phosphorylation, and NO production.

Besides the imposed physical forces, local ECM stiffness has important mechanical effects on cell function. Live cells follow a pattern called "stiffness sensing", which denotes that cells can sense their outer environment as they adhere and respond to mechanical resistivity of ECM. Cells can recognize substrate mechanical properties through receptors attached to the substrate (Cines et al., 1998; Krishnan et al., 2010; Pelham & Wang, 1997; Yeung et al., 2005).

As substrate stiffness can affect cell behavior in response to imposed forces from the substrate, this effect can be greater in dynamic situation such as tensile loading. Studies showed that eNOS phosphorylation and NO production is reduced in dynamic situation as vessel stiffness increase (Blackwell et al., 2004; Lakatta et al., 2009; Soucy et al., 2006).

The potential mechanisms in reduction of NO production with stiffness enhancement include 1) substrate scavenging through competitive enzymes such as arginase; 2) high production of superoxides (Reactive Oxygen Species (ROS) and O_2^-); 3) less superoxide dismutase (SOD) activation; 4) endogenous inhibition of eNOS by asymmetric dimethyl arginin; 5) reduction in eNOS activation; and 6) modulation of upstream activators (kinases) (Soucy et al., 2006; Sun et al., 2004).

Studies done on aged aorta showed that mechanical forces increase O_2^- production and reduce SOD activation in aged-arterials, in which NADPH is the main

source. eNOS can be nitrated and uncoupled by peroxynitrite caused from the reaction NO and O_2^- within the aged vessels (Blackwell et al., 2004; Sun et al., 2004).

Li et al. (2005) triggered phosphorylation in Akt by only shear stress. They observed that p-Akt level remained unchanged with this stimulus; hence, they concluded that stretch has more potential to trigger kinases for phosphorylation (Li et al., 2005).

Peng et al. (2003) revealed that tube distensibility affect cell adhesion and survival when those are under stress (Peng et al., 2003). They also showed that substrate stiffness alters endothelial mechano-signaling and cell susceptibility to stress in the presence of shear stress and stretch. Therefore, cells on stiff substrates are more vulnerable to oxidative stress. This mechanism somehow explains why pulse pressure in aging contributes to vascular risk. The endothelial cell function is not the only contributing factor in arterial stiffness, stiffness of arterial wall can also influence endothelial function in the other side (Peng et al., 2003).

Therefore, the availability of proper stiffness profiles can elevate the feasibility of biophysical studies on cell-substrate interaction (Yeung et al., 2005).

Cell response to substrate was evaluated through cell growing on polyacrylamide (PA) and polycaprolactone (PCL) (Tan & Teoh, 2007; Yeung et al., 2005). However, these materials are not stretchable, whereas Polydimethylsiloxane (PDMS) elastomeric materials have shown potential biocompatibility for vascular and nerve tissue applications (Johansson et al., 2009). PDMS has attracted research attention in the field of cell biology because of its biocompatibility, simple fabrication, tuneable flexibility, gas permeability, high oxidative and thermal stability, and low cost (Lee et al., 2004; Takeda et al., 2006; Zhang et al., 2013).

PDMS can exhibit specific mechanical properties such as high stiffness in its native flexibility by adding a second phase material.

From the available second phase materials for controlling substrate-stiffness, α-alumina (Al_2O_3), which has a well-known biocompatibility, thermal and electrical resistivity, thermal and chemical stability, and abundance availability (Leukers et al., 2005), was chosen in this study. The stability of α-phase Al_2O_3 at conditions similar to the present operational conditions is one of the main reasons for its selection in our study (Boumaza et al., 2009). A stable phase helps minimize deviations in physical properties at different processing conditions, whereas an unstable phase shows different physical properties anonymously.

CHAPTER 3

MATERIALS AND METHODS

The initial sage of the study involves the optimization of bovine aortic endothelial cell (BAEC) isolation. The techniques were optimized and an improvement was proposed to commercial enzymatic method. The second part of the study involves the preparation of substrates with different stiffness, and those were characterized by mechanical, structural, and morphological analysis. Moreover, BAEC adhesion, proliferation and morphology on the substrates were characterized. Finally, 10% stretch loading for 3 h was applied on substrates, in which NO production and phosphorylation of eNOS (p-eNOS) at Ser^{1177} were evaluated by enzyme-linked immunosorbent assay (ELISA) (Figure 3.1).

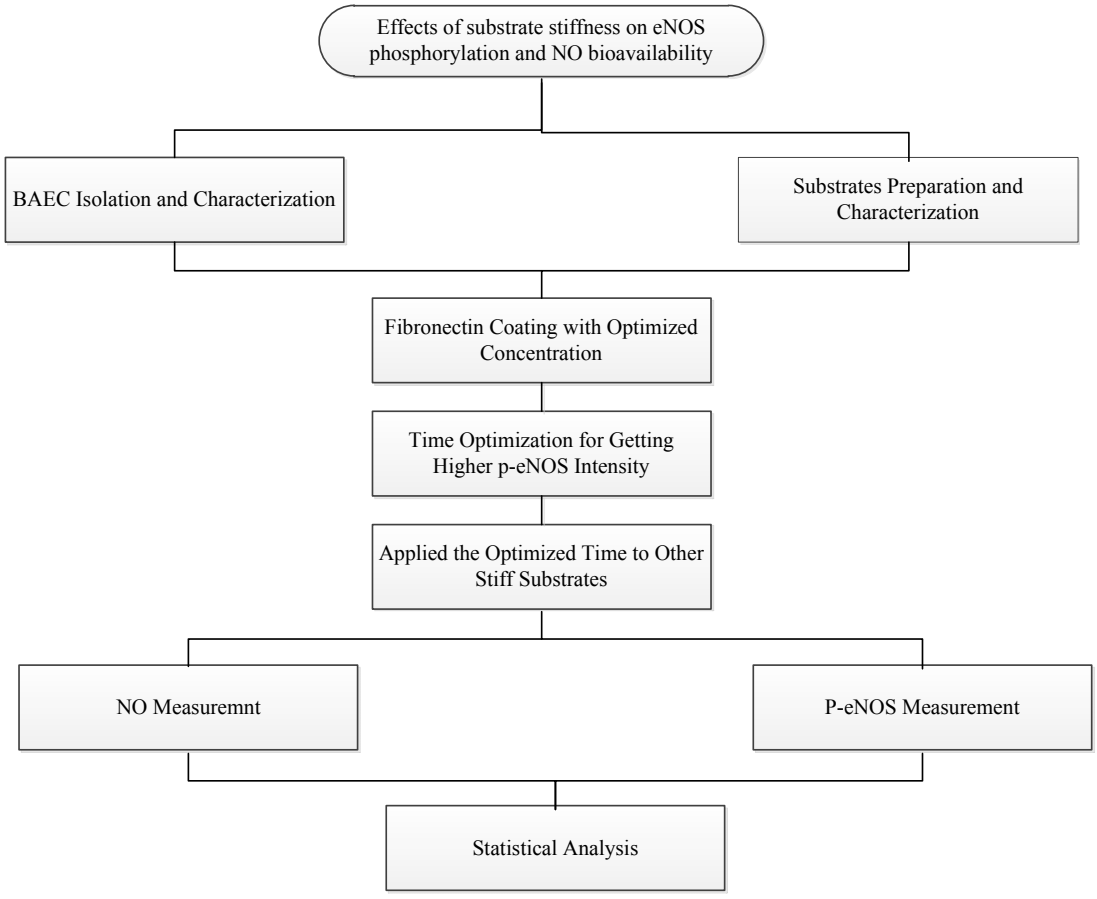

Figure 3.1: A summary of the stages conducted in this study

3. 1. Endothelial cell isolation

Fresh bovine aorta (descending part) was obtained from a local slaughterhouse (Chang Fatt Sing slaughter house, Shah Alam, Malasyia). Immediately after excision, both ends of the samples were clamped using sterilized plastic tie wraps, and the inner lumen was filled with wash medium [Dulbecco's Modified Eagle Medium (DMEM) (Sigma #D5921) containing 2% penicillin-streptomycin (Sigma #30002210) and 120 µg/l Amphotericin B]. The clamped aorta was then dipped in 70% ethanol for 30 s to clean the outer surface, stored in 4 °C phosphate buffered saline (PBS; Sigma #P4417) with 6% penicillin-streptomycin and 120 µg/l amphotericin B, and transported to the laboratory in an ice box.

The samples were unclamped and washed with PBS in a laminar flow hood; after which, the adventitia was removed using a scissor. The aorta was cut into two or three 5 cm long pieces, and each piece was opened with a longitudinal incision. Afterward, 0.1% collagenase type II solution was prepared by dissolving 0.1 g of collagenase II (Gibco #1115455) in 100 ml of Hank's balanced salt solution (HBSS) (Hyclone® #SH30268.02). The specimens were then laid in separate dishes with the endothelium facing up and covered with sterile filter paper (Fisher, #FB59023). About 2 to 3 ml of 0.1% (w/v) collagenase type II solution was dripped onto each filter paper.

Both samples were placed in an incubator with 5% CO_2 at 37 °C for 30 min which is the optimum condition for collagenase enzyme to act properly. After incubation, the solution containing the endothelial cells was collected to centrifuge tubes. Then, each sample and filter paper was rinsed gently with pre-warmed PBS to remove cells which were still intact in the tissues. Also, the PBS used for washing the samples was collected in centrifuge tubes. The cells remaining in the collagenase

solution were collected through centrifuging at 1500 rpm for 10 min. The pellets were re-suspended in endothelial cell-specific culture medium [M200 (Gibco, #M200-500) containing 1% penicillin-streptomycin-amphotericin, 0.1 mg/ml heparin sodium (Rotex Medica, #ETI3L184-10), 50 µg/ml bovine endothelial supplement (Sigma-Aldrich, #E0760), and 20 vol% fetal bovine serum (FBS) (Sigma-Aldrich, #F1051)], and then seeded in Nunc EasYFlask™ Nunclon™ T25 tissue culture flasks (Figure 3.2). The culture medium was changed every 3 days.

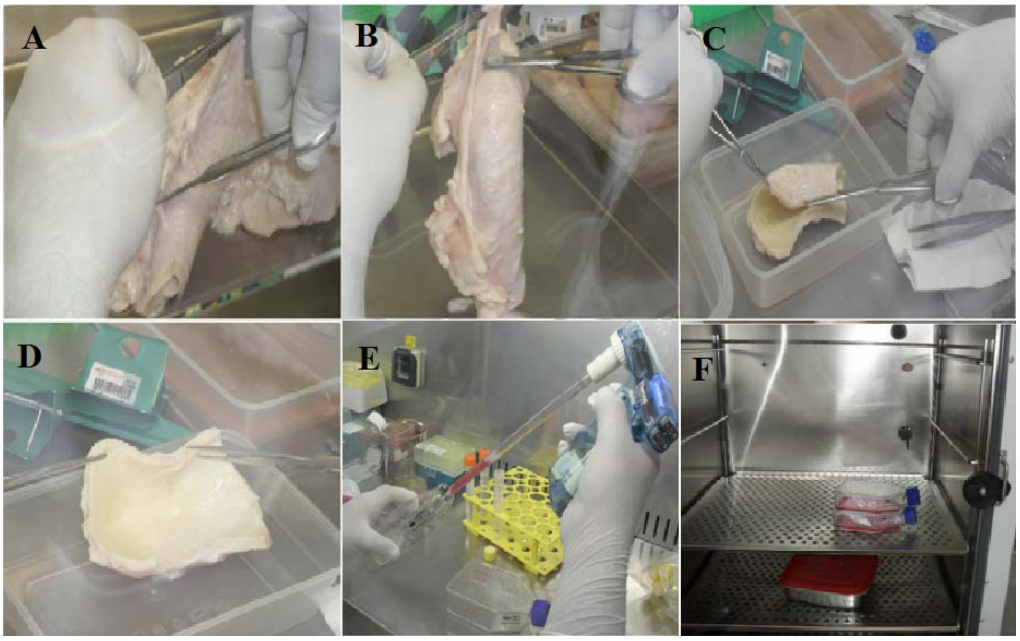

Figure 3.2: Stages of endothelial cell isolation from bovine aorta B) Removing adventitia tissue C) Cutting aorta samples longitudinal D) Putting samples in dishes with endothelium facing up E) Re-suspending cell plate in T25 flasks F) Adding medium to flasks and keeping in incubators.

Cell passaging was performed using TryPLE Select® (GIBCO #12563011) when the cells reached 80% to 90% confluence. Cells washed with pre-warmed PBS, and then 10 ml of TryPLE Select® was added to each T75 flasks. Flasks were kept inside an incubator at 37 °C for 8 min. After incubation, the cells attached to the

flasks were detached by gentle shaking, and their detachment was verified under light microscope. TryPLE deactivation was carried out by adding a medium containing FBS to each flask. Cells were harvested in centrifuge tube and pellet was formed at 1500 rpm for 10 minutes. The supernatant was then discarded and the formed pellet was re-suspended in 1 ml of complete medium and counted by haemocytometer and 0.2 (w/v)% Trypen Blue (Sigma #T6146) in PBS. Endothelial cells with density 5,000 cells per cm^2 were seeded on flasks. The culture medium was changed every 3 days.

3. 2. Cell counting and viability

Hemocytometry, a manual method for cell counting, was used. Cell suspension was mixed with Trypen Blue with proportion 1:1. Meaning, 15 µl of cell suspension was mixed with 15 µl of 0.2% Trypen Blue (0.2 gr Trypen Blue in 100 ml PBS). Before placing the cell suspension into the hemocytometer, the glass cover must have proper contact with both counting chambers. Afterward, cell suspension was applied to the edge of cover slip and the cell number was counted under light microscope in the 5 areas mentioned in Figure 3.3. Live cells appeared bright under the microscope, whereas dead cells appeared dark because the dye can pass through the membrane of dead cells. The number of live cells counted in the 5 squares was timed in 4000. The calculated number was considered as cell number per 1 ml of cell suspension.

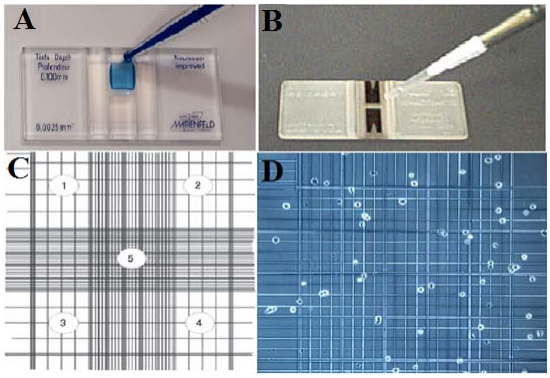

Figure 3.3: Cell counting through hemocytometer A) How cell suspension should be applied in hemocytometere chamber B) Cell suspension in both sides of the hemocytometere chamber C) Area which should be counted for cell counting D) Living cells with bright appearance, and dead cells with dark appearance.

3. 3. Endothelial cell cryopreserving

Cell preserving can be done at freezer with −80 °C or at liquid nitrogen with −196 °C. In this study, the cells were preserved in liquid nitrogen. After cell detachment and centrifugation, cells were suspended in 7% Dimethyl sulfoxide (DMSO) (7 ml of DMSO (Sigma, #D2650) (Kofron et al., 2003; Reed, 2004) with 93 ml of completed medium or FBS). Cell suspension was kept 20 min at room temperature, and then placed inside a freezing container (Mr. Frosty), because it induces constant reduction in temperature. The freezing container was then placed in a freezer at −80 °C for at least 4 h, and the cell samples were then transferred to the liquid nitrogen tank. Cells can be maintained in liquid nitrogen for several years.

3. 4. Cell characterization

Cell characterization was used to confirm that the isolated cells were the cells that we were looking for. The isolated cells were identified as BAEC by specific markers including CD-31 as a surface marker, Von Willbrand factor, and Dil-Ac-LDL as cytoplasmic markers, and the formation of blood vessel-like structure

(angiogenesis), as described in the literature (Nicosia et al., 1994b; Phillips et al., 1979). Therefore, detection of CD-31 was done through flowcytometry, followed by immunofluorescence staining for factor VIII and Dil-Ac-LDL. Characterization of the endothelial cells was conducted in Passage 4 (Shimizu et al., 1999).

3. 4. 1. Factor VIII staining

Thermanox® plastic cover slips with dimension of 2 cm×2 cm were placed inside 6 well plates (Nunc®), and then pre-wetted by small volume of warm culture medium and kept in incubator until cell seeding. Approximately, 80000 endothelial cells suspended in 200 µl of medium were seeded on each cover slip. After incubating the cover slips at 37 °C for 4 h, 200 µl of medium was added to the cover slips. Cells with 400 µl medium were kept for 24 h. Medium volume then increased to 1 ml after 24 h of incubation.

A confluent monolayer of endothelial cells on thermanox® plastic cover slips was subjected to immunofluorescence staining to determine the Von Willebrand factor and Dil-Ac-LDL. After reaching 70% confluence, cells were washed with cold PBS and fixed with paraformaldehyde 4% (Sigma #HT501128) for 10 min at 4 °C. Afterward, paraformaldehyde was discarded and cells were washed with cold PBS for three times, with each time took 5 min. Permeabilization was conducted by 0.02% Triton X-100 (OmniPure #9410) for 20 min at room temperature. Permeabilization helped the penetration of antibody to the cells because factor VIII is a cytoplasmic marker. After one time washing with PBS, the cells should be blocked with 3% bovine serum albumin (BSA) to remove the false positive results (unwanted bonds). Blocking was performed using 3% BSA (Amresco #0332) for 30 min. Cells were then incubated overnight with rabbit anti-human factor VIII as primary antibody

(Dako #ab6997; diluted 1:200) at 4 °C. After discarding the primary antibody, cells were washed with PBS three times, which took 5 min each time to remove unbonded antibody. The staining process was continued through cell staining with donkey anti-rabbit IgG H&L FITC as secondary antibody (Dako, #ab7079; diluted: 1:500) for 1.5 h at room temperature. Cells were then washed with PBS three times. ProLong® Gold Antifade Reagent (Invitrogen, P36935) was used to fix the cover slips on the glass slides. The slides were observed using confocal microscope (Leica Microsystems, Heidelberg GmbH).

3. 4. 2. Dil-Ac-LDL uptake

The uptake of Dil-Ac-LDL was examined after 4 h of incubation of the endothelial cells with 10 μg of stock solution of Dil dye (Invitrogen, #D282) in 1 ml of endothelial cell complete medium. The protocol was followed according to the study of Ando et al.(Ando et al., 1999) and Nicosia et al.(Nicosia et al., 1994b) . The stained cells were observed using confocal microscope.

(Stock solution of Dil-Ac-LDL was prepared through dissolving 15 mg of Dil-Ac-LDL in 1 ml of DMSO as solvent. Working solution with concentration of 10 μg/ml of Dil dye was added to the medium of seeded cells on the cover slides.

3. 4. 3. CD-31 detection

Endothelial cells were detached from the flasks and counted using haemocytometer. Cells were re-suspended in PBS, divided, and placed in centrifuge tubes at a density of 1×10^6 cells per tube. Three tubes were used for three applications: without treatment, cells with Mouse IgG2a isotype control antibody [HOPC-1] (FITC), and cells with Mouse Monoclonal antibody to CD31 (Gene Text,

#GTX 43622). The cells were then centrifuged at 1500 rpm for 10 min. The platelets were re-suspended in 90 µl of sheath fluid (BD FACSFlow #342003) and combined with 10 µl of Mouse Monoclonal antibody to CD31 and Mouse IgG2a isotype control antibody, and then incubated for 45 min at room temperature. The control group was kept at the same situation, but without treatment. Isotype control was used to eliminate the probability of obtaining false positive results.

Cells were washed twice with sheath fluid and re-suspended in 500 µl of sheath fluid after incubation. The same procedure was carried out for controls, but no treatment was administered. The percentage of pure endothelial cells stained by CD-31 was evaluated through flowcytometry (FACSDiva Version 6.1.3, USA) (Grover-Páez & Zavalza-Gómez, 2009).

3. 4. 4. Angiogenesis

Endothelial cells were placed in a fibrin construct, which was used as three dimension (3D) environment to demonstrate angiogenesis as a specific dynamic behavior of endothelial cells (Fariha et al., 2013). Briefly, blood was collected into citrate coated tubes from one donor. Plasma was separated from blood through centrifugation at 700×g for 10 min. Approximately, 6×10^6 BAEC were suspended in 6 ml of human plasma and poured into a six well plate (1 ml plasma/1 well). Afterward, 10 µl of 1 M calcium chloride ($CaCl_2$) (Sigma-Aldrich, St. Louis, MO, USA) and 1 IU of thrombin (Sigma-Aldrich, #T9326) was added into each well and stored at 37 °C. Fibrin existed in the plasma polymerized to the 3D fibrin construct after 15 min. After polymerization, 2 ml of the completed medium was added to each well. Cell response to the 3D environment was monitored under inverted light microscopy for 1, 3, 5, and 7 days.

3. 5. Substrate preparation and characterization

3. 5. 1. Membrane preparation

PDMS/Al_2O_3 composite substrates with different stiffness were prepared by mixing PDMS gel (Sylgrade 184 Silicon Elastomer Base; Dow Corning, USA) as base matrix with 5 wt% and 10 wt% Al_2O_3 (Sigma-Aldrich, # 265497), which served as second phase ceramic particle (particle size:<10 μm, density: 3.97 g/cm^3, ball and sphere shape) using a planetary ball mill (Retsch, PM200, Germany). Ball milling of ceramic particles with PDMS was done for 4 h at a speed of 300 rpm. A curing agent from Dow Corning with a 1:10 proportion (v/v) (curing agent: PDMS gel) was then added to the PDMS/Al_2O_3 mixture. The curing agent was used as a cross-linker at the base of PDMS polymeric chains. PDMS/Al_2O_3/curing agent mixture was also subjected to ball milling for 10 min at a speed of 300 rpm. The required amount of uncured mixtures of different Al_2O_3 concentrations was poured into different suitable shaped molds used for different characterizations. The dumb bell, TPP® 12-well plate molds, and membrane mold were used for tensile test, cell culture studies, and tensile loading studies, respectively (Figures 3.4 and 3.5). The molds were then kept under vacuum pump (GAST, #DOA-P504-BN) for 30 min to remove bubbles. Each mold was placed in an oven (Lab Companion) at 50 °C for 4 h to ensure proper curing of elastomers. Pure PDMS elastomer was also prepared by mixing the PDMS gel with the curing agent (i.e., 10% volume of PDMS gel) using the ball mill without the addition of Al_2O_3 particles. The mixture was then cured at 50 °C for 4 h (Figures 3.6) (Huh et al., 2013; Mata et al., 2005).

Extensive cleaning was conducted by washing the substrate specimens, which includes all composite substrates and pure PDMS elastomers, with 1 N hydrochloric

acid (HCl) for 2 min to remove non-bonded PDMS particles (Ziegler et al., 1998). After several rinses with distilled water, the substrates were dried and submitted to the University Malaya Hospital (UMMC), Malaysia for sterilization using ethylenoxid (EO).

Figure 3.4: Mold used for preparation of membranes with different stiffness

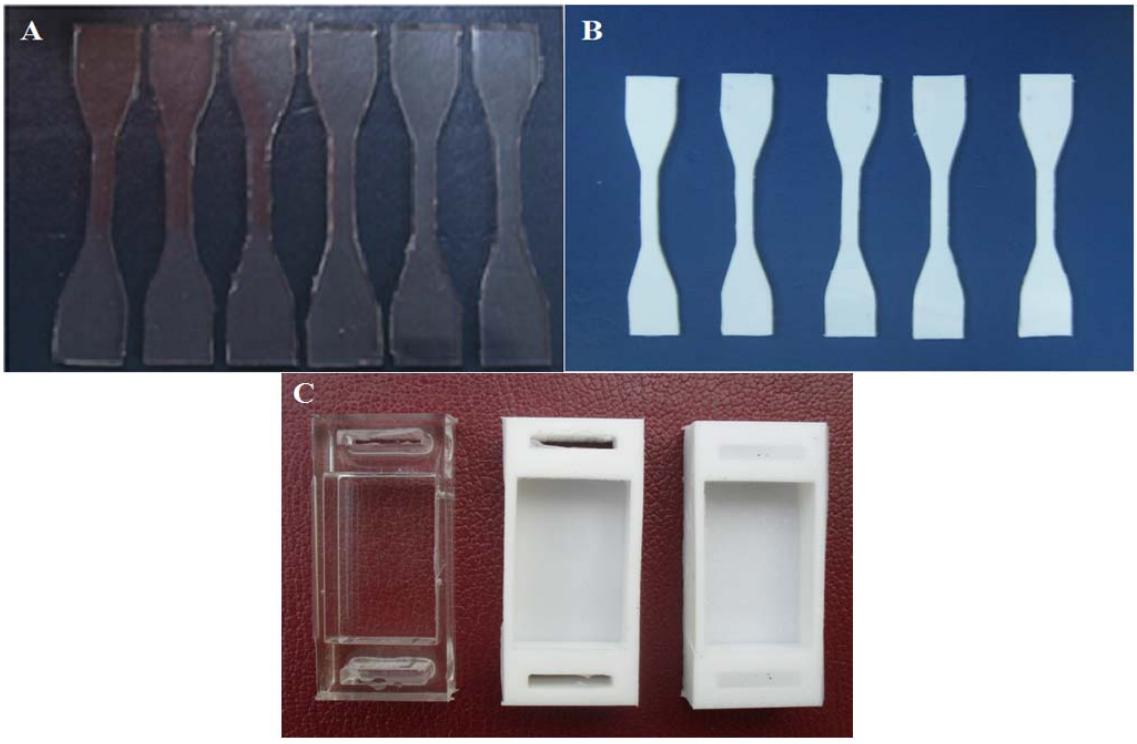

Figure 3.5: A, B) I-shaped mold prepared according to ASTM D 412 test standard for vulcanized rubber and thermoplastic elastomers C) Substrates with different stiffness (pure PDMS, PDMS/5% Al_2O_3, and PDMS/10% Al_2O_3)

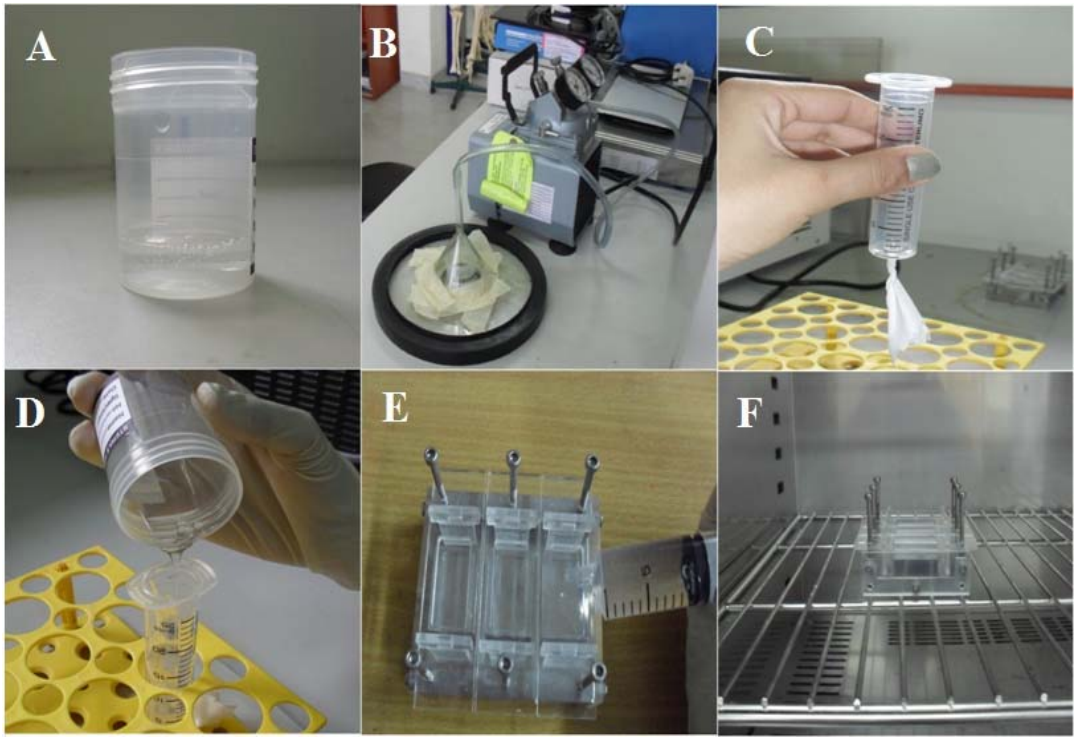

Figure 3.6: Membrane preparation process A) PDMS base and curing agent mixture B) Using a vacuum pump for removing bubbles C) Clamping the end of a syringe by tissue and tacking out piston D) Pouring the mixture in the syringe E) Pouring the PDMS mixture in membrane mold by syringe F) Placing the membranes in a 50 °C oven for 4h

3. 5. 2. Tensile test

The mechanical properties of pure PDMS elastomer and its composites with different Al_2O_3 concentrations (5% and 10%) were characterized according to the American Society for Testing and Materials (ASTM) D 412 test standard for vulcanized rubber and thermoplastic elastomers (Figure 3.7) (Institute, 1968). The test standard requires the use of a universal testing machine, (Instron Micro Tester, # 5848) (Figures 3.8) at a constant crosshead speed of 1 $mm.min^{-1}$ to evaluate the stiffness of the materials in tensile mode. The dimensions of the tensile specimen are 25 mm×6 mm×2 mm (actual gauge length × width × thickness) (Figure 3.7). At least three identical specimens were tested to obtain the average and standard deviation values.

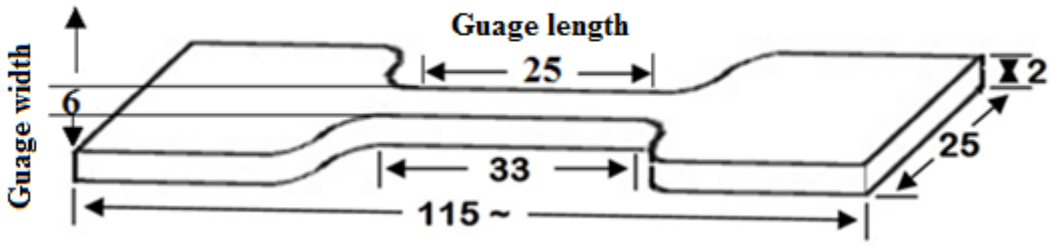

Figure 3.7: Specimen shape and size according to ASTM D 412 test standard for vulcanized rubber and thermoplastic elastomers

Figure 3.8: Insteron machine used for tensile test and Young's Modulus measurement

3. 5. 3. X-Ray diffraction (XRD)

The crystal structures and crystalline phases of the pure PDMS and its composites with Al_2O_3 were identified by XRD analysis using an X-ray diffractometer (DKSH Technology, # DY/032) (Figure 3.9). The scanning angle (2θ) ranges for this study were from 10° to 70° using CuKα radiation (λ=1.54056 Å).

Figure 3.9: X-ray diffractometer used for detecting crystalline phases of pure PDMS and its composites with Al_2O_3

3. 5. 4. Fourier transforms infrared spectroscopy (FTIR)

The molecular structure and functional groups presented in the materials section (i.e., PDMS, PDMS / Al_2O_3 composites, and pure Al_2O_3) was detected using attenuated total reflectance-FTIR (ATR–FTIR) spectroscopy (Perkin Elmer, # 400) (Figure 3.10) within the wavelength range of 4000 cm^{-1} to 500 cm^{-1} at a resolution of 4 cm^{-1}.

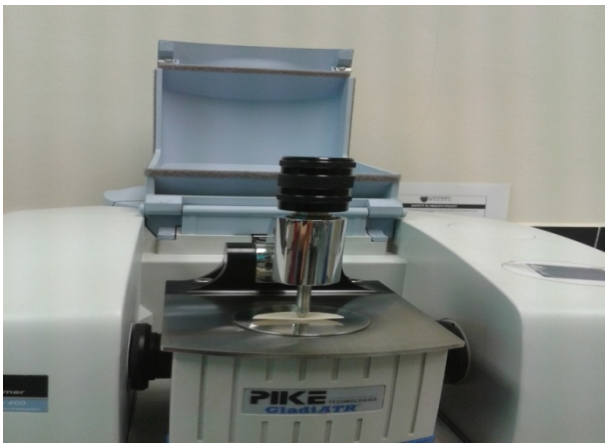

Figure 3.10: ATR-FTIR spectroscopy used for detecting molecular and functional structure of materials

3. 5. 5. Atomic force microscope (AFM)

An AFM (Ambios Technology, USA; Q-scope TM) was used to evaluate the surface properties seen in the 3D images of the material surface under the non-contact mode (Figure 3.11).

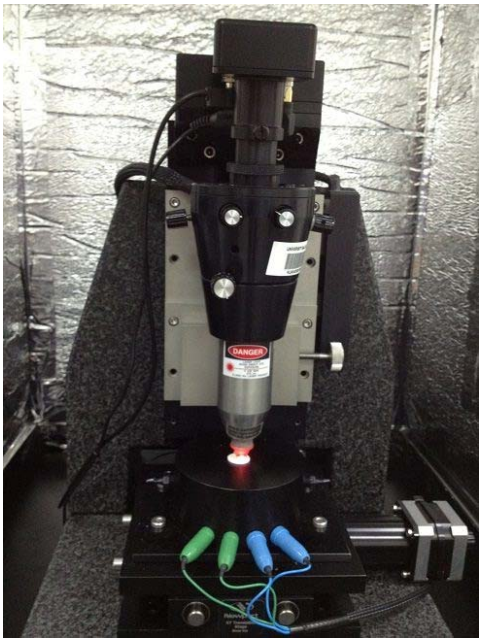

Figure 3.11: AFM machine used to examine surface morphology

3. 5. 6. Field emission scanning electron microscopy (FESEM)

Samples were separated into cross sections to show the matrix-particle bonding in the composites using FESEM (Zeiss, # Auriga) at different magnifications (Figure 3.12).

Figure 3.12: Electron microscopy used to show substrate structure and homogeneity

3. 5. 7. Surface hydrophobicity

The water contact angle test was used to characterize the surface hydrophobicity of pure PDMS and its composites using a sessile contact angle meter (OCA15E, Germany) (Figure 3.13) with a droplet size of 2 µl deionized water at room temperature. The contact angle was detected after 20 s when the droplet stabilized (Yang et al., 2010).

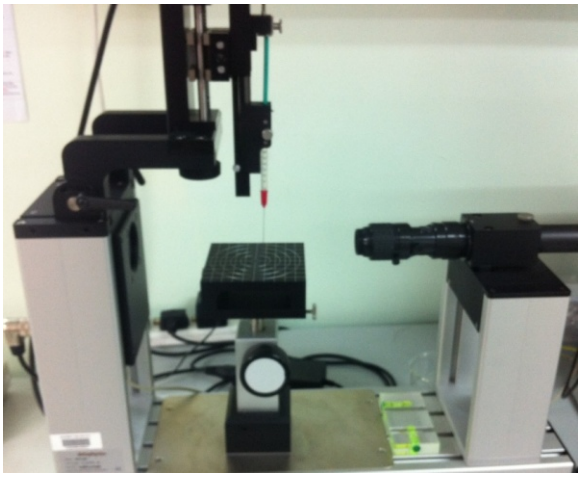

Figure 3.13: Optical contact angle measuring instrument for the detection of surface hydrophobicity

3. 6. Preparation of coating agent used to improve hydrophilicity

Given that the substrates were highly hydrophobic, coating substrates with extra cellular proteins such as fibronectin improved the hydrophilicity.

A stock solution of bovine fibronectin (Gibco, # 33010-018) was prepared by dissolving 1 ml of distilled water in 1 mg of bovine fibronectin to obtain 1 µg/µl concentration. The stock solution was stored in low-binding protein tubes (eppendorf, # C150327G) and kept at −20 °C until use. The desired protein (working solution) was prepared using double distilled water.

Fibronectin concentration was optimized by measuring cell attachment using a DNA measurement assay.

However, three concentrations were considered for optimization, namely, 10, 50, and 100 µg/ml. Five membranes were used for each concentration. Up to 700 µl of the desired concentration (working solution) was added to the substrates, and the mixtures were then incubated overnight. Afterward, extra fibronectin was discarded and substrates were left to dry in a laminar flow hood. A total of 6×10^5 cells suspended in 500 µl of completed medium were seeded on substrates and kept for 24 h in an incubator. The culture medium was discarded after 24 h, and the cells were washed with pre-warmed PBS once. Approximately, 1 ml of digest buffer (contains 0.1576 gr of L-cystein HCL (Sigma, # C1276) and 0.0806 gr of Ethylene diamine tetra acetic acid (EDTA) (Sigma, # E6758) in 100 ml PBS), 3 KU of papain, which acts as a protease was added to substrates with cell. Substrates with digest buffer and papain were kept in an oven for at least 1 h because the temperature needed to activate the protease function of papain is 60 °C. The cells were then centrifuged at 10000 ×*g* for 10 min. The cell supernatant was used for DNA measurement using the Hoechst method.

3. 6. 1. Hoechst method

DNA content should be expected in the samples before the assay starts. Total DNA content can be calculated using the cell number and DNA content of each cell type. Standard concentrations were arranged according to the total DNA content of the samples. Based on the 6×10^5 cell number seeded on the membranes and the fact that each endothelial cell has 6 ± 1.7 pg.cell^{-1} DNA (Hayes et al., 1979), the first standard concentration for our study was 5 µg/ml. Six standards for each measurement were prepared. A serial dilution was prepared by diluting the first standard concentration with phosphate buffer EDTA (PBE). An undiluted standard served as the high standard (5 µg/ml). Based on the dilution serial, the high concentration standard had 5 µg/ml, whereas the less concentrated standard had 0 µg/ml (S0–S6). The other standards that followed the first standard were 2.5, 1.25, 0.625, and 0.3125 µg/ml. Tubes were vortexed thoroughly before each transfer. Up to 40 µl of triplicate standards and samples were placed in a 96-well plate, and then 200 µl of Hoechst was added to each well as dyeing agent. The plate was shaken gently for a few seconds and immediately read with two wavelengths, namely, OD_{530} and OD_{590}, using a microplate reader.

After reading the samples using a microplate reader, the standard curve ($r^2 = 0.99$) was drawn by the microplate reader. Based on the standard curve, sample concentrations were calculated per 1 ml.

3. 6. 2. Standard content and preparation

1) Up to 5 mg calf thymus DNA was dissolved overnight at 37 °C in 5 ml of sterile phosphate, EDTA (PBE), or Tris/EDTA/Nacl (TEN) buffers.
2) For shearing of DNA, calf thymus DNA was pipetted around 40 times with a sterile glass pasteur pipette and filtered through a 0.45 µm syringe filter.

3) For DNA measurement concentration, optical density (OD) 260/OD280 was read to ensure that the DNA is fully dissolved. The ratio 280/260 should be above 1.8.
4) According to the DNA concentration, 10 ml of each diluted standards with following concentrations 1, 2, 4, 6, 8, and 12.5µg/ml in PBE was prepared.
5) Standards were liquated to 100 µl packs and stored at –20 °C until use.

PBE: PBE made from 100 mM sodium phosphate buffer and 10 mM Na_2EDTA

Hoechst solution: Hoechst preparation was carried out in two stages. First, the stock solution was prepared by mixing 2 mg of Hoechst powder (Sigma, # 861405) with 1 mL of ddH2O to obtain 100000 × stock. The working solution was the result of diluting 3 µl of Hoechst stock solution with 30 ml (30000µl) Ten.

Ten contents: 10 mM Tris-HCl, 1 mM EDTA, and 100 mM NaCl. For the preparation of 1 litter of ten with using the components above, 1.21 g of Tris-HCl, 5.84 g of NaCl, and 2 ml of 500 mM of EDTA were dissolved in 800 ml of ddH2O. Moreover, pH was adjusted to 7.5 before adding ddH20 up until1 L. A chance of contamination with DNAase during the preparation is present, so the solution was filtered.

3. 7. Effects of substrate stiffness on cell attachment, proliferation, and morphology in a static environment

Substrates (PDMS, PDMS/5% Al_2O_3, and PDMS/10% Al_2O_3) with 2.5 mm thickness were prepared in 24-well plates, which were washed and sterilized with EO.

Substrates were coated with 100 µg fibronectin. Endothelial cells at passage nine with density of 10^4 cells were seeded on substrates.

3. 7. 1. Resazurin assay

The Resazurin test measured the metabolism rate of BAEC according to protocol (Shum et al., 2008). The Resazurin assay was performed at four time points, namely, 3, 6, 12, and 18 days.

The Resazurin powder (Sigma-Aldrich, # R7017) used in the assay was first dissolved in PBS at a concentration of 140 mg/l to create the stock solution according to the instructions from Sigma Technical Support. The stock solution was then re-diluted with PBS to obtain a 10% working solution.

For the detection of cell metabolism rate using the assay, the culture medium was removed; the cells were gently washed with pre-warmed PBS, and then incubated at 37 °C for 4 h with 1.5 ml of 10% Resazurin working solution at each time point. Triplicates of 100 µl of Resazurin working solution incubated with cells grown on different elastomer/composites were obtained for absorbance measurements at λ_1 = 570 nm and λ_2 = 600 nm by FLUOstar OPTIMA microplate reader (BMG LABTECH) (Shum et al., 2008). The percentage reduction of Resazurin was evaluated to determine the metabolism and proliferation rate of endothelial cells using the following equation (1) (Gang et al., 2004).

$$\frac{(\varepsilon_{OX})\lambda_2 A\lambda_1 - (\varepsilon_{OX})\lambda_1 A\lambda_2}{(\varepsilon_{RED})\lambda_1 A^o\lambda_2 - (\varepsilon_{RED})\lambda_2 A^o\lambda_1} \times 100 \qquad (1)$$

Where:
ε_{OX} = molar extinction coefficient of AlamarBlue® oxidized form (BLUE)
ε_{RED} = molar extinction coefficient of AlamarBlue® reduced form (RED)
A = absorbance of test wells
$A°$ = absorbance of negative growth control well
$\lambda 1$ = 570nm
$\lambda 2$ = 600nm

3. 7. 2. Cell morphology

BAEC were seeded on pure PDMS, PDMS/5% Al_2O_3 composite and PDMS/10% Al_2O_3 composite for 4 d, and then stained with Dil-Ac-LDL, a specific marker for endothelial cells. After 4 d of culturing, the medium was discarded from the endothelial cells. The uptake of Dil-Ac-LDL was examined after 4 h of incubation of endothelial cells with 10 μg of Dil dye in 1 ml of endothelial cell complete medium (Ando et al., 1999; Nicosia et al., 1994b). The stained cells were observed using a confocal microscope

3. 8. Effect of membrane stiffness on eNOS phosphorylation and NO production in a dynamic environment

3. 8. 1. Tensile jig

A tensile jig was developed to provide a dynamic environment for this study. A specially designed test jig, as illustrated in figure 3.14, was used to apply tensile loading on BAEC seeded on substrates with different stiffness and investigate the influence of tensile loading on BAEC. The tensile jig, machined from stainless steel, included one small metal mold for substrate fitting and a big metal mold that connects the substrates to the power through wire. Transferring the force to the mold for stretching was the main role of the wire. One ruler was used to check the movement of membranes (Figure 3.14).

Figure 3.14: Parts of tensile-jig inside the incubator1) Screw for fixation of membrane position 2) Screw for transferring power to membranes 3) Screws to keep the relaxation position of membranes 4) Wire that connects power to the mold 5) Power 6) controls 7) Membranes fitted in the small metal mold.

3. 8. 2. Cell seeding on membranes

Up to 6×10^5 cells suspended in 1 ml complete medium were seeded on each substrate (five substrates were used as sample and five substrates were considered as control) coated with 100 µg fibronectin and kept inside an incubator for 2 d in a static environment. After 2 d, substrates were visualized under the microscope to check cell

attachment and replace the culture medium with fresh medium. The substrates were incubated for one more day in incubator.

At the time of tensile loading, the medium of membranes was discarded and membranes were placed in the small metal mold of tensile jig. Fresh and serum free medium was then added to the membranes and placed in an incubator. Five membranes were stretched by 10% with 1 Hz (60cycle/min) frequency which modeled physiologically relevant levels of stretch (Awolesi et al., 1995) (Figure 3.15). Control membranes were kept with the membrane samples, but in a static environment.

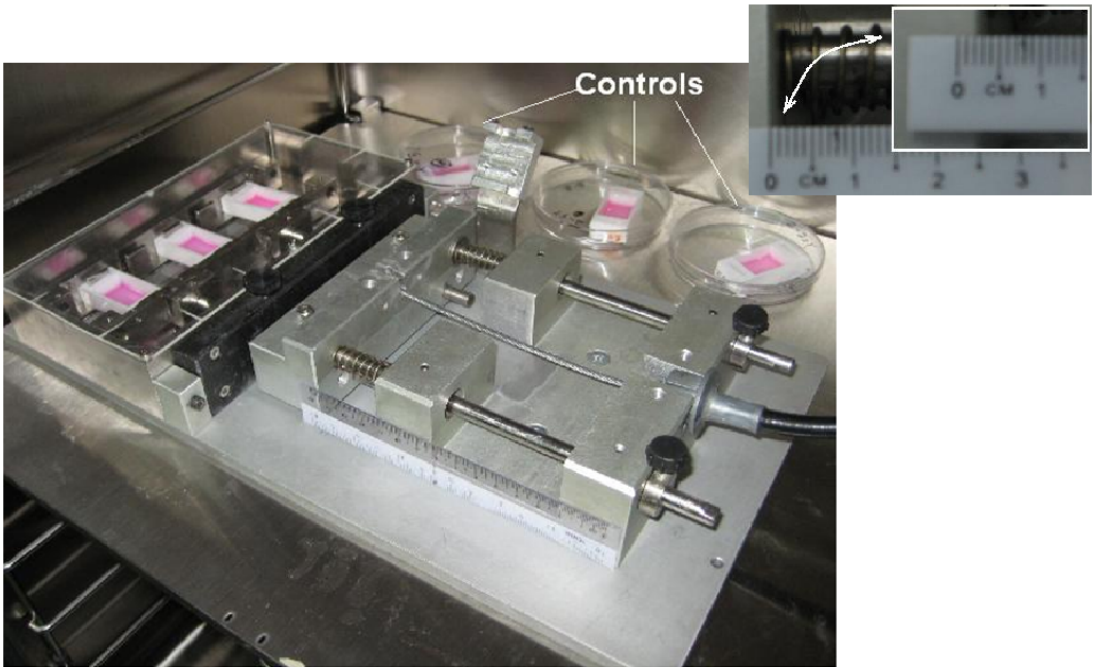

Figure 3.15: Fitting of substrates to the bioreactor and applying 10% strain with 1 Hz frequency. Substrates considered as control were kept in a static environment.

3. 8. 3. Effect of loading time on p-eNOS intensity and applying optimized time on stiff substrates

According to the literature, 2, 3, and 6 h are the possible time points in which eNOS phosphorylation reaches peak activity (Chen et al., 2008; Hu et al., 2013). All three time durations were applied on 5 PDMS substrates and 5 more PDMS substrates were used as controls. Each time point was repeated for three trials.

After finishing the time durations, the culture medium of substrates were collected in micro centrifuge tubes, which were labeled properly based on loading time, stretching date, and substrate type. Samples were immediately kept at –80 °C for NO measurement.

The substrates were washed with cold PBS immediately to remove residual media, and then removed from the metal part and placed on ice. Afterward, 30 µl of lysate buffer (cell signalling, #9803) was added to each membrane. Substrates were kept on ice for 5 min, and the cells were scraped and collected in micro-centrifuge tubes. Cell lysate was kept for 5 min and sonicated briefly with an ultrasonic sonicator for 5 s three times. The cell lysate was then centrifuged for 10 min at 14000×*g* and 4 °C. The supernatant was kept in low bind protein tubes at –80 °C.

Applying tensile loading on stiff substrates: Based on the results achieved from tensile loading at different time points, 3 h stretch with 1 Hz frequency was applied on stiff substrates (PDMS/5% Al_2O_3 and PDMS/10% Al_2O_3).

3. 8. 4. Bradford protein assay

Total protein should be measured to apply the same total protein concentration for target protein measurement. The common method used in protein measurement is the Bradford protein assay, a simple and accurate procedure used for protein detection. The basis of the Bradford protein assay is the binding of the coomassie brilliant blue G-250 dye to proteins, which convert red color into blue. Purified BSA was used as standard. The quick start Bradford protein assay kit (Bio-Rad, #500-0205) was used in this study. Standard concentrations were considered based on cell numbers and the protein content of each endothelial cell. Each endothelial cell has 307±71 $pg.cell^{-1}$. The cell number was roughly 576×10^3 cells (based on cell attachment optimization in respond to fibronectin concentration). Therefore, total

protein concentration was calculated around 172.8 µg. The serial concentration of standards was started from 2 mg/ml, which served as the high concentration standard and continued with 1.5, 1, 0.75, 0.5, 0.25, and 0.125 mg/ml as lower concentration standards and 0 mg/ml as blank. The area covered by standards can cover the total protein concentration of our samples; hence, the samples were not diluted. According to the microplate assay of standard protocol, 5 µl of samples and standards were added to wells, followed by the addition of 250 µl of dye. The microplate was incubated for at least 15 min at room temperature and shaken gently during the incubation period. The absorbance of the plate was read at wavelength 595 nm by the FLUOstar OPTIMA microplate reader (BMG LabTech).

3. 8. 5. p-eNOS intensity by ELISA kit

PathScan phspho-eNOS sandwich ELISA kit (Cell Signaling, #7980) was used to determine the endogenous levels of p-eNOS as Ser^{1177}. Based on the instructions for cell signaling technical support, samples were diluted 1:1 with sample diluents because proteins were extracted using the instructions for cell digestion. Regarding the total protein concentration measured by the Bradford assay, 100 µg of protein from each sample was diluted1:1 with sample diluents and applied to each well in duplicate. The plate was sealed properly and incubated overnight at 4 °C to obtain the best detection of target protein. After incubation time, the plate contents were discarded and plate was washed with 1× ELISA wash buffer. During the washing stage, the residual solution was removed from each well. Following extensive washing, 100 µl of eNOS mouse monoclonal detection antibody was added (this antibody detected the captured p-eNOS protein). Plate was sealed and incubated for 1 h at 37 °C. The incubation stage was followed by well washing for four times. In

the next stage, 100 µl of horseradish peroxidise (HRP)-linked secondary antibody was added to the wells and incubated at 37 °C for 30 min. The HRP-linked streptavidin recognized the bound detection antibody. Washing procedure was repeated after this stage for four times. Afterward, 100 µl of HRP substrate (TMB) was added and incubated at 37 ºC for 10 min. TMB was used to develop color. In the last stage, 100 µl of stop solution was added to each well to stop the reaction. The mixture was then shaken gently for a few seconds. The underside of the wells was wiped with a lint-free tissue and absorbance was read at wavelength 450 nm by FLUOstar OPTIMA (BMG LABTECH) micro plate reader.

3. 8. 6. NO concentration by ELISA kit

Endothelial cells can produce NO as a result of eNOS phosphorylation. However, NO has a short half-life, and disappears after a few seconds, and is converted to nitrate (NO_3^-) and nitrite (NO_2^-) (Hakim et al., 1996; Lundberg et al., 2008). The used ELISA kit (Cusavio, #CSB-E15884B) has the ability to measure nitrite released to the culture medium. The ELISA kit contained a nitrite standard with 20 ng concentration and was freeze-dried. Therefore, standards were prepared during the first stage. The standard was dissolved at 1 ml of sample diluents to reach 20 ng/ml concentrations and was diluted in a serial. The standard was diluted two folds. The highest concentrated standard was 20 ng/ml followed by 10, 5, 2.5, 1.25, 0.625, 0.312, and 0 ng/ml. According to the instruction of the Cusabio technical support, samples were diluted 1000 times. Up to 50 µl of samples and standards were added to wells twice, and then 50 µl of HRP- conjugate was added to the wells immediately. Two wells were left as blank. The plate was mixed properly through shaking for 60 s, and then sealed. The plate was incubated for 40 min at 37 °C. After

incubation, the wells were washed thoroughly for four times. Up to 200 µl of wash buffer was used for every wash. In each stage, the complete removal was done by striking the plate with clean tissue. In the next stage, 90 µl of TMB substrate was added to each well to develop HRP. Incubation time was 20 min at 37 °C. TMB was light sensitive and was protected from light**.**

In the last stage, 50 µl of stop solution was added to the TMB substrate to the stop reaction. The plate was shaken gently for a few seconds and absorbance was read at 450 nm.

The standard curve was constructed by plotting the mean standard absorbance on the x-axis against the concentration on the y-axis. NO concentration of the sample was determined by standard curve.

3. 9. Statistical analysis

All statistical analyses were conducted using SPSS for windows (SPSS Inc, Chicago, USA, # Release 21). One way ANOVA was used to evaluate the significant differences between substrate roughness value and substrate hydrophilicity with pure PDMS and composites in AFM and surface hydrophobicity, respectively. Two-way ANOVA was used to detect the significant difference between endothelial cell reduction percentages with substrate stiffness at different time points. One-way ANOVA was conducted to detect the significant relationship between eNOS phosphorylation and NO concentration with substrate stiffness. The critical level for consideration of the null hypothesis was a P_{value} less than 5%, two-tailed.

CHAPTER 4

RESULTS

4. 1. Endothelial cell isolation and characterization

In the samples that underwent the isolation process with the use of filter paper, more than 98% of the cells were identified as endothelial cells according to cell morphology visualized by light microscopy (Eclipse TS100). Figure 4.1 shows the gradual growth process of endothelial cells during days 1, 3, 6, 9, and 12. At day 12, cells reach the confluent cell layer.

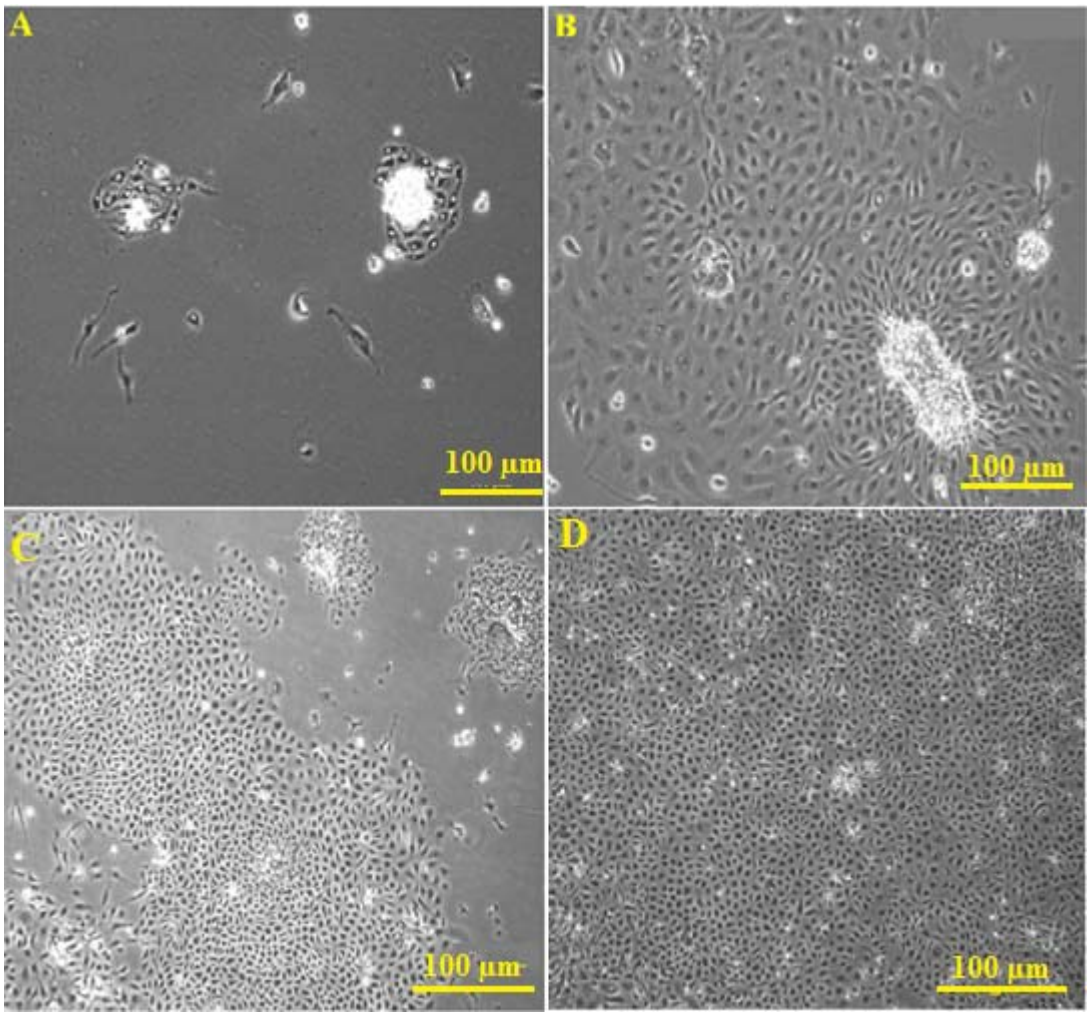

Figure 4.1: BAEC isolation using filter paper in enzymatic digestion method A) First day after isolation B) 6th day after isolation C) 9th day after isolation D) 12th day after isolation

While the endothelial cell isolated from the samples floated in enzyme solution without filter paper had high contamination with other kind of the cells. Figure 4.2 shows cell growth and minimal fibroblast cell population at day 3 (panel A). Fibroblast population increased in day 6 (panel B) and occupied half of the total cell population by day 9 (panel C), indicating that fibroblast cells grew faster than endothelial cells. Therefore, fibroblast contamination became more obvious as time passed.

Endothelial cells are polygonal cobblestone. They cover the inner surface (tunica intimae) of blood vessel and are in direct contact of blood. Endothelial cells after the isolation are like the bright particles which are endothelial cell clumps. A few days after cell isolation endothelial cells sprouted out.

However, fibroblast cells are elongated and spindle like. They are morphologically heterogeneous with diverse appearances depending on their location and activity. These cells are normally found in the tunica adventitia (outer layer) of blood vessel.

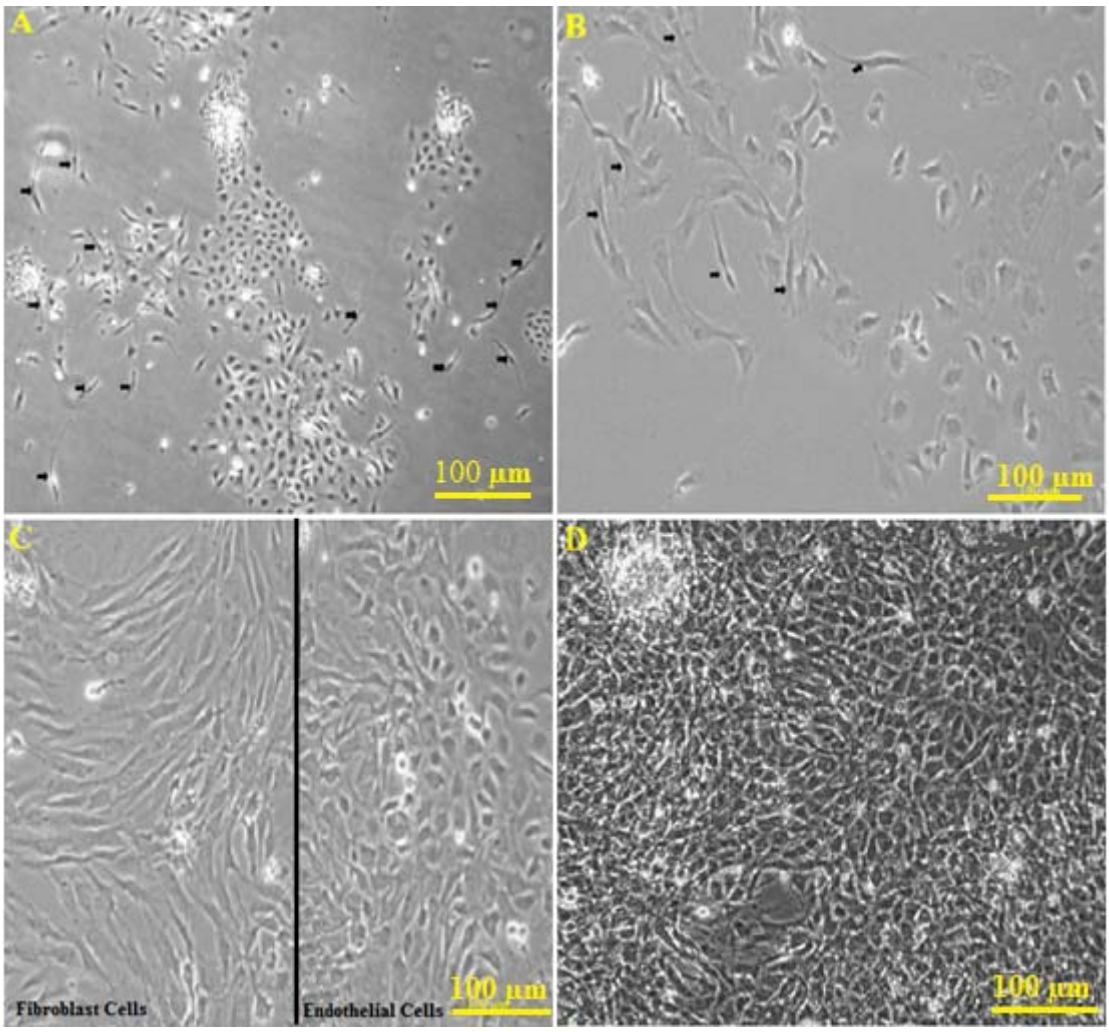

Figure 4.2: The vessel pieces were immersed in enzyme solution without wrapping in filter paper and incubated for 30 min, and then cultured in T25 Flasks A) 3rd day after isolation B) 6th day after isolation C) 9th day after isolation D) 12th day after isolation

➡ The arrows show the fibroblast cells

4. 1. 1. CD-31

CD-31 was used as a surface marker to evaluate the purity of isolated endothelial cells through flow cytometry. Unstained cells were the negative control located in Q3 quarter (Figure 4.3-A) in which cells did not show any signal for CD-31 marker. The probability of obtaining false positive results was eliminated by using an isotype control (Figure 4.3-B), whereas cells with positive results for CD-31 alone

were located in the Q4 quarter (Figure 4.3-C). Histogram of cells stained with Mouse Monoclonal antibody to CD-31 is shown in Figure 4.4.

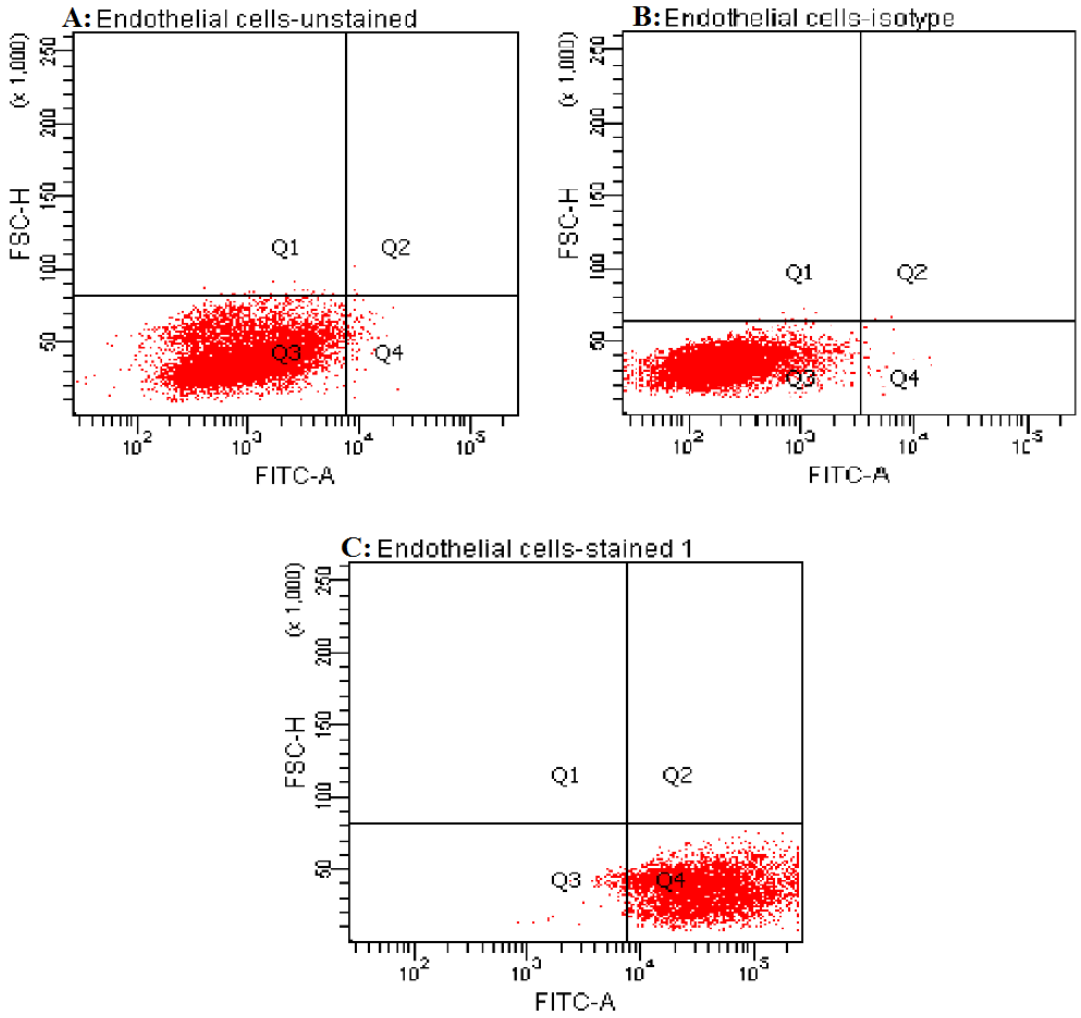

Figure 4.3: Flow Cytometry dot plots of isolated BAEC from Bovine Aorta

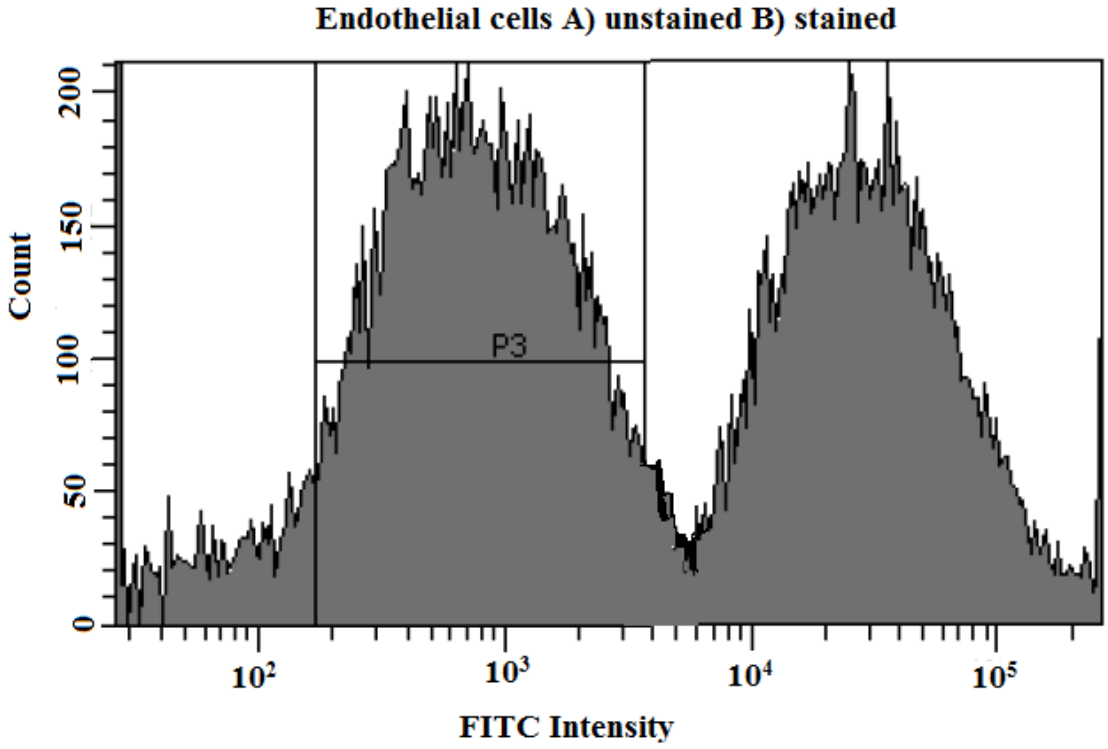

Figure 4.4: Histogram related to samples treated with Mouse Monoclonal antibody to CD31

4. 1. 2. Factor VIII and Dil-Ac-LDL

Cells were characterized by cytoplasmic markers, such as factor VIII and Dil-Ac-LDL. Our results revealed that over 95% of the cells expressed factor VIII (Figure 4.5-A and B). This proportion is achieved by judging of the proportion of cell nuclei stained with 40-6-diamino-2-phenylindole as dapi compared with that of the cells stained with factor VIII. Endothelial cells had the ability to uptake Dil-Ac-LDL (Figure 4.5-C and D).

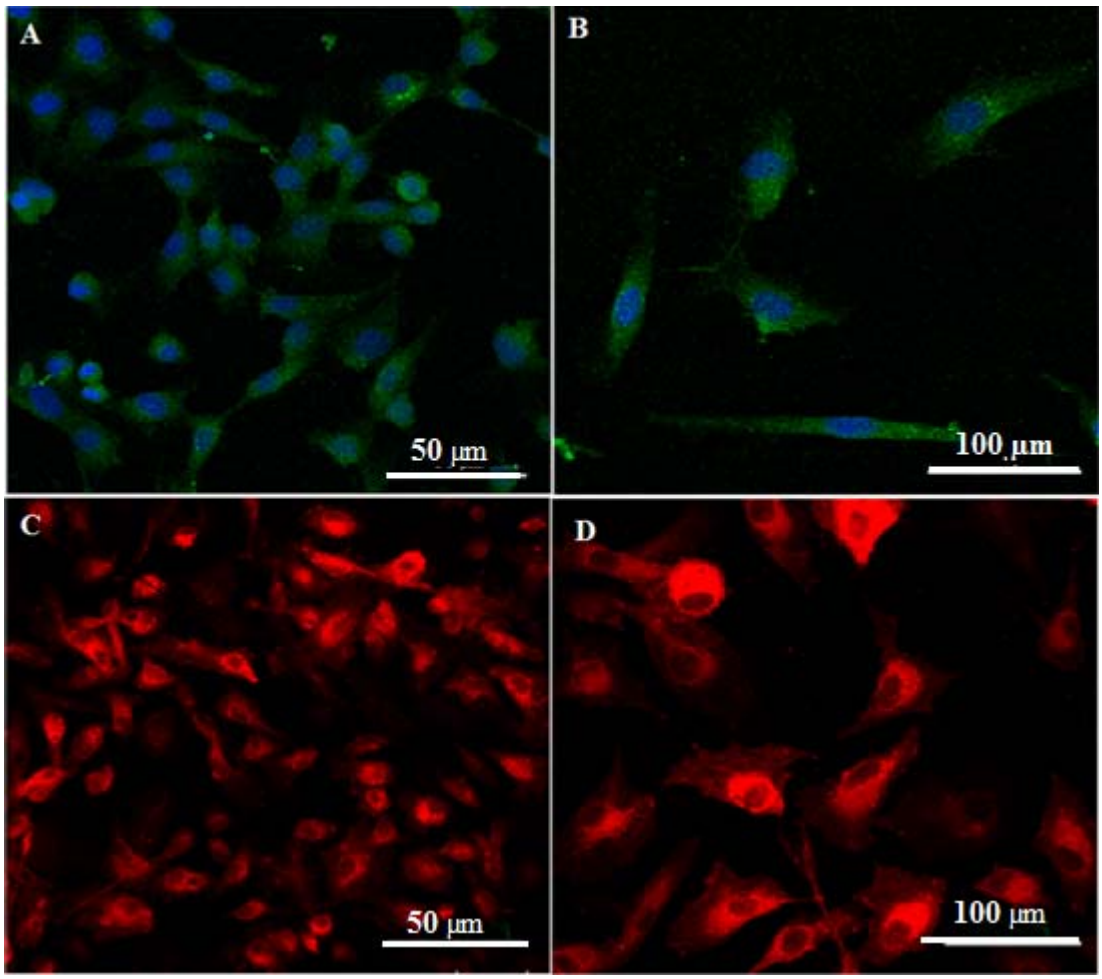

Figure 4.5: BAEC immunostaining by DiI-Ac-LDL and Von Willebrand factor
A, B) Endothelial cells labeled by rabbit anti-human factor VIII as primary antibody and donkey anti-rabbit IgG H&L FITC as the secondary antibody C, D) Uptake of DiI-Ac-LDL by endothelial cells

4. 1. 3. Angiogenesis

Blood vessel formation happens in multiple stages, such as endothelial cell proliferation, directional cell migration, and appropriate cell connections (Eilken & Adams, 2010). The standard test for detection of this behavior in endothelial cells is placing cells in 3 dimension environment. Cells proliferate, migrate and arrange in the shape of blood vessels. Then, endothelial cells start to digest fibrin for making tube. Therefore, cells were characterized through angiogenesis behavior in this study. Figure 4.6 shows the gradual process of angiogenesis for endothelial cells seeded on fibrin construct over 7 d.

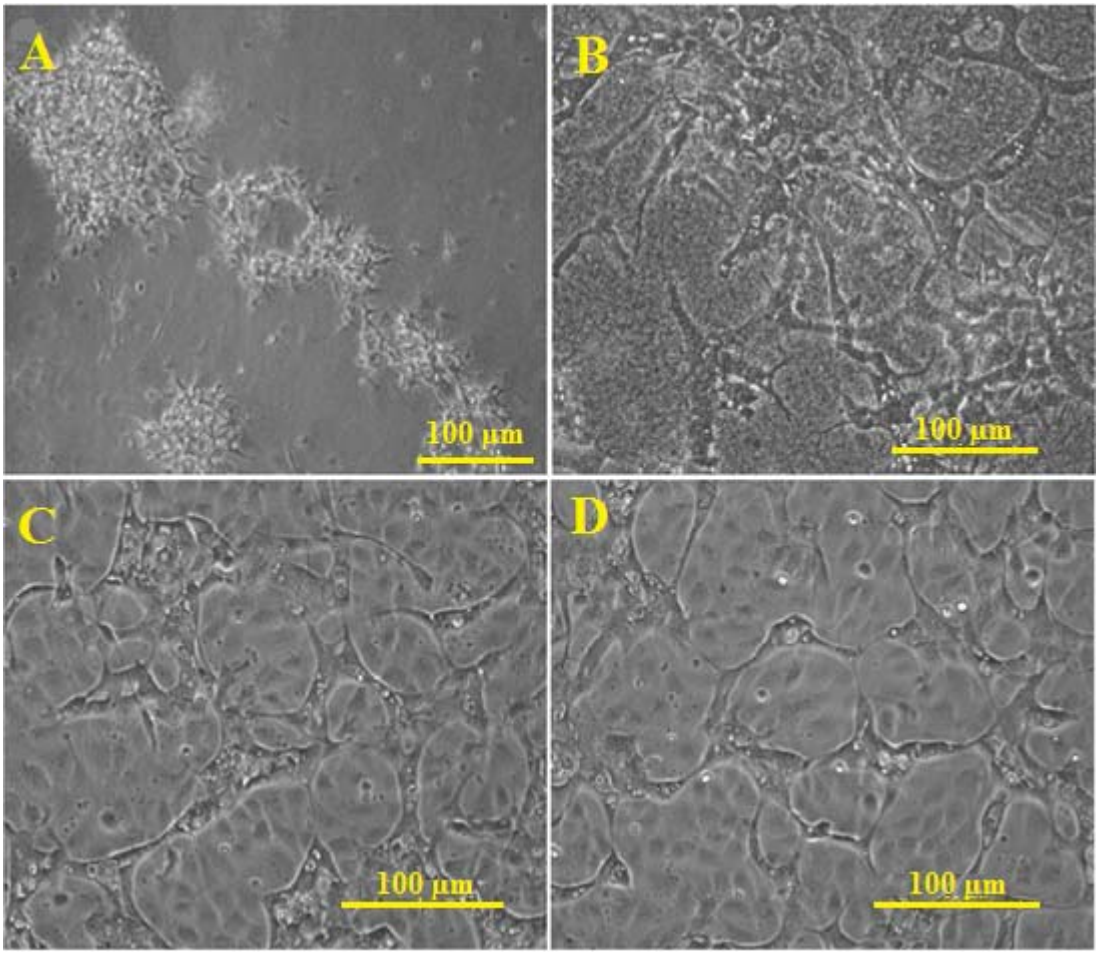

Figure 4.6: Formation of blood vessel-like structure by endothelial cells in fibrin construct A) First day B) 3th day C) 5th day, and D) 7th day

4. 2. Membrane characterization

4. 2. 1. Stiffness measurement

To understand the contribution of substrate stiffness on endothelial cell behavior, PDMS elastomer and its composites with 5%, and 10% Al_2O_3 were subjected to mechanical tests. Table 1 shows the results of the tensile test. Young's modulus was elevated when Al_2O_3 was added to PDMS. The highest obtained value for the Young's modulus was 1.08 MPa for PDMS/10% Al_2O_3 composite, whereas the lowest value belonged to pure PDMS with 0.32 MPa. The stress–strain behavior of the composites was compared with pure PDMS elastomer (Figure 4.7). Given that

the Young's modulus is directly proportional to stiffness, stiffness values were measured in this study following the trend of Young's modulus. Substrate stiffness was measured by using the following equation (2).

$$k = \frac{AE}{L} \tag{2}$$

Where, k is stiffness, A is area, E is Young's modulus and L is actual gauge length. Maximum stress and maximum strain or elongation (%) were also considered as rupture strength and rupture strain (%), respectively, for all specimens, including pure PDMS and its composites. The results are shown in the Figure 4.7 and Table 4.1.

Table 4.1: Substrate contents, Young's modulus, stiffness variation, maximum stress, maximum strain, maximum elongation in PDMS membrane and PDMS/Al_2O_3 composites. The results of Young's modulus and stiffness show that PDMS has the less stiffness and highest stiffness is for PDMS/10% Al_2O_3. Because failure occurred at maximum stress and maximum strain or elongation (%), these were considered as rupture strength and rupture strain (%), respectively, for all the specimens, including pure PDMS and its composites.

Sample Code	PDMS (wt %)	Al_2O_3 (wt %)	Young's modulus (MPa)	Stiffness	Maximum stress (MPa)	Maximum Strain (%)	Maximum Elongation (mm)
Pure PDMS	100	0	0.331±0.006	0.031	0.567	219.25	54.788
PDMS/5% Al_2O_3	95	5	0.592±0.04	0.044	1.890	278.75	69.675
PDMS/10% Al_2O_3	90	10	1.076±0.01	0.104	2.545	226.99	56.748

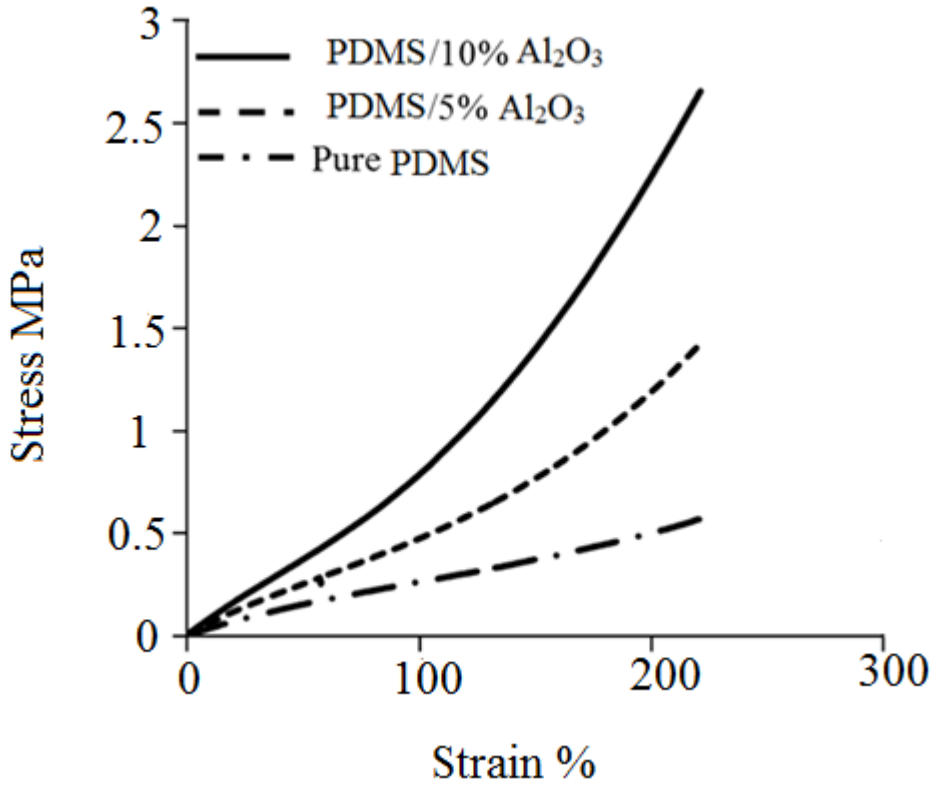

Figure 4.7: Stress vs. strain behavior of PDMS/ Al_2O_3 composites compared to the pure PDMS elastomer. PDMS/10% Al2O3 has the highest stiffness based on the pure PDMS, while the lowest stiffness is for pure PDMS.

Our results illustrated that ceramic Al_2O_3 particles have a major function in the PDMS matrix for the improvement of the stiffness. The digital images in Figure 4.8 depicted the behavior of all elastomeric specimens and indicated the change in flexibility of the composites under the same pressure exerted by normal adhesive tape with increasing Al_2O_3 concentration.

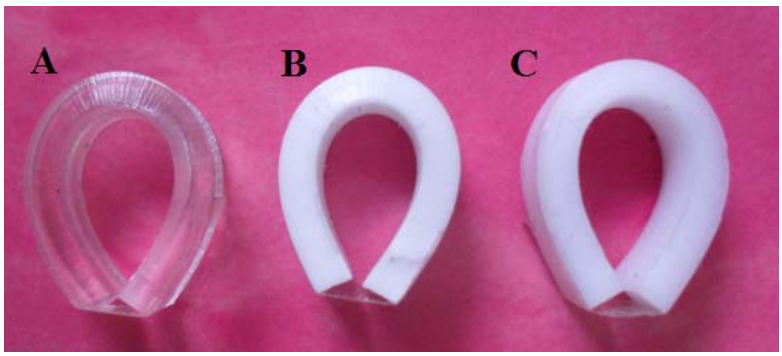

Figure 4.8: Flexibility of PDMS and its composites A) Pure PDMS, B) PDMS/5% Al_2O_3, and C) PDMS/10% Al_2O_3. The quality of bending easily without breaking is called flexibility. Adding Al_2O_3 to PDMS did not affect the substrate flexibility significantly; therefore, substrates are proper for researches dynamic environment which is necessary for cardiovascular studies.

4. 2. 2. XRD

Figure 4.9 represents the XRD pattern of pure PDMS elastomer and its composites with different Al_2O_3 percentages. The crystalline peaks of Al_2O_3 α-phase were compared with the standard JCPDS-ICDD file no. 46-1212 and JCPDS file no. 42-1468, which were identified from pure alumina (Boumaza et al., 2009; Feret et al., 2000; Su & Li, 2011). The broad amorphous peak of the composites near 2θ =11.5° was an indication of PDMS elastomer, similar to what was found in the XRD pattern of pure PDMS. The XRD patterns of the composites show the crystalline peaks of the Al_2O_3 α-phase (JCPDS-ICDD file no. 46-1212) and the broad amorphous peak of inorganic PDMS elastomer near 2θ =11.5°.The intensity of all crystalline peaks of α-Al_2O_3 was elevated with increasing Al_2O_3-concentration in the composites.

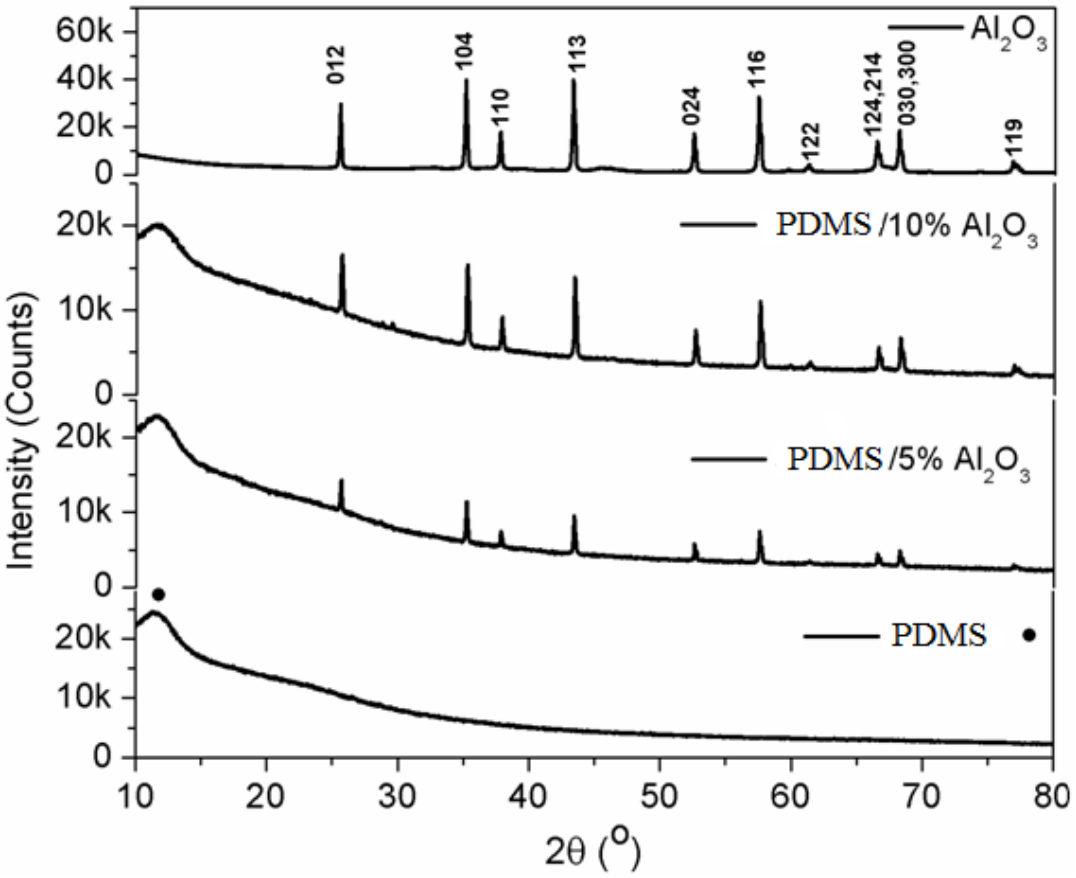

Figure 4.9: XRD patterns of pure PDMS, PDMS/5% Al_2O_3, PDMS/10% Al_2O_3, and pure Al_2O_3 composites.

4. 2. 3. FTIR

Figure 4.10 shows the transmittance FTIR spectra of pure PDMS, pure Al_2O_3, and PDMS/Al_2O_3 composites. All FTIR peaks for pure PDMS elastomer at 601 cm^{-1} corresponding to Si-C stretching (Jantová et al., 2011), 699 cm^{-1} corresponding to Si-O-Si stretching, 787 and 843 cm^{-1} corresponding to Si-CH_3 stretching, 1009 and 1055 cm^{-1} corresponding to Si-O-Si stretching, 1258 cm^{-1} corresponding to Si-CH_3 rocking, 1412 cm^{-1} corresponding to Si-CH=CH_2, and 2963 cm^{-1} corresponding to C-H stretching from CH_3 were all present in both composites (Awolesi et al., 1995; Jantová et al., 2011; Lin & Hwang, 1996; Shivakumar et al., 2005).

In the Al_2O_3 spectra, the FTIR peaks at 570 and 640 cm^{-1} correspond to the translational peak of Al-O and bending mode of O-Al-O, respectively (Boumaza et al., 2009; Katamreddy et al., 2006; Kloprogge et al., 2004).

The two transmittance peaks near 570 and 640 cm^{-1} from the Al_2O_3 were found in both composites (5% and 10% Al_2O_3) with slight deviations in peak width and position (Figure 4.11). A new bond Si-O-Al in the composites spectra is the result of PDMS and Al_2O_3 interaction. The peaks showed a downward trend and increase in width with increasing Al_2O_3 concentration in the composites. All FTIR peaks for different chemical bands present with pure and composite materials with their peak positions are illustrated in Table 4.2.

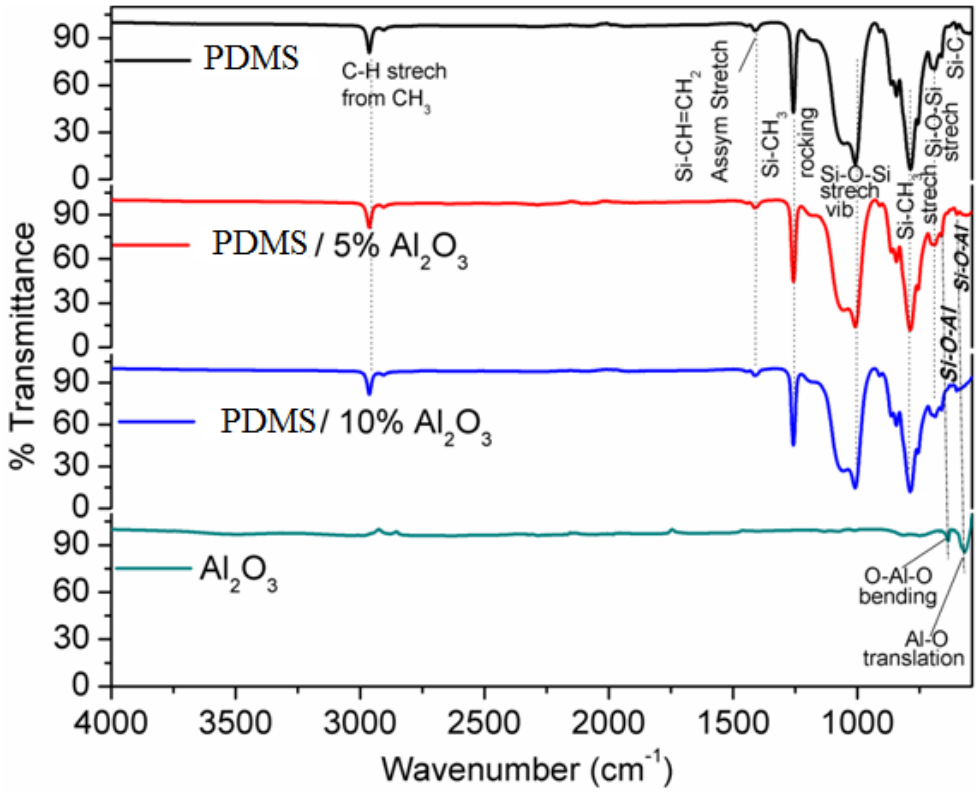

Figure 4.10: FTIR spectra of pure PDMS, PDMS/5% Al_2O_3, and PDMS/10% Al_2O_3 composites

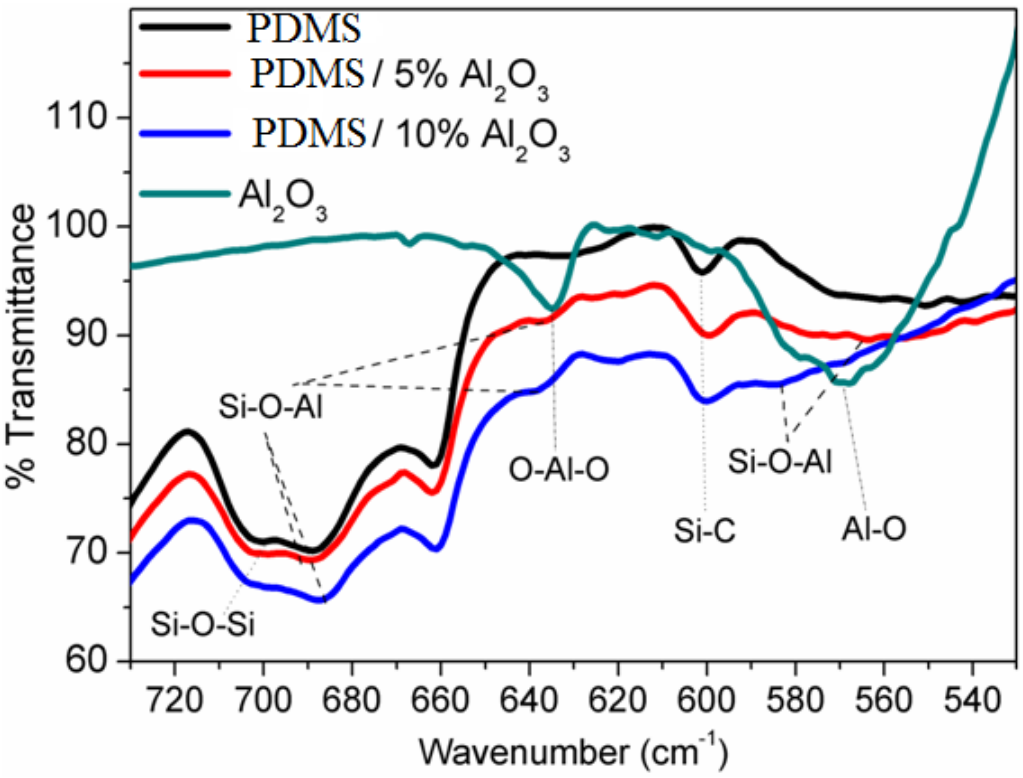

Figure 4.11: Magnified part of FTIR spectra of pure PDMS, pure Al_2O_3, and their composites- mentioning a new Si-O-Al bond formation in the composites.

Table 4.2: List of FTIR bands for pure PDMS, PDMS/5% Al_2O_3, PDMS/10% Al_2O_3, and pure Al_2O_3

Type of FTIR peak bands	Pure PDMS	PDMS /5%Al_2O_3	PDMS /10%Al_2O_3	Pure Al_2O_3	Reference
	Wave number (cm^{-1})				
Al-O translation	-	-	-	570	(Shum et al., 2008; Su & Li, 2011)
Si-O-Al	-	564	584	-	(Shivakumar et al., 2005; Su & Li, 2011)
Si-C stretching	601	600	599	-	(Res et al., 1986)
O–Al–O bending	-	638	639	640	(Awolesi et al., 1995; Shivakumar et al., 2005; Shum et al., 2008)
Si-O-Si stretching* or Si-O-Al	699*	690	688	-	(Feret et al., 2000; Su & Li, 2011)
Si-CH_3 stretching	787, 843	787, 843	787, 843	-	(Takeda et al., 2006)
Si-O-Si stretching vibration	1009, 1055	1008, 1056	1009, 1056	-	(Feret et al., 2000; Res et al., 1986)
Si-CH_3 rocking	1258	1257	1258	-	(Yeung et al., 2005)
Si-CH=CH_2	1412	1412	1412	-	(Ando et al., 1999)
C-H stretching from CH_3	2963	2963	2963	-	(Su & Li, 2011)

4. 2. 4. AFM

The 3-D images of the AFM study showed the surface morphology of substrates. The surface uniformity and morphology of the thin film produced on the substrate surface was verified for composites and compared with pure PDMS substrate using the 3D images (Figure 4.12). The surfaces of pure PDMS and both composites were almost similar. According to the results of the one-way ANOVA conducted to determine the effect of Al_2O_3 addition on roughness values, there is no significant difference between pure PDMS and composites with regard to Ra values of the substrate surfaces (P_{Value}= 0.118), our results revealed that surface roughness is similar for all substrates.

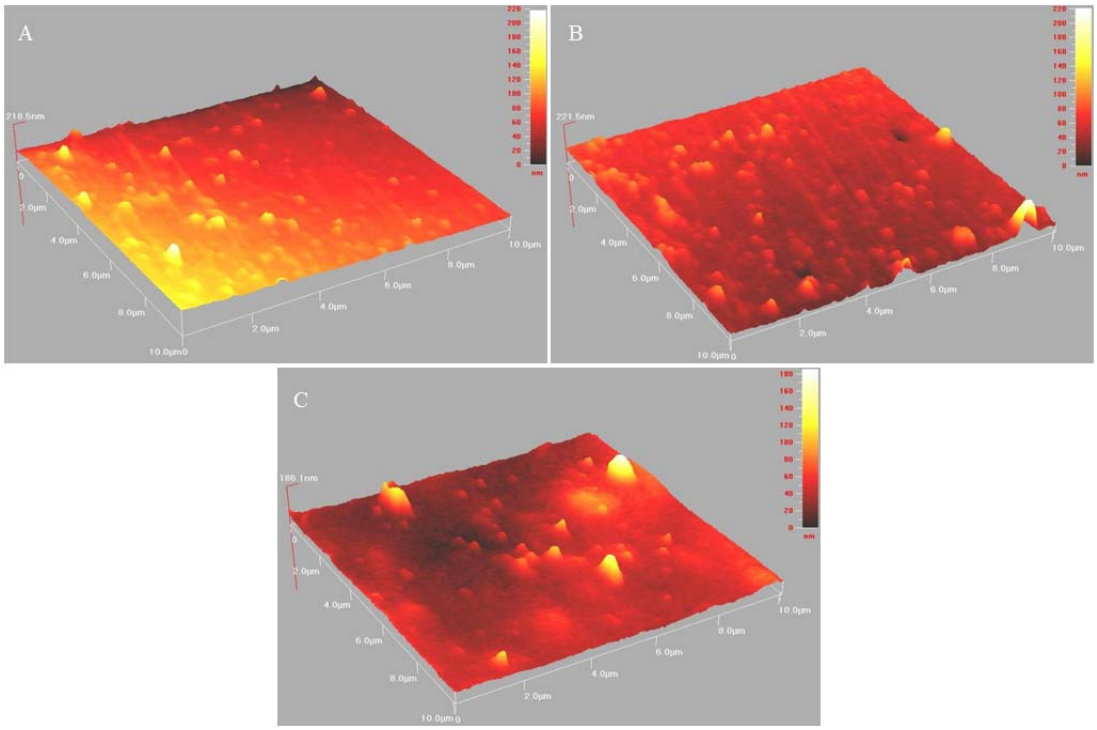

Figure 4.12: 3-D AFM images of A) Pure PDMS, B) PDMS/5% Al_2O_3 substrate surfaces E) PDMS/10% Al_2O_3 composites

4. 2. 5. FESEM

FESEM was used to investigate the matrix–particle bonding in the composites. FESEM verified the shape and homogenous distribution of Al_2O_3 particles in the PDMS matrix after the samples were cross-sectioned. The morphology of Al_2O_3 particles and PDMS matrix was clearly revealed in the FESEM micrographs (Figure 4.13). The FESEM images showed the uniform distribution of the tiny Al_2O_3 particles, which are bonded with the PDMS-matrix.

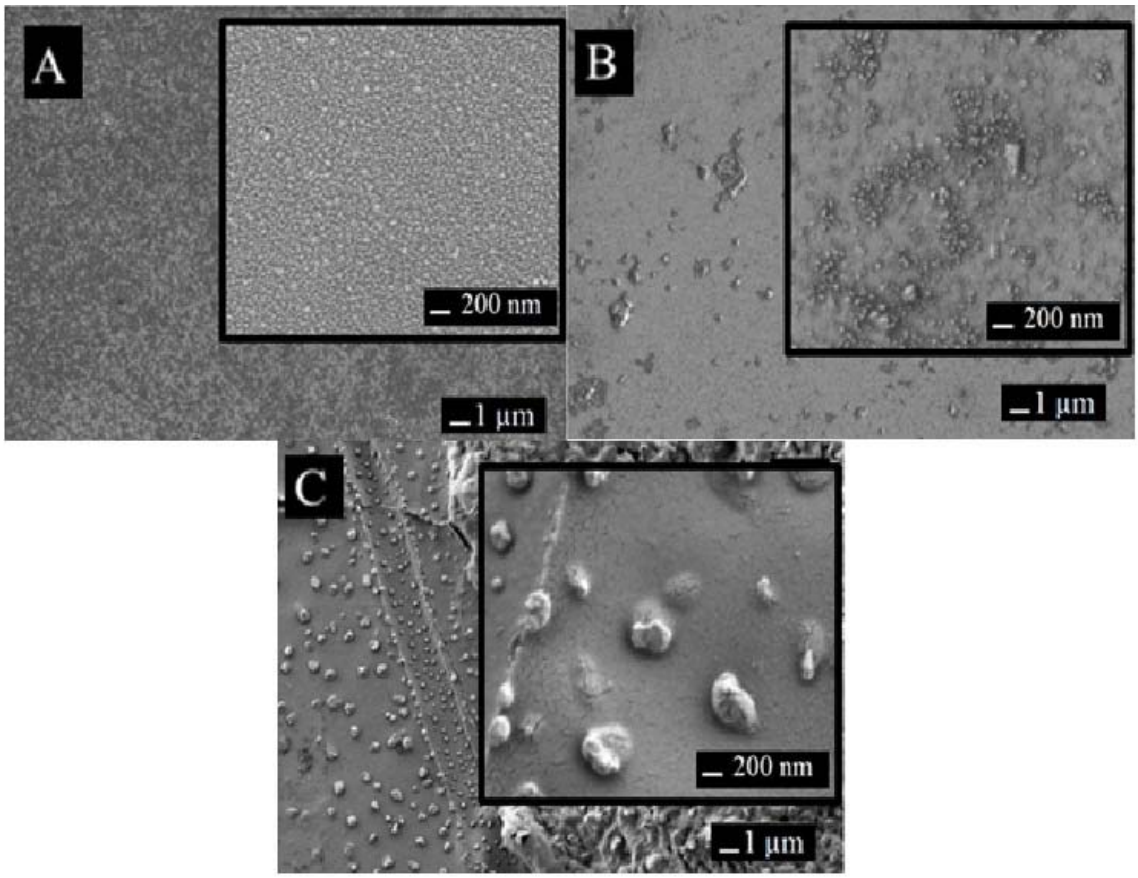

Figure 4.13: FESEM surface morphology A) Pure PDMS B) PDMS/5% Al_2O_3 and C) PDMS/10% Al_2O_3 composites

4. 2. 6. Substrate hydrophobicity

Surface hydrophobicity was assessed by measuring water contact angle on the surface. A lower contact reflected better hydrophilic surface properties. The water contact angles were 114.7 ± 2°, 112.3 ± 4°, 107.2 ± 3° for PDMS, PDMS/5% Al_2O_3, and PDMS/10% Al_2O_3 composite, respectively (Figure 4.14).

Statistical analysis on surface hydrophobicity showed no significant difference between substrates, but the addition of Al_2O_3 is expected to enhance surface hydrophilicity (P_{value} = 0.4).

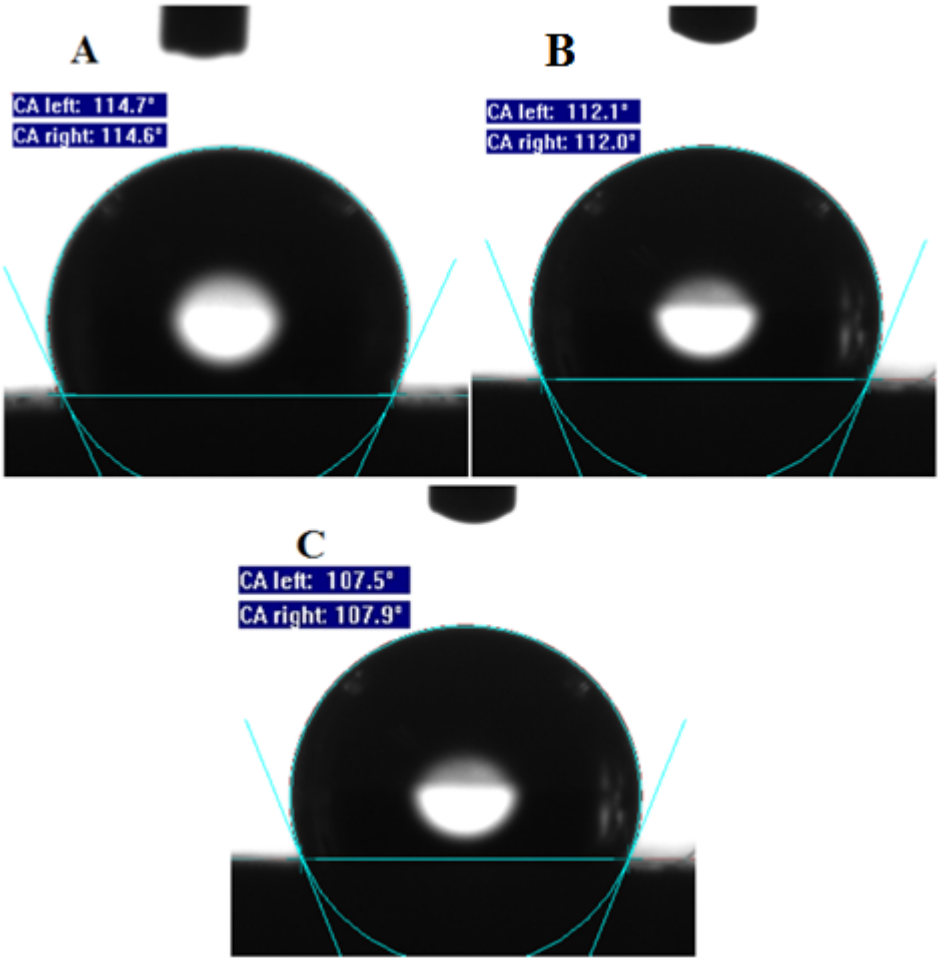

Figure 4.14: Hydrophobic properties of PDMS and its composites A) Pure PDMS B) PDMS/5% Al_2O_3 C) PDMS/10% Al_2O_3

4. 3. Optimized concentration of fibronectin

Results obtained using the Hoechst method revealed that approximately 96% of the cells were attached on PDMS substrates coated with 100 µg/ml of fibronectin. However, 10µg and 50 µg of fibronectin increased cell attachment to 32% and 71%, respectively (Figure 4.15). Thus, the 100 µg concentration of fibronectin, with significant result, was selected for substrate coating in next stages of the study.

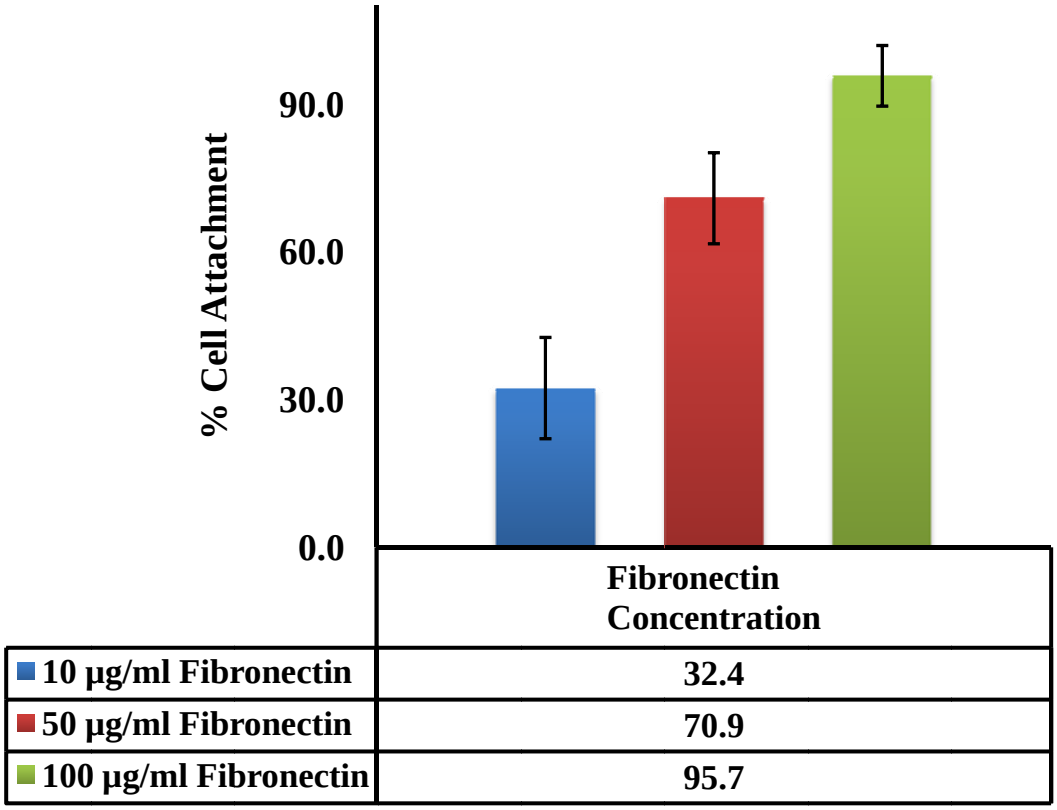

Figure 4.15: Measurement of cell attachment on membranes coated with 10, 50, and 100 µg/ml of fibronectin using the Hoechst dye method. Based on this result, 100 µg/ml of fibronectin increased cell attachment significantly.

4. 4. Evaluation of endothelial cell proliferation and morphology in response to substrate stiffness in static environment

The biological performance of the composites was evaluated through in vitro adhesion and proliferation of endothelial cells. Figure 4.16 shows the proliferation behavior of the endothelial cells on pure PDMS and PDMS/Al_2O_3 composites at 3, 6,

12, and 18 d after cell culture. The attachment and proliferation of the endothelial cells increased as the substrate stiffness increased. The percentage reduction for the PDMS/10% Al_2O_3 composite was the highest in the Resazurin assay, whereas pure PDMS had the lowest percentage reduction in all time points. Cell proliferation significantly improved during the experiment so as to the highest cell growth occurred at day 18 for all composites (Figure 4.16).

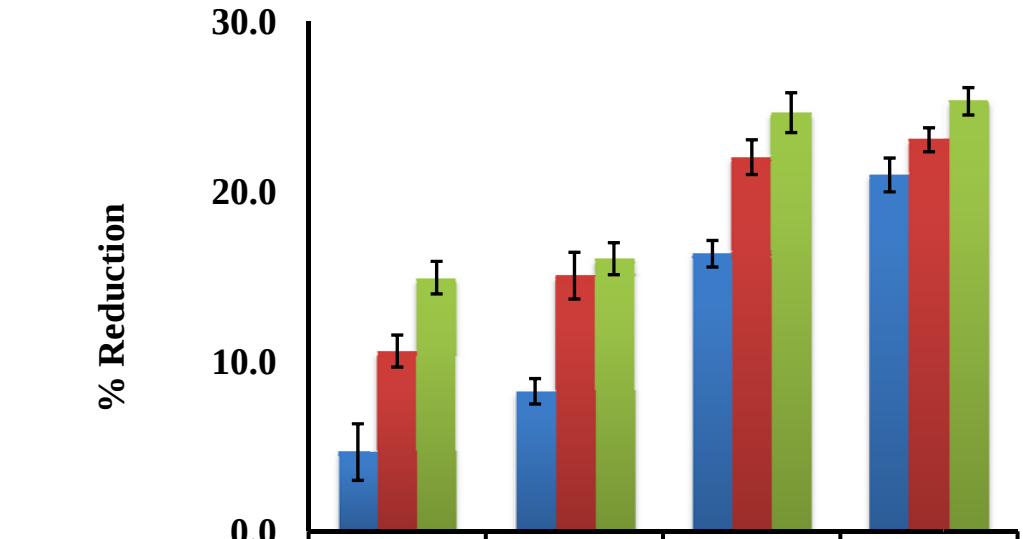

	Day 3	Day 6	Day 12	Day 18
PDMS	4.7	8.3	16.3	21.0
PDMS/5% Alumina	10.6	15.1	22.0	23.1
PDMS/10% Alumina	14.9	16.1	24.7	25.3

Figure 4.16: Percentage reduction of Resazurin as a function of adhesion and proliferation of endothelial cells cultured on different composites during various time points.

The endothelial cells cultured on substrates with low, middle, and high stiffness showed different shapes under the confocal microscope, ranging from round in pure PDMS with lower stiffness to spindle-shaped in the PDMS/10% Al_2O_3 composite with higher stiffness (Figure 4.17). The spindle-shaped endothelial cells in the

PDMS/10% Al_2O_3 composite were larger than the round cells in pure PDMS substrate.

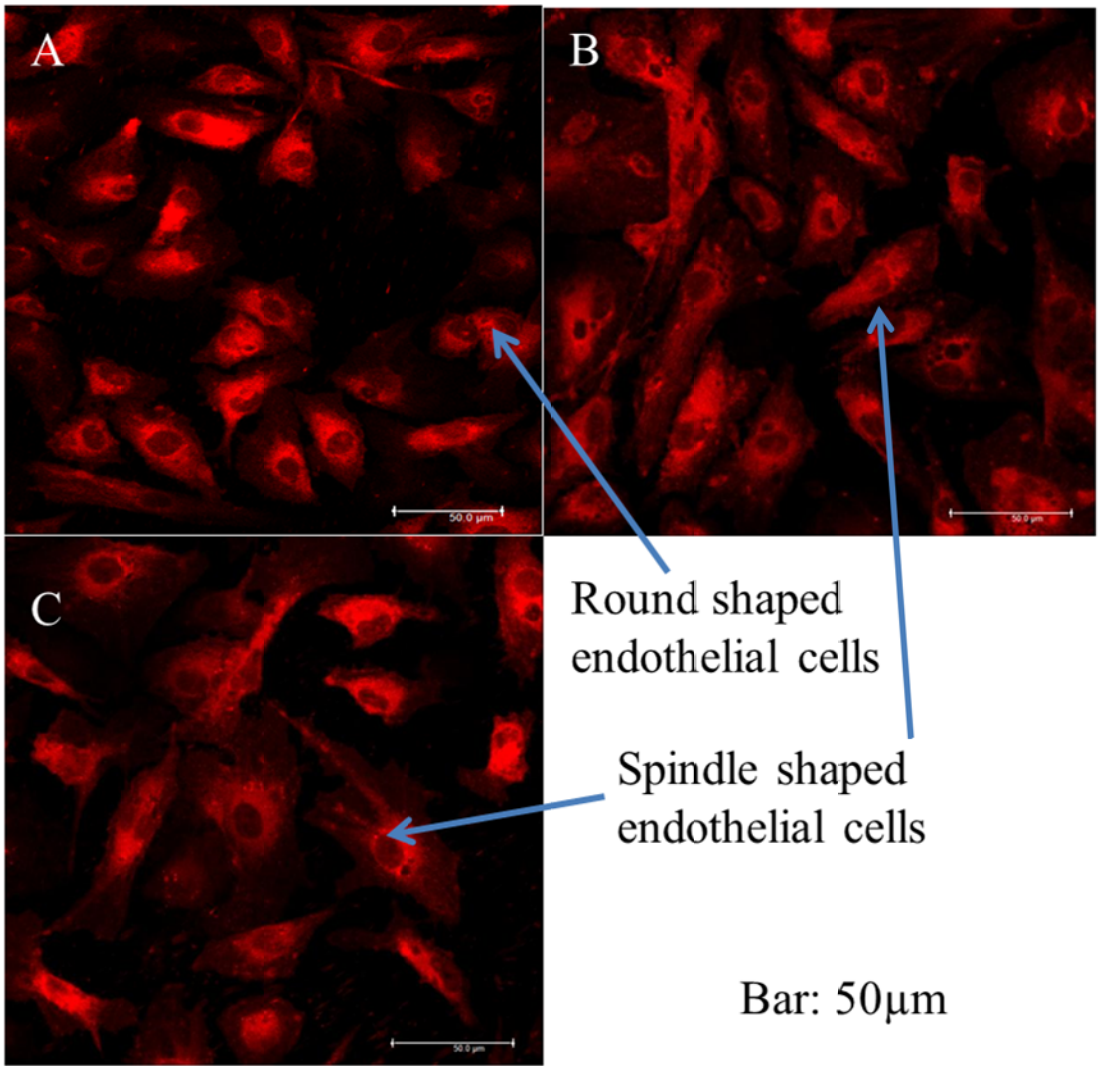

Figure 4.17: Effects of substrate stiffness on BAEC morphology under confocal microscope for the substrates. A) Stained cell on pure PDMS, B) Stained cells on PDMS/5% Al_2O_3, and C) Stained cells on PDMS/10% Al_2O_3

Statistical analysis was performed to understand the significant difference between different composites and days. The samples were divided into three groups based on substrate stiffness (group 1 = pure PDMS, group 2 = PDMS/5% Al_2O_3, and group 3 = PDMS/10% Al_2O_3). Time and substrate stiffness were found to significantly affect (P_{value}=0.001) percentage reduction. This result indicates that the

effect of time on the reduction percentage depends on the considered stiffness. The reduction percentages for all substrates were relatively low at day 3, and significantly high at day 18 (fourth time point). PDMS/10% Al_2O_3, as a stiff substrate, had the highest percentage reduction in all time points.

4. 5. Effect of stiffness on eNOS phosphorylation and NO production in a dynamic environment

4. 5. 1. Cells remaining on substrates after 9 h of tensile loading

The endothelial cells attached on the substrates were stretched for 9 h to ensure that the cells still remain attached to the membranes after tensile loading. The cells were counted through the Hoechst method assay. The obtained results revealed that the difference between treatment group and control group which is equal to detached cell per cent is negligible and suggest that 9 h of stretch loading did not significantly detach the cells (Figure 4.18).

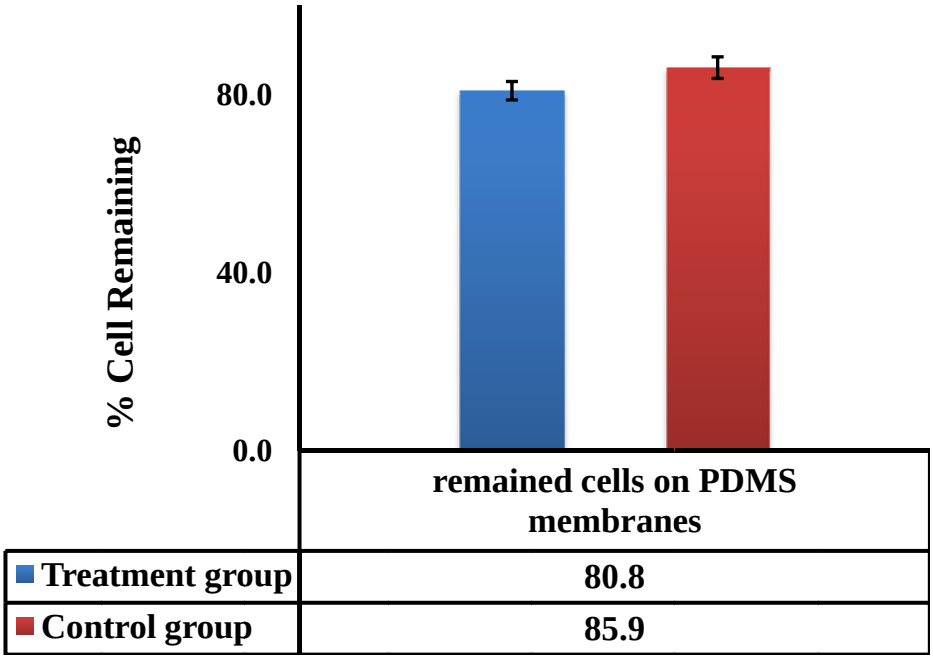

Figure 4.18: Cells remaining on the pure PDMS substrates after 9 h of stretch loading. There is significant difference between treated group and control group.

Some substrates were removed from the metal mold and placed inside sterile Petri dishes after tensile loading, and were observed under a normal microscope to observe the cells remaining attached to the membranes and the alterations in cell morphology, which are shown in Figure 4.19. The morphology of the cells immediately after tensile loading revealed that the cells were subjected to high stress caused from tensile loading (Peng et al., 2003), because the cells were observed to look like bright particles.

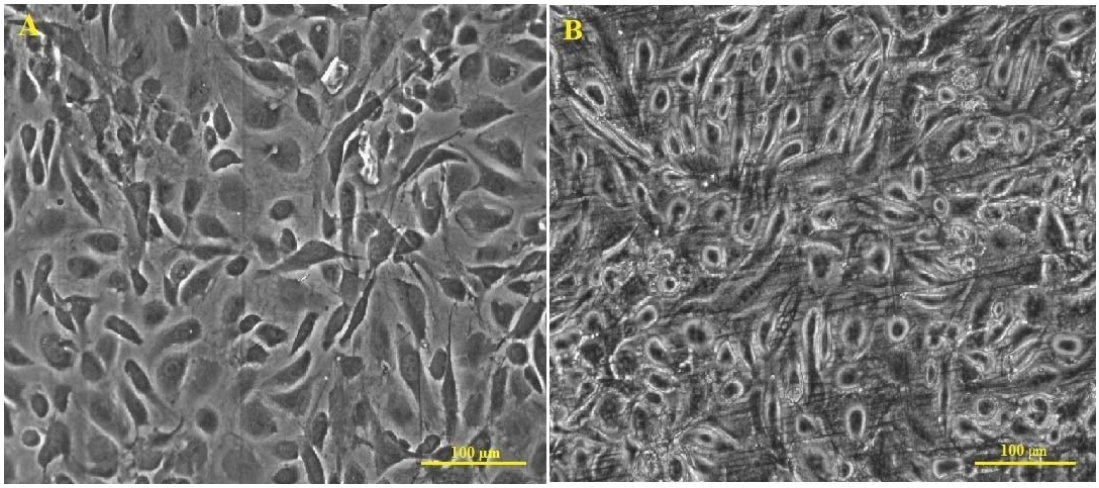

Figure 4.19: Changes in endothelial cell morphology in response to tensile loading A) Endothelial cell morphology without applying tensile loading (control) B) Endothelial cell morphology after 9 h of tensile loading (treated cells)

4. 5. 2. eNOS phosphorylation at different time points

The eNOS phosphorylation at Ser^{1177} is important in NO production. Two aspects, namely, the hypothesized change in eNOS phosphorylation at Ser^{1177} under physiological cyclic stretching, and the eNOS phosphorylation peaks at different time points, were investigated. Three time points, namely, 2, 3, and 6 h, were selected based on reports to determine which time point induces the highest eNOS

phosphorylation in pure PDMS. Our results showed that cyclic stretching induced more eNOS phosphorylation compared with the static condition (no stretching). Non-stretched cells displayed low-basal p-eNOS levels at Ser^{1177}, whereas the p-eNOS levels in the stimulated cells (3 and 6 h) were higher than the basal level. Moreover, eNOS phosphorylation hit the peak point after 3 h of stretching (Figure 4.20). Therefore, this time point was selected for applying tensile loading on stiff substrates (PDMS/5% Al_2O_3 and PDMS/10% Al_2O_3).

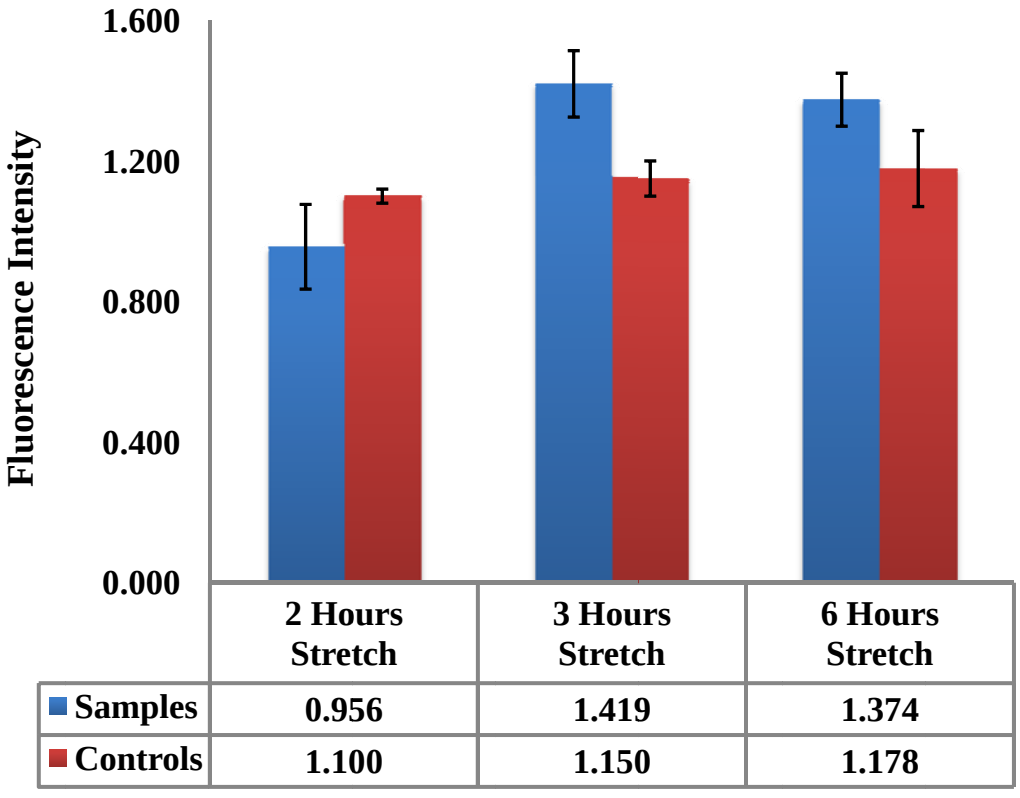

Figure 4.20: eNOS phosphorylation intensity after 2 h, 3 h, and 6 h of tensile loading time.

4. 5. 3. eNOS phosphorylation intensities in substrates with different stiffness values

The 3 h tensile loading with 1Hz frequency was also applied for stiff substrates, based on the p-eNOS intensity at different time points. The p-eNOS intensity was measured with and without cyclic stretch loading. Results showed that substrate stiffness decreased p-eNOS intensity in response to 10% stretch with 1 Hz frequency for 3 h compared with the static samples. The highest p-eNOS intensity (1.50) was related to PDMS membranes as compliant membranes, whereas the p-eNOS intensity in stiff membranes (roughly 1.05) was nearly at the low-basal level (Figure 4.21).

A one-way ANOVA was conducted to analyze the effect of substrate stiffness on eNOS phosphorylation at Ser^{1177} between groups. The samples were divided into three groups according to substrate stiffness (PDMS, PDMS/5% Al_2O_3, and PDMS/10% Al_2O_3). The three groups were significantly different at $p<0.05$: $F(2, 6) = 48.255$, $P < 0.001$. The actual difference in mean scores between the groups and the effect size calculated using eta squared (0.94) were quite high. Post hoc comparisons using the Tukey HSD test indicated that the mean score for group 1 ($M = 1.66$, $SD = 0.09$) is significantly different from both group 2 ($M = 1.05$, $SD = 0.13$) and group 3 ($M = 1.03$, $SD = 0.07$), whereas group 2 is not significantly different from group 3.

*P<0.05 VS. PDMS/5% Al_2O_3,
PDMS/10% Al_2O_3, and their controls

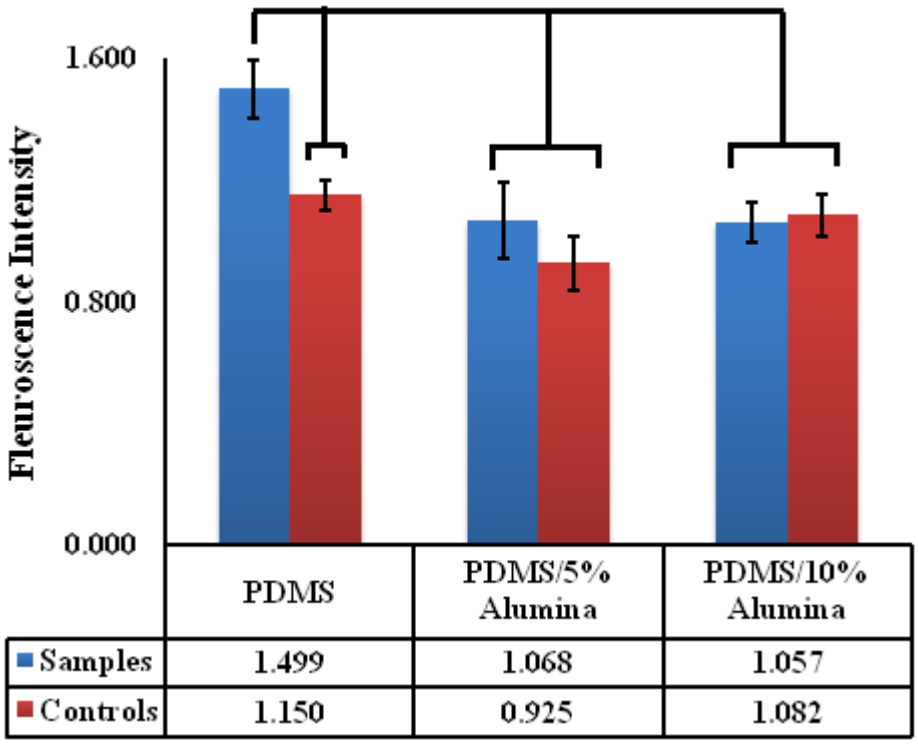

Figure 4.21: Effect of substrate stiffness (PDMS, PDMS/5% Al_2O_3, PDMS/10% Al_2O_3,) on p-eNOS intensity

4. 5. 4. Effect of substrate stiffness on NO concentration

The effect of cyclic tensile loading on NO production was examined. The effect of substrate stiffness on NO production was also assessed by preparing PDMS, and its composites. Cyclic tensile loading significantly increased NO basal production three times in PDMS as a compliant membrane (600 µg/ml) compared with stationary controls (200 µg/ml), whereas NO production significantly decreased as stiffness was increased. NO concentration was undetectable in the untreated cells cultured on stiff substrates and the treated cells on PDMS/10% Al_2O_3 membranes, but the NO concentration of the cells cultured on PDMS/5% Al_2O_3 under stretching was 50 µg/ml, significantly different from the NO concentrations on the compliant membranes (pure PDMS) (Figure 4.22).

The analysis of the NO results through one-way ANOVA shows the effect of substrate stiffness on NO concentration. The samples were divided into three groups according to substrate stiffness (PDMS, PDMS/5% Al_2O_3, and PDMS/10% Al_2O_3). There was a significant difference at the $p<0.05$ level between three groups, $F(2, 6) = 1491.43$, $P=0.001$. The actual difference of effect size calculated through eta squared is quite high (0.99). These results indicate that the difference between groups was significantly high. Group 1 (M = 590, SD = 10) is significantly different from groups 2 (M = 50.66, SD = 2.08) and group 3 (M = 1.00, SD = 1), whereas groups 2 and 3 were not significantly different.

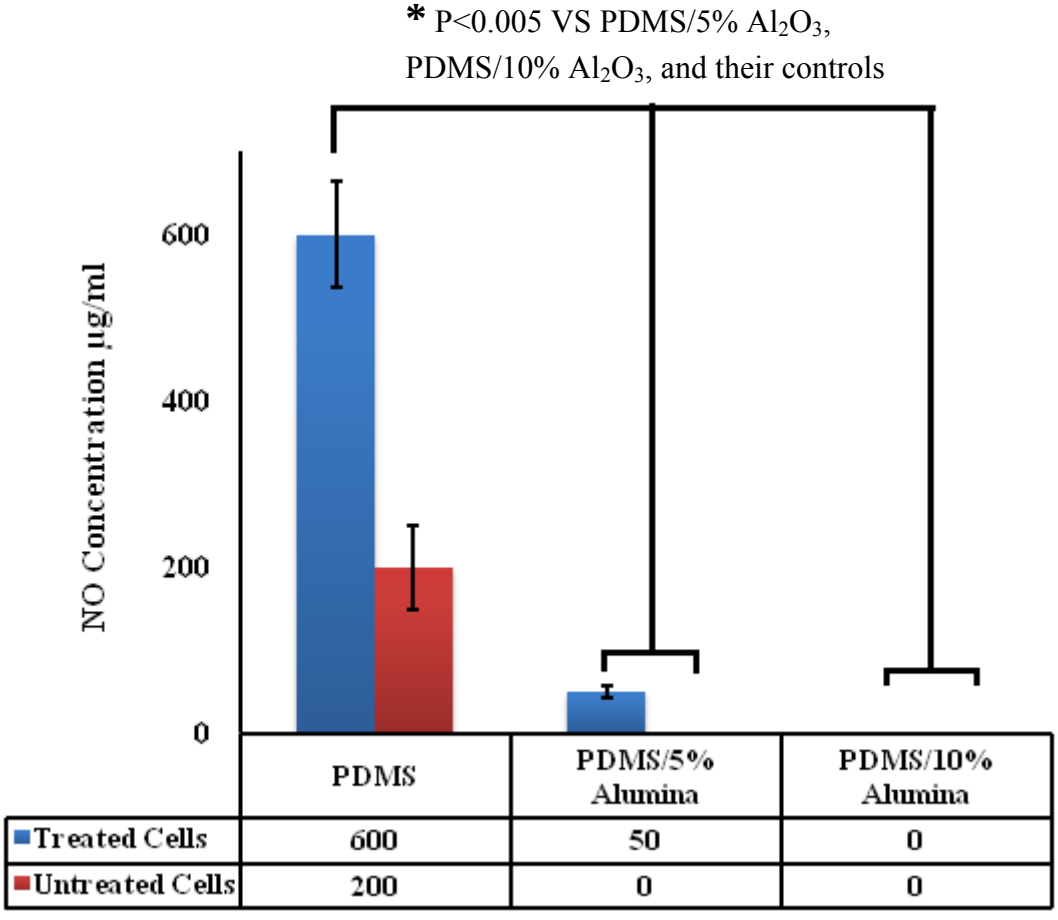

Figure 4.22: NO concentration increase in response to cyclic tensile loading compared with un-stimulated cells.

CHAPTER 5

DISCUSSION

5. 1. Endothelial cell isolation

Endothelial cell isolation methods include the physical removal of the endothelium, outgrowth method, use of magnetic beads, and enzymatic digestion. These methods have some disadvantages despite evidence which shows the effectiveness of the mentioned methods in endothelial cell isolation. The physical cell removal using a scraper can indirectly break cell membranes by over-scraping and decreases cell viability. Fibroblast contamination may also occur.

Many cells can be isolated from small pieces of tissue using the outgrowth method, but fibroblast cells sprout from tissue pieces faster than endothelial cells, thereby increasing the likelihood of fibroblast contamination. Fibroblast cells also grow faster and occupy more space than endothelial cells. This method is time consuming because the first cells emerge after a few weeks.

Using magnetic beads coated with CD31 is more accurate for obtaining pure endothelial cells; however, production of sensitive cells with low proliferative capacity is common issues in using magnetic beads in cell isolation (Figure 5.1). Contamination with other cell types is likely in this method because of the non-specific binding of magnetic beads.

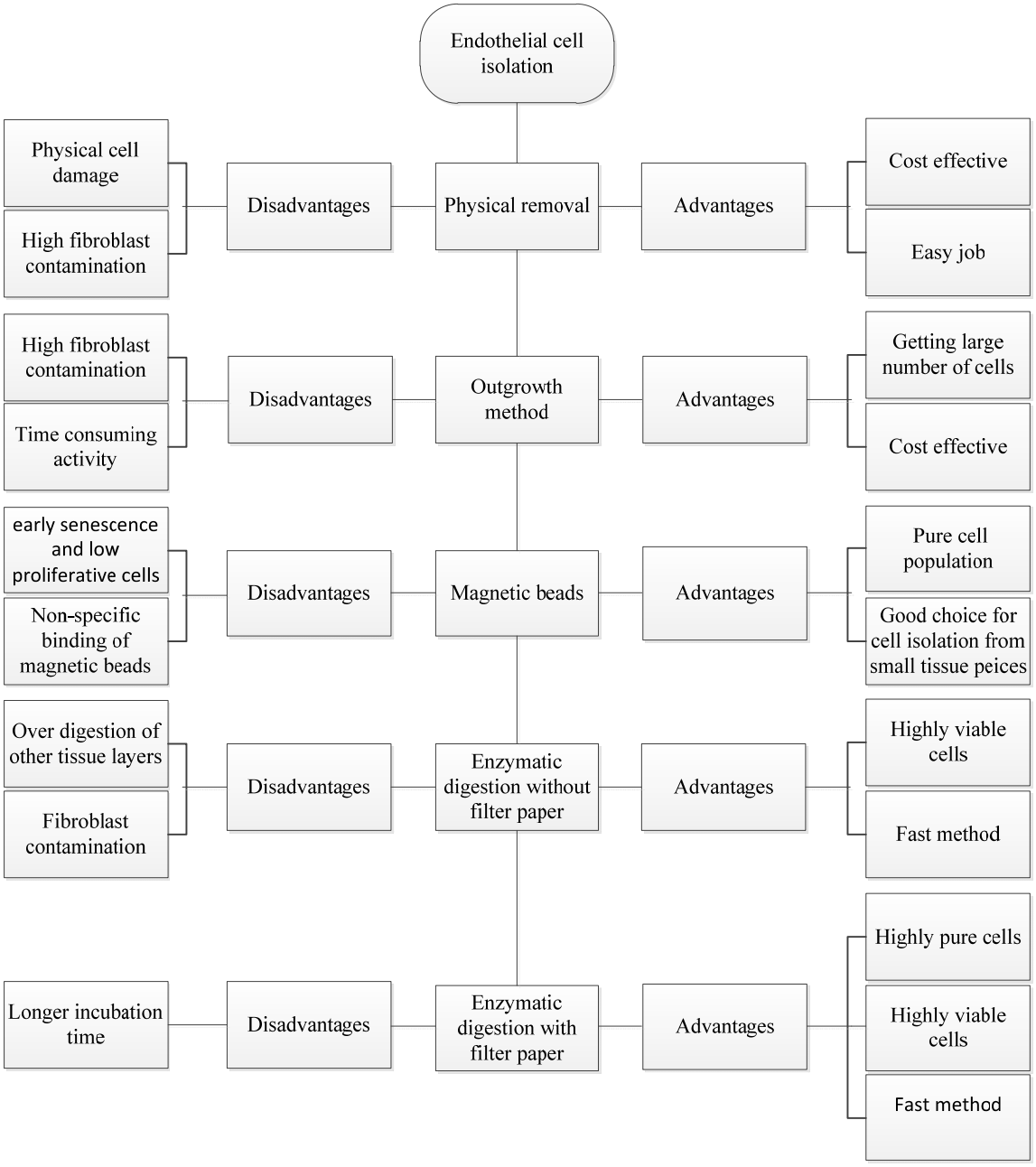

Figure 5.1: Summary of the benefits and disadvantages of common methods for endothelial cell isolation

The well-known enzymatic method was used with a filter paper in the enzymatic digestion step in this study. The additional step improves the purity of the isolated endothelial cells because the over digestion of the cell layers beside the endothelium using collagenase II is the main reason for the contamination with other kinds of cells in the enzymatic digestion method without filter paper.

The proposed method has several advantages over the conventional enzymatic method. The filter paper absorbs collagenase type II and maintains the direct and continuous contact of the endothelial cells with the enzyme. Additional enzyme was prevented from dripping on the filter paper to prevent the digestion of other tissue layers. Digestion is therefore limited to only the endothelium and prevents the over-digestion of neighboring tissues, thereby minimizing fibroblast contamination. Endothelial cell viability was reasonable, and the cells appeared to be less sensitive to their environment because the endothelial cells isolated in this study were sustained up to Passage 10.

Cobblestone appearance of endothelial cells has been clearly shown at Figure 4.1 as present cells after enzymatic digestion with filter paper. Panels A and B of this figure present the typical appearance of aggregated endothelial cells because endothelial cells tend to form cell clumps (Machi et al., 1990). There are some round shape cells in this figure which did not still spread their cytoplasm out.

The digestion of the aortic samples in the enzyme solution without filter paper increases the likelihood of enzyme digestion of tissues other than the endothelium because the enzyme is in direct contact with all three layers of the vessels (intimae layer, media layer, and adventitia layer). Fibroblast cells exist in all three layers, thus immersing the tissue pieces in the enzyme solution promotes fibroblast contamination.

The purity of the isolated cells must be established after cell isolation. Von Willbrand factor expression, CD31, Dil-Ac-LDL, and the formation of blood vessel-like structures (termed angiogenesis) in the 3D environment are the most commonly used markers in endothelial cell characterization (Nicosia et al., 1994a; Phillips et al., 1979).

Pure cells population was measured using CD31 as a surface marker by flowcytometry. The flowcytometry results show that 89.4% of the isolated cells are endothelial cells (Figure 4.3-C) (Ataollahi et al., 2014a). However, the results are underestimated because cells are commonly damaged during flowcytometry as a result of multiple centrifugations. The purity of the isolated endothelial cells is nearly identical to that obtained by Beijnum et al., (Van Beijnum et al., 2008), who obtained 90% pure endothelial cells from fresh tissues using magnetic beads. The use of magnetic beads favorably isolate endothelial cells from small-sized tissues, microvascular tissues, and tumors (Drake & Loke, 1991; Hewett & Clifford, 1996; Matsubara et al., 2000); however, this method is not cost effective for use in the isolation of the endothelial cells of large vessels.

The histogram of the cells stained with Mouse Monoclonal antibody to CD31is shown in Figure 4.4. The X-axis of the histogram represents the value of the parameter signals in channel numbers, and the y-axis represents the number of events per channel number in flow cytometry. Signals with identical intensities accumulate in the same channel. Therefore, this histogram shows that most events accumulated in the FITC channel, and were positive for CD31.

The flowcytometry results are supported by the immunostaining results, which revealed the high purity of the isolated endothelial cells through the proportion of cell nuclei stained with dapi to the stained cells with von willbrand factor (Figure 4.5).

The blood vessel network is a major part of the vertebrate body structure. This extensive network forms from endothelial cells growing from existing vessels. This cell behavior, termed angiogenesis, results from the interaction of endothelial cells with their environment (Deroanne et al., 2001; Eilken & Adams, 2010; Lei et al., 2012). Blood vessel formation happens in multiple stages, such as endothelial cell

proliferation, directional cell migration, and appropriate cell connection (Eilken & Adams, 2010). The endothelial cells in this study readily displayed angiogenesis and formed tubes.

The isolated cells from bovine aorta were finally confirmed to be BAEC based on the characterization methods because the cells were positive for all the characterization methods normally used for endothelial cells.

5. 2. Membrane characterization

Vessel stiffness increases in physiological situations such as aging and pathological situations such as atherosclerosis. Cells also sense the mechanical properties of the substrate and forces imposed from the environment through their receptors. Therefore, according to the importance of vessel stiffness and its effects on cell responds, the feasibility of suitably stiff substrates helps to understand the involved cellular mechanism.

Substrates with different stiffness ranges are prepared as scaffolds for endothelial cells to observe endothelial cell responses in terms of cell adhesion, proliferation, morphology, and synthetic profiles, such as eNOS phosphoryation and NO production in response to static and dynamic environments. The mechanisms underlying eNOS phosphorylation and NO production in response to tensile loading have been studied in physiological situations (Feliers et al., 2005; Jin et al., 2005; Motley et al., 2007); however, little information about the mechanisms involved in eNOS phosphorylation and NO production in cells cultured on stiff substrates in response to tensile loading exists.

Substrates with different stiffness ranges were prepared by adding 5% and 10% Al_2O_3 to PDMS. The pure PDMS substrate serves as the compliant scaffold. PDMS elastomer is a common substrate for cell cultures (Awolesi et al., 1995; Takeda et al., 2006) because of its biocompatibility, low toxicity, high flexibility, gas permeability, and thermal stability. These advantages make this material more suitable than the other materials, such as polyacrylamide gels (Pelham & Wang, 1997; Yeh et al., 2012). The flexibility of PDMS makes it much more suitable for cardiovascular studies because the tensile loading during each pulse is common in the cardiovascular system.

To investigate the effects of substrate stiffness on endothelial cell behavior, 5% and 10% Al_2O_3 were added to PDMS to enhance stiffness. Al_2O_3 is used for controlling substrate-stiffness because of its biocompatibility, thermal and electrical resistivity, thermal and chemical stability, and availability (Leukers et al., 2005). The Al_2O_3 stability (corundum) in α-phase (Boumaza et al., 2009) is one of the reasons for its selection in this study. A stable phase helps minimize deviations in physical properties at different processing conditions, whereas an unstable phase rapidly shows different physical properties.

The tensile test results show that the addition of Al_2O_3 to PDMS enhanced the substrate stiffness in the PDMS elastomeric matrix (Table 4.1). Therefore, the PDMS/10% Al_2O_3 composite, with 1.1 MPa, is stiffer than pure PDMS (300 KPa) which showed the lowest stiffness. This finding is attributed to the interfacial bonding between Al_2O_3 particles and the PDMS matrix. Alumina concentrations of 5% and 10% were selected to enhance PDMS stiffness because the Young's modulus values obtained from these concentrations are significantly different from those of pure PDMS. The change in Al_2O_3 concentration altered substrate stiffness. The distance between the two ends of a specimen enhanced with increased Al_2O_3 concentration in

the PDMS base at almost the same pressure exerted by normal adhesive tape which is an indicator of increased stiffness. Thus, the PDMS/Alumina composite is a potential scaffold for studies on the effects of stiffness, especially on the cardiovascular system.

Structural and morphological tests are performed to confirm the existence of PDMS and Al_2O_3, the bonds between them, membrane hemogenicity, and hydrophilicity.

XRD is performed to confirm the crystalline phase of Al_2O_3 in the composites. The pure PDMS elastomer is an amorphous material that showed a broad peak near $2\theta = 11.5°$. Thus, the PDMS elastomer did not show any crystalline peak in the XRD results, whereas all the sharp crystalline peaks observed in the composites are attributed to Al_2O_3. The peak intensity increased with increasing Al_2O_3 concentration. Thus, the PDMS/10% Al_2O_3 composite substrate shows the highest crystalline peaks among the composites. The XRD patterns show that the peak intensities for Al_2O_3 form (119) and (122) planes are still visible in the PDMS/10% Al_2O_3 composite substrate, but are almost negligible in the PDMS/5% Al_2O_3 composite substrate. This result indicates that Al_2O_3 and PDMS elastomer matrix materials interacted, which increased with elevated Al_2O_3 concentrations. FTIR spectroscopy also confirms this result.

FTIR spectra as complementary results confirmed the existence of PDMS and Al_2O_3 in the substrates. The composites comprised functional groups of pure PDMS, pure Al_2O_3, and Si-O-Al. The slight deviation of the FTIR peaks near 700 and 640 cm^{-1} indicates the interaction between Si-O-Si and Al-O-Al, and the deviation near 570 cm^{-1} indicates an interaction between Si-C and Al-O groups, resulting in a new bond between PDMS and Al_2O_3 as a function of Si-O-Al (Águila Rodríguez et al., 2007; Awolesi et al., 1995; Lin & Hwang, 1996; Ochoa et al., 2012).

The surface morphology and roughness of the PDMS membrane and its composites are analyzed through AFM. Neither 3D images of the surface nor the statistical analysis show any significant changes in the roughness values observed in AFM. This result is attributed to the high surface affinity of the viscous PDMS gel toward the mold-surfaces and the lower density of PDMS (2.21 g/cc) than the Al_2O_3 particles (3.97 g/cc). A thin PDMS film always formed at the membrane surfaces of both composites. Thus, the surface roughness of both composites is almost similar (nearly 14.2 μm Ra value) to that of the pure PDMS substrate, which indirectly affects cell adhesion or proliferation.

The degree of the dispersion of the Al_2O_3 particles and interfacial bonding with the PDMS matrix in the composites are examined under FESEM. The smaller Al_2O_3 particles (<100 nm) gradually agglomerated with increasing Al_2O_3 concentrations in the composites. The 200 nm Al_2O_3 particles bonded and homogeneously distributed in the PDMS matrix in the PDMS/10% Al_2O_3 composite substrate. Hence, the PDMS/10% Al_2O_3 composite substrate show higher Young's modulus and stiffness than the substrates made of pure PDMS and other composites.

Low hydrophobicity is obtained with increasing Al_2O_3 concentrations in the PDMS matrix (Khumrak & Sukree, 2012), but the surface hydrophobicity value of the pure PDMS and the composites are not significantly different, according to the statistical analysis.

The characterization process showed that PDMS and PDMS/Al_2O_3 composites are mono-phase, homogeneous, flexible and hydrophobic scaffolds. Al_2O_3 addition did not significantly affect the surface roughness and hydrophilicity.

The extra cellular protein fibrinectin is used to increase surface hydrophilicity. The results of the optimization of the fibronectin concentration show that cell attachment with 100 μg/ml fibronectin is the most reasonable (96%), and higher

fibronectin concentration does not significantly increase cell attachment. Hence, this concentration is selected for the next stage of the project, and higher fibronectin concentrations were not used.

5. 3. Cell response to substrate stiffness in a static environment

The attachment, proliferation, and morphology of the endothelial cells seeded on membranes with different stiffness are assessed because cells sense the mechanical stiffness of both ECM and other cells through integrin receptors and cadherin receptors, respectively (Wells, 2008). This process may explain why ECM is a scaffold where surface topography and mechanical properties affect cellular morphology, locomotion, proliferation, and cytoskeletal protein expression (Pramanik et al., 2012; Sunyer et al., 2012). Cell proliferation, arrangement, and differentiation have been reported to be controlled in part by substrate rigidity, depending on substrate stiffness (Engler et al., 2006). Therefore, the change in ECM density affects binding efficiency and adherent receptor activation, which consequently trigger intracellular signaling pathways. Cell responses to mechanical forces are specific to cell types, and are related to the nature of the adherent receptors through which the cell is attached to its substrate because cell responses to the environment depend on how the receptors transduce the mechanical stresses into biochemical signals. Yeunget al.(Yeung et al., 2005) showed that fibroblast cells tend to grow on stiff substrates without the appearance of stress fibers, whereas endothelial cells show stress fibers and a well-spread shape on stiff substrates (Califano & Reinhart-King, 2008).

The time-dependent characteristic of substrate stiffness on cell function and the morphology of cultured endothelial cells were evaluated at various durations in this

study. The results indicate that the cell attachment and proliferation in stiff substrates are higher than those of soft substrates. Cell attachment and proliferation are not affected by surface roughness because the surface roughness of the substrates is not significantly different, according to the statistical analysis. The cell proliferation (a function of absorbance percentage) in the PDMS /10% Al_2O_3 composite, which is stiffer than the other substrates, increased over time and remained high until the end of the study (day 18) compared with the other time points. The statistical analysis shows that the effect of time on cell proliferation depends on scaffold stiffness despite the significant effect of time on cell proliferation. This phenomenon is the reason for the high percentage reduction of the stiff substrates in the Resazurin assay in all time points.

The endothelial cells cultured on PDMS/10% Al_2O_3 appeared to be well-spread compared with those cultured on pure PDMS or PDMS/5% Al_2O_3 composite substrates, as revealed by the confocal microscope. The morphological changes in the endothelial cells on different composite substrates are also a significant evidence of the effect of stiffness on endothelial cell morphology (Ataollahi et al., 2014b). The results of this study are consistent with those of Yeh *et al.* (Yeh et al., 2012), who cultured endothelial cells on polyacrylamide gels with various stiffness. This phenomenon is associated with cell receptors. Cells have a binary sensor in their membrane junction sites, which can obtain signals for relaxed and spindle morphologies when the substrate is stiffer than or as stiff as the intrinsic elastic modulus of the cells. Zeng et al., (2010) showed that the Young's Modulus values of endothelial cells range from 1000 Pa to 7000 Pa, which are less than the Young's modulus of the substrates in this study (Zeng et al., 2010).

5. 4. Cell response to tensile loading

Investigations on the geometric features of blood vessels indicate that wall excursion during systole under normal physiologic conditions is 5% to 6%, and increases to 10% in hypertensive conditions (Steinman & Ethier, 1994). The literature shows that 10% cyclic stretch alters some cell parameters, such as the production of vasoactive substances (Awolesi et al., 1995; Takeda et al., 2006; Throm Quinlan et al., 2011). eNOS is a crucial vasoactive protein in endothelial cells that can be activated by physical stimuli, such as tensile loading and be phosphorylated in various sites, but the vital phosphorylated site leading to NO production is the p-eNOS at Ser^{1177} (Awolesi et al., 1995; Takeda et al., 2006).

A study has shown that 6% and 10% cyclic stretch up-regulate eNOS gene expression and eNOS protein production of the strain treated cells for 24 h (Awolesi et al., 1995).

Another study revealed that cyclic strain phosphorylates eNOS at Ser^{1177} through two pathways, one of which is related to Ca release from the SA channel in the early stages, which continues in the late stages through the PI3K-Akt pathway (Takeda et al., 2006).

Stretching induces the eNOS phosphorylation at Ser^{1177} to reach the maximum level, and then reduces and remains in an unchanged and detectable level during the continuous cyclic tensile loading. Chen et al (Chen et al., 2008) mentioned that eNOS activity rapidly increased and reached the maximum level within 3 h to 6 h, whereas eNOS activity reached the maximum level after 6 h of tensile loading in their study. The eNOS activity in another study reached the highest value after 2 h (Hu et al., 2013).

Therefore, loading-induced eNOS phosphorylation is time dependent and does not affect the total eNOS amount in short durations. Hence, 2, 3, and 6 h were selected as loading times to measure eNOS phosphorylation. However, the cells remaining attached are critical in applying tensile loading. As long as cell adhesion increases with increasing stiffness, the PDMS base construct was considered in cell attachment optimization in response to tensile loading. Stretch loading was applied for 9 h on PDMS membranes to determine the likelihood of cell detachment during stretching by observing cells under a normal microscope and using the Hoechst method. The cell morphologies and the results of the Hoechst method after applying tensile loading revealed that 9 h of stretch, as coverage for 2, 3, and 6 h mentioned in literature, does not detach the cells.

Comparisons between eNOS intensities in the three time points selected in this study indicate that 2 h of stretching is not enough to trigger cell signals for eNOS phosphorylation, whereas phosphorylation peaked after 3 h of stretching. The eNOS phosphorylation seems to have increased and peaked after 3 h and declined from then on because the p-eNOS intensity at 6 h is less than that in 3 h. The phosphorylated form of eNOS seems to approach a constant level.

Results show that 10% cyclic stretch significantly induced the highest eNOS phosphorylation level after 3 h of stretching. The possible mechanism involved in eNOS phosphorylation is the Ca^{2+} release from the SA channel, which stimulates eNOS phosphorylation in its early phases (Sunyer et al., 2012).

Physical forces affect the integrins in adhesion sites to ECM and induce the phosphorylation of the tyrosine of the focal adhesion kinase. Phosphorylation is then continued by the PI3K-Akt pathway. This enzyme elevates the sensitivity of eNOS to Ca^{2+}, such that eNOS shows maximum activity at sub-physiologic Ca^{2+}

concentrations and facilitates NO production (Dimmeler et al., 1998; Takeda et al., 2006).

ECM is a scaffold whose surface topography and mechanical properties affect cellular morphology, locomotion, proliferation, and cytoskeletal protein extraction (Pramanik et al., 2012; Sunyer et al., 2012). Cells sense the mechanical properties of both the ECM and other cells through integrin receptors and cadherin receptors, respectively (Wells, 2008).

Earlier studies investigated the effects of substrate stiffness on eNOS gene expression, mRNA and protein production in silico tubes (Peng et al., 2003; Ziegler et al., 1998). Ziegler et al. discovered using a novel perfusion apparatus that the combination of shear stress and pressure upregulated eNOS and ET mRNA levels and protein production, whereas 4% stretching of endothelial cells with all levels of shear stress did not significantly change eNOS mRNA or protein production (Ziegler et al., 1998).

Peng et al. evaluated the effect of pulse perfusion on the eNOS and Akt phosphorylation of cells seeded in tubes with different stiffness. The results revealed that pulse perfusion phosphorylated eNOS and Akt, but the perfusion of the phosphorylated eNOS and Akt at stiff tubes was less than the compliant tubes, and the cells in stiff tubes were more vulnerable to oxidative stress (Peng et al., 2003).

The mechanical environment in the tubes is a complicated system that combines shear stress, stretch, and pressure, whereas these factors involve different mechanisms and thereby have single effects. Hence, the effects of only cyclic tensile loading on eNOS phosphorylation in response to substrate stiffness were investigated in this study.

This study is the first to demonstrate that substrates with only cyclic tensile loading alter eNOS phosphorylation depending on substrate stiffness. The p-eNOS

intensity in the cells seeded on the compliant membranes (PDMS) was higher than those cultured on PDMS/5% Al_2O_3, whereas the lowest point was related to PDMS/10% Al_2O_3 as the stiffest substrate, even less than the basal level in response to cyclic stretching.

This result suggests that a possible mechanism whereby the forces applied to the endothelial cells by the stiff substrates during the cycle tensile loading alter the eNOS phosphorylation of the endothelial cells and are a matter of debate. The possible reasons through which substrate forces affect eNOS phosphorylation during tensile loading probably are the reduction in eNOS activation, high superoxide production, and thereby, eNOS uncoupling as a result of protein nitration by peroxynitrite, endogenous NOS inhibitors (asymmetric dimethyl arginin), upstream activator modulation (kinases) - including p-Akt and PI3K- which regulate eNOS activity, and the vulnerability of endothelial cells to stress. These reasons can be considered to have impaired the sensitivity of eNOS to mechanical forces (Peng et al., 2003; Soucy et al., 2006). The possibility of high superoxide production, which led to high cell vulnerability to superoxides, eNOS nitration, and thereby, eNOS uncoupling and reduction in NO bioavailability, is the most probable, because the p-eNOS intensity in the control group was higher than that of the stimulated group. However, the exact mechanisms involved in these effects are unknown. The current results demonstrate the importance of the mechanical properties of ECM in eNOS regulation.

Stretching enhances the involvement of PI3K-dependent phosphorylation, which contributes to the activation of Akt/PKB and finally eNOS. The eNOS phosphorylation produces NO by metabolizing L-arginin. Therefore, the reduction in eNOS phosphorylation decreases NO concentration.

The NO concentration was the highest in the PDMS membranes, but decreased in the treated PDMS/5% Al_2O_3 group, and was undetectable in the cells seeded on PDMS/10% Al_2O_3 membranes. The reason is probably mainly related to the attenuated eNOS activity and the NO scavenging by ROS and the O_2^- produced by the cell mitochondria in response to substrate forces. The reaction between NO and O_2^- creates peroxynitrite, which scavenges BH4. When BH4 concentration reaches less than the level required for eNOS enzymatic activity, eNOS cannot catalyse L-arginin oxidation to NO and thereby increases superoxide production. This can be considered to be synergistic with the NO level reduction in the cells seeded on stiff substrates (Blackwell et al., 2004; Delp et al., 2008). These oxidants scavenge NO and L-arginin as substrate for NO production. This phenomenon is called endothelial dysfunction (Soucy et al., 2006).

CONCLUSION, FUTURE WORKS, AND LIMITATIONS

6. 1. Conclusions

In conclusion, the incorporation of a new stage (filter paper) during the collagenase digestion in endothelial cells isolation has successfully produced a pure population of endothelial cells with purity 89.4%. Limiting of collagenase to endothelium by filter paper is the main merit of this method. Also, the quality of isolated cells is quite reasonable for further studies.

The stiffness of PDMS-based substrate, as scaffold for endothelial cells, was manipulated by incorporating biocompatible reinforcements, such as alumina. Statistical analysis revealed that substrates with different stiffness are not different in surface roughness and hydrophilicity significantly. The percentage of maximum strain or elongation of all the specimens indicates the high flexibility of each material. Among these flexible elastomers, the stiffer materials, the cell proliferation as well as cell adhesion, and induced the well-spread morphology of endothelial cells in static environment.

eNOS intensity and NO concentration in endothelial cells cultured on PDMS membranes as compliant substrate was significantly higher which is an indication of eNOS phosphorylation at Ser^{1177} in respond to tensile loading after 3h. However, phosphorylation intensity and NO concentration in stiff membranes were in base level and even undetectable level, which suggest that substrate stiffness might decline eNOS phosphorylation and also NO bioavailability in dynamic condition by oxidative agents. The oxidative agents increase cell vulnerability and induce eNOS nitration and uncoupling. Also, NO can be scavenged by O_2^- that produces

peroxynitrite. These results indicate that mechanical properties of vessel walls play critical factor in the regulation of eNOS and NO by cyclic stretch.

6. 2. Future works

6. 2. 1. Applying shear stress on endothelial cells seeded on substrates with different stiffness

Endothelial cells are involve in cardiovascular system, in which three factors, shear stress, tensile loading, and pressure are subsequently applied. These factors have their own effects. Therefore, further work on the direct shear stress applied on endothelial cells seeded on stiff substrates will provide useful information about the effects of each factor on eNOS intensity and NO production in physiological conditions.

6. 2. 2. Evaluation of the points in which p-eNOS intensity peaks in substrates with different stiffness values

The eNOS phosphorylation increases in response to a dynamic environment but peaks and then declines to a detectable level. The time to reach the peak possibly increases as stiffness increases. Therefore, not only, the decline in p-eNOS intensity is attributed to the decrease in shear stress and tensile loading, but also the delay in reaching the peak point, may have a synergistic effect on the reduction of p-eNOS intensity and NO production in stiff substrates. Therefore, this hypothesis must be investigated in further studies.

6. 2. 3. Applying a mixture of shear stress and tensile loading on endothelial cells

Applying shear stress and tensile loading on endothelial cells seeded in tubes with different stiffness may be used to investigate whether the reduction in vessel distensibility affects p-eNOS intensity. These situations somehow simulate the endothelial cell conditions in the body. The results of this study may be compared with the results achieved from the effects of shear stress and tensile loading alone, which may provide researchers a useful conclusion.

6. 3. LIMITATIONS

The tensile jig available in the lab is a manual instrument in which the tensile loading applied on cells should be controlled using a ruler, promoting hand errors and eye errors. Moreover, this system exerts extreme forces on cells when returned to the relaxed position. These high forces may increase cell vulnerability and induce cell death.

REFERENCES

Águila Rodríguez, G., García-Salgado, G., Romero-Paredes, G., & Peña-Sierra, R. (2007). FTIR and photoluminescence studies of porous silicon layers oxidized in controlled water vapor conditions. *Revista Mexicana DeFísica*, 53 (6), 431-435.

Ando, H., Kubin, T., Schaper, W., & Schaper, J. (1999). Cardiac microvascular endothelial cells express α-smooth muscle actin and show low NOS III activity. *American Journal of Physiology - Heart and Circulatory Physiology*, 276 (5), 1755-1768.

André, P., Michel, M., Schott, C., & Stoclet, J. C. (1992). Characterization of cultured rat aortic endothelial cells. *Journal of Physiology-Paris*, 86 (4), 177-184.

Ataollahi, F., Pingguan-Murphy, B., Moradi, A., Abas, A. B. W. A., Chua, K. H., & Osman, N. A. A. (2014a). A new method in the isolation of large vessels endothelial cells. *Cythotherapy*, 16, 1145-1152.

Ataollahi, F., Pramanik, S., Moradi, A., Dalilottojari, A., Pingguan-Murphy, B., Wan Abas, W. A. B., & Abu Osman, N. A. (2014b). Endothelial cell responses in terms of adhesion, proliferation, and morphology to stiffness of polydimethylsiloxane elastomer substrates. *Journal of Biomedical Materials Research Part A*, DOI: 10.1002/jbm.a.35186 In press.

Averna, M., Stifanese, R., De Tullio, R., Passalacqua, M., Salamino, F., Pontremoli, S., & Melloni, E. (2008). Functional Role of HSP90 Complexes with Endothelial Nitric-oxide Synthase (eNOS) and Calpain on Nitric Oxide Generation in Endothelial Cells. *Journal of Biological Chemistry*, 283 (43), 29069-29076.

Awolesi, M. A., Sessa, W. C., & Sumpio, B. E. (1995). Cyclic strain upregulates nitric oxide synthase in cultured bovine aortic endothelial cells. *The Journal of Clinical Investigation*, 96 (3), 1449-1454.

Birdwell, C. R., Gospodarowicz, D., & Nicolson, G. L. (1978). Identification, localization, and role of fibronectin in cultured bovine endothelial cells. *Proceedings of the National Academy of Sciences of the United States of America*, 75 (7), 3273-3277.

Blackwell, K. A., Sorenson, J. P., Richardson, D. M., Smith, L. A., Suda, O., Nath, K., & Katusic, Z. S. (2004). Mechanisms of aging-induced impairment of endothelium-dependent relaxation: role of tetrahydrobiopterin. *American*

Journal of Physiology - Heart and Circulatory Physiology, 287 (6), 2448-2453.

Boo, Y. C., Sorescu, G., Boyd, N., Shiojima, I., Walsh, K., Du, J., & Jo, H. (2002). Shear stress stimulates phosphorylation of endothelial nitric-oxide synthase at Ser1179 by Akt-independent mechanisms. *Journal of Biological Chemistry*, 277 (5), 3388-3396.

Boumaza, A., Favaro, L., Lédion, J., Sattonnay, G., Brubach, J. B., Berthet, P., Huntz, A. M., Roy, P., & Tétot, R. (2009). Transition alumina phases induced by heat treatment of boehmite: An X-ray diffraction and infrared spectroscopy study. *Journal of Solid State Chemistry*, 182 (5), 1171-1176.

Cai, H., & Harrison, D. G. (2000). Endothelial dysfunction in cardiovascular diseases: the role of oxidant stress. *Circulation Research*, 87 (10), 840-844.

Califano, J. P., & Reinhart-King, C. A. (2008). A Balance of substrate mechanics and matrix chemistry regulates endothelial cell network assembly. *Cellular and Molecular Bioengineering*, 1 (2-3), 122-132.

Carrillo, A., Chamorro, S., Rodríguez-Gago, M., Álvarez, B., Molina, M. a. J., Rodríguez-Barbosa, J. I., Sánchez, A., Ramírez, P., Muñoz, A., Domínguez, J.*, et al.* (2002). Isolation and characterization of immortalized porcine aortic endothelial cell lines. *Veterinary Immunology and Immunopathology*, 89 (1–2), 91-98.

Chen, S. C., Cheng, J. J., Wu, S. E., Shen, H. C., Shyu, K. G., & Wang, D. L. (2008). Cyclic strain-induced thrombomodulin expression in endothelial cells is mediated by nitric oxide, but not hydrogen peroxide *Acta Cardiological Sinica*, 24, 114-150.

Cines, D. B., Pollak, E. S., Buck, C. A., Loscalzo, J., Zimmerman, G. A., McEver, R. P., Pober, J. S., Wick, T. M., Konkle, B. A., Schwartz, B. S.*, et al.* (1998). Endothelial cells in physiology and in the pathophysiology of vascular disorders. *Blood*, 91 (10), 3527-3561.

Dao, H. H., Essalihi, R., Bouvet, C., & Moreau, P. (2005). Evolution and modulation of age-related medial elastocalcinosis: Impact on large artery stiffness and isolated systolic hypertension. *Cardiovascular Research*, 66 (2), 307-317.

Dart, A. M., & Kingwell, B. A. (2001). Pulse pressure—a review of mechanisms and clinical relevance. *Journal of the American College of Cardiology*, 37 (4), 975-984.

Delp, M. D., Behnke, B. J., Spier, S. A., Wu, G., & Muller-Delp, J. M. (2008). Ageing diminishes endothelium-dependent vasodilatation and tetrahydrobiopterin content in rat skeletal muscle arterioles. *The Journal of Physiology*, 586 (4), 1161-1168.

Deroanne, C. F., Lapiere, C. M., & Nusgens, B. V. (2001). In vitro tubulogenesis of endothelial cells by relaxation of the coupling extracellular matrix-cytoskeleton. *Cardiovascular Research*, 49 (3), 647-658.

Dimmeler, S., Assmus, B., Hermann, C., Haendeler, J., & Zeiher, A. M. (1998). Fluid shear stress stimulates phosphorylation of Akt in human endothelial cells. *Circulation Research*, 83 (3), 334-341.

Djassemi, N. (2012). Tissue Engineering A Blood Vessel Mimic While Monitoring Contamination Through Sterility Assurance Testing.

Drake, B. L., & Loke, Y. W. (1991). Isolation of endothelial cells from hunan first trimester decidua using immunomagnetic beads. *Human Reproduction*, 6 (8), 1156-1159.

Dudzinski, D. M., & Michel, T. (2007). Life history of eNOS: partners and pathways. *Cardiovascular Research*, 75 (2), 247-260.

Eilken, H. M., & Adams, R. H. (2010). Dynamics of endothelial cell behavior in sprouting angiogenesis. *Current Opinion in Cell Biology*, 22 (5), 617-625.

Engler, A. J., Sen, S., Sweeney, H. L., & Discher, D. E. (2006). Matrix elasticity directs stem cell lineage specification. *Cell*, 126 (4), 677-689.

Farber, H. W., & Loscalzo, J. (2004). Pulmonary arterial hypertension. *New England Journal of Medicine*, 351 (16), 1655-1665.

Fariha, M.-M. N., Chua, K.-H., Tan, G.-C., Lim, Y.-H., & Hayati, A.-R. (2013). Pro-angiogenic potential of human chorion-derived stem cells: in vitro and in vivo evaluation. *Journal of Cellular and Molecular Medicine*, 17 (5), 681-692.

Feliers, D., Xiaoyan, C., Akis, N., Choudhury, G. G., Madaio, M., & Kasinath, B. S. (2005). VEGF regulation of endothelial nitric oxide synthase in glomerular endothelial cells. *Kidney International*, 68 (4), 1648-1659.

Feret, F. R., Roy, D., & Boulanger, C. (2000). Determination of alpha and beta alumina in ceramic alumina by X-ray diffraction. *Spectrochimica Acta Part B: Atomic Spectroscopy*, 55 (7), 1051-1061.

Feron, O., & Balligand, J.-L. (2006). Caveolins and the regulation of endothelial nitric oxide synthase in the heart. *Cardiovascular Research*, 69 (4), 788-797.

Fisslthaler, B., Dimmeler, S., Hermann, C., Busse, R., & Fleming, I. (2000). Phosphorylation and activation of the endothelial nitric oxide synthase by fluid shear stress. *Acta Physiologica Scandinavica*, 168 (1), 81-88.

Fleming, I., & Busse, R. (1999). NO: the primary EDRF. *Journal of Molecular and Cellular Cardiology*, 31 (1), 5-14.

Fukumura, D., Gohongi, T., Kadambi, A., Izumi, Y., Ang, J., Yun, C.-O., Buerk, D. G., Huang, P. L., & Jain, R. K. (2001). Predominant role of endothelial nitric oxide synthase in vascular endothelial growth factor-induced angiogenesis and vascular permeability. *Proceedings of the National Academy of Sciences*, 98 (5), 2604-2609.

Gang, E. J., Hong, S. H., Jeong, J. A., Hwang, S. H., Kim, S. W., Yang, I. I. H., Ahn, C., Han, H., & Kim, H. (2004). In vitro mesengenic potential of human umbilical cord blood-derived mesenchymal stem cells. *Biochemical and Biophysical Research Communications*, 321 (1), 102-108.

Gnasso, A., Carallo, C., Irace, C., De Franceschi, M. S., Mattioli, P. L., Motti, C., & Cortese, C. (2001). Association between wall shear stress and flow-mediated vasodilation in healthy men. *Atherosclerosis*, 156 (1), 171-176.

Grover-Páez, F., & Zavalza-Gómez, A. B. (2009). Endothelial dysfunction and cardiovascular risk factors. *Diabetes Research and Clinical Practice*, 84 (1), 1-10.

Hakim, T. S., Sugimori, K., Camporesi, E. M., & Anderson, G. (1996). Half-life of nitric oxide in aqueous solutions with and without haemoglobin. *Physiological Measurement*, 17 (4), 267-277.

Hamilton, P., Lockhart, C., Quinn, C., & Mcveigh, G. (2007). Arterial stiffness: clinical relevance, measurement and treatment. *Clinical Science*, 113 (4), 157-170.

Harrison, D. G. (1997). Cellular and molecular mechanisms of endothelial cell dysfunction. *The Journal of clinical investigation*, 100 (9), 2153-2157.

Hayes, L. W., Goguen, C. A., Stevens, A. L., Magargal, W. W., & Slakey, L. L. (1979). Enzyme activities in endothelial cells and smooth muscle cells from swine aorta. *Proceedings of the National Academy of Sciences*, 76 (6), 2532-2535.

Hewett, P. W., & Clifford, M. J. (1996). Isolation of microvascular endothelial cells using magnetic beads coated with anti-pecam-1 antibodies. *In Vitro Cellular & Developmental Biology - Animal*, 32 (8), 462-462.

Hu, Z., Xiong, Y., Han, X., Geng, C., Jiang, B., Huo, Y., & Luo, J. (2013). Acute Mechanical Stretch Promotes eNOS Activation in Venous Endothelial Cells Mainly via PKA and Akt Pathways. *PLoS ONE*, 8 (8), e71359.

Huh, D., Kim, H. J., Fraser, J. P., Shea, D. E., Khan, M., Bahinski, A., Hamilton, A. G., & Ingber, E. D. (2013). Microfabrication of human organs-on-chips. *Nature protocol*, 8 (11), 2135-2157.

Ignarro, L. J. (2000). *Nitric oxide: biology and pathobiology*: Academic press.

Institute, A. N. S. (1968). standard method of tension testing of vulcanized rubber *21 CFR 801.410 (d)(2)*. American National Standard J2.1: ASTM D 412-68.

Jantová, S., Theiszová, M., Matejov, P., & Bakoš, D. (2011). Biocompatibility and cytotoxicity of bioglass-ceramic composite with various P2O5 content in Li2O–SiO2–CaO–CaF2–P2O5 system on fibroblast cell lines. *Acta Chimica Slovaca*, 4 (1), 15-30.

Jin, Z.-G., Wong, C., Wu, J., & Berk, B. C. (2005). Flow shear stress stimulates gab1 tyrosine phosphorylation to mediate protein kinase B and endothelial nitric-oxide synthase activation in endothelial cells. *Journal of Biological Chemistry*, 280 (13), 12305-12309.

Johansson, F., Wallman, L., Danielsen, N., Schouenborg, J., & Kanje, M. (2009). Porous silicon as a potential electrode material in a nerve repair setting: tissue reactions. *Acta Biomaterialia*, 5 (6), 2230-2237.

Kals, J., Kampus, P., Kals, M., Pulges, A., Teesalu, R., & Zilmer, M. (2006). Effects of stimulation of nitric oxide synthesis on large artery stiffness in patients with peripheral arterial disease. *Atherosclerosis*, 185 (2), 368-374.

Kang, S. D., Carlon, T. A., Jantzen, A. E., Lin, F.-H., Ley, M., Allen, J. D., Stabler, T. V., Haley, N. R., Truskey, G. A., & Achneck, H. E. (2013). Isolation of functional human endothelial cells from small volumes of umbilical cord blood. *Annals of Biomedical Engineering*, 41 (10), 1-12.

Katamreddy, R., Inman, R., Jursich, G., Soulet, A., & Takoudis, C. (2006). ALD and characterization of aluminum oxide deposited on Si (100) using tris(diethylamino) aluminum and water vapor. *Journal of The Electrochemical Society*, 153 (10), 701-706.

Khumrak, S., & Sukree, K. (2012). Ceramic on ceramic bearings. *The Bangkok Medical Journal* 4, 93-103.

Kloprogge, J. T., Hickey, L., & Frost, R. L. (2004). FT-Raman and FT-IR spectroscopic study of synthetic Mg/Zn/Al-hydrotalcites. *Journal of Raman Spectroscopy*, 35 (11), 967-974.

Kofron, M. D., Opsitnick, N. C., Attawia, M. A., & Laurencin, C. T. (2003). Cryopreservation of tissue engineered constructs for bone. *Journal of Orthopaedic Research*, 21 (6), 1005-1010.

Krishnan, R., Klumpers, D. D., Park, C. Y., Rajendran, K., Trepat, X., Bezu, J. v., Hinsbergh, V. W. M. v., Carman, C. V., Brain, J. D., Fredberg, J. J*., et al.* (2010). Substrate stiffening promotes endothelial monolayer disruption through enhanced physical forces. *American Journal of Physiology - Cell Physiolog*, 300 (1), 146-154.

Lakatta, E. G., & Levy, D. (2003). Arterial and cardiac aging: major shareholders in cardiovascular disease enterprises: part I: aging arteries: a "set up" for vascular disease. *Circulation*, 107 (1), 139-146.

Lakatta, E. G., Wang, M., & Najjar, S. S. (2009). Arterial aging and subclinical arterial disease are fundamentally intertwined at macroscopic and molecular levels. *Medical Clinics of North America*, 93 (3), 583-604.

Lee, J. N., Jiang, X., Ryan, D., & Whitesides, G. M. (2004). Compatibility of mammalian cells on surfaces of poly(dimethylsiloxane). *Langmuir*, 20 (26), 11684-11691.

Lee, S.-J., & Park, S.-H. (2013). Arterial Ageing. *Korean Circulation Journal*, 43 (2),

Lei, Y., Zouani, O. F., Rémy, M., Ayela, C., & Durrieu, M.-C. (2012). Geometrical microfeature cues for directing tubulogenesis of endothelial cells. *PLoS ONE*, 7 (7), e41163.

Leukers, B., Gülkan, H., Irsen, S. H., Milz, S., Tille, C., Seitz, H., & Schieker, M. (2005). Biocompatibility of ceramic scaffolds for bone replacement made by 3D printing. *Materialwissenschaft und Werkstofftechnik*, 36 (12), 781-787.

Li, M., Chiou, K.-R., Bugayenko, A., Irani, K., & Kass, D. A. (2005). Reduced wall compliance suppresses Akt-dependent apoptosis protection stimulated by pulse perfusion. *Circulation Research*, 97 (6), 587-595.

Liao, D., Arnett, D. K., Tyroler, H. A., Riley, W. A., Chambless, L. E., Szklo, M., & Heiss, G. (1999). Arterial stiffness and the development of hypertension: The ARIC study. *Hypertension*, 34 (2), 201-206.

Libby, P. (2002). Inflammation in atherosclerosis. *Nature* 420 (868), 868-874.

Lin, S. L., & Hwang, C. S. (1996). Structures of CeO2-A1203-SiO2 glasses. *Journal of Non-Crystalline Solids*, 202 (1), 61-67.

Lundberg, J. O., Weitzberg, E., & Gladwin, M. T. (2008). The nitrate-nitrite-nitric oxide pathway in physiology and therapeutics. *Nature Reviews. Drug Discovery*, 7 (2), 156-167.

Machi, T., Kassell, N. F., & Scheld, W. M. (1990). Isolation and characterization of endothelial cells from bovine cerebral arteries. *In Vitro Cellular & Developmental Biology*, 26 (3), 291-300.

Mancia, G., Fagard, R., Narkiewicz, K., Redon, J., Zanchetti, A., Böhm, M., Christiaens, T., Cifkova, R., De Backer, G., Dominiczak, A.*, et al.* (2013). 2013 ESH/ESC guidelines for the management of arterial hypertension: The task force for the management of arterial hypertension of the european society of hypertension (ESH) and of the european society of cardiology (ESC). *European Heart Journal*, 31 (7), 1281-1357.

Mata, A., Fleischman, A., & Roy, S. (2005). Characterization of polydimethylsiloxane (PDMS) properties for biomedical micro/nanosystems. *Biomedical Microdevices*, 7 (4), 281-293.

Matsubara, T. A., Murata, T. A., Wu, G. S., Barron, E. A., & Rao, N. A. (2000). Isolation and culture of rat retinal microvessel endothelial cells using magnetic beads coated with antibodies to PECAM-1. *Current Eye Research*, 20 (1), 1-7.

Mookadam, F., Moustafa, S. E., Lester, S. J., & Warsame, T. (2010). Subclinical atherosclerosis: evolving role of carotid intima-media thickness. *Preventive Cardiology*, 13 (4), 186-197.

Morello, F., Perino, A., & Hirsch, E. (2009). Phosphoinositide 3-kinase signalling in the vascular system. *Cardiovascular Research*, 82 (2), 261-271.

Motley, E. D., Eguchi, K., Patterson, M. M., Palmer, P. D., Suzuki, H., & Eguchi, S. (2007). Mechanism of endothelial nitric oxide synthase phosphorylation and activation by thrombin. *Hypertension*, 49 (3), 577-583.

Napoli, C., de Nigris, F., Williams-Ignarro, S., Pignalosa, O., Sica, V., & Ignarro, L. J. (2006). Nitric oxide and atherosclerosis: An update. *Nitric Oxide*, 15 (4), 265-279.

Nicosia, R. F., Villaschi, S., & Marion, S. (1994a). Isolation and characterization of vasoformative endothelial cells from the rat aorta. *In Vitro Cellular & Developmental Biology. Animal*, 30A (6), 394-399.

Nicosia, R. F., Villaschi, S., & Smith, M. (1994b). Isolation and characterization of vasoformative endothelial cells from the rat aorta. *In Vitro Cellular & Developmental Biology - Animal*, 30 (6), 394-399.

Ochoa, M., Durães, L., Beja, A., & Portugal, A. (2012). Study of the suitability of silica based xerogels synthesized using ethyltrimethoxysilane and/or methyltrimethoxysilane precursors for aerospace applications. *Journal of Sol-Gel Science and Technology*, 61 (1), 151-160.

Oemar, B. S., Tschudi, M. R., Godoy, N., Brovkovich, V., Malinski, T., & Lüscher, T. F. (1998). Reduced endothelial nitric oxide synthase expression and production in human atherosclerosis. *Circulation*, 97 (25), 2494-2498.

Park, S., & Lakatta, E. G. (2012). Role of Inflammation in the pathogenesis of arterial stiffness. *Yonsei Medical Journal*, 53 (2), 258-261.

Pelham, R. J., & Wang, Y. l. (1997). Cell locomotion and focal adhesions are regulated by substrate flexibility. *Proceedings of the National Academy of Sciences*, 94 (25), 13661-13665.

Peng, X., Haldar, S., Deshpande, S., Irani, K., & Kass, D. A. (2003). Wall stiffness suppresses Akt/eNOS and cytoprotection in pulse-perfused endothelium. *Hypertension*, 41 (2), 378-381.

Phillips, P., Kumar, P., Kumar, S., & Waghe, M. (1979). Isolation and characterization of endothelial cells from rat and cow brain white matter. *Journal of Anatomy*, 129 (2), 261-272.

Pramanik, S., Pingguan-Murphy, B., & Osman, N. A. A. (2012). Progress of key strategies in development of electrospun scaffolds: bone tissue. *Science and Technology of Advanced Materials*, 13 (4), 043002.

Reed, B. M. (2004). Shoot-tip cryopreservation manual. *USDA-ARS National Clonal Germplasm Repository. Oregon: Corvallis*,

Res, M. A., Bednarik, J., & Blum, F. (1986). Transformation of Na2O-CeO2-B2O3 glass into a material with interconnected pores. *Journal of Materials Science*, 21 (5), 1758-1764.

Resnick, N., & Gimbrone, M. A. (1995). Hemodynamic forces are complex regulators of endothelial gene expression. *The FASEB Journal*, 9 (10), 874-882.

Richards, O. C., Raines, S. M., & Attie, A. D. (2010). The role of blood vessels, endothelial cells, and vascular pericytes in insulin secretion and peripheral insulin action. *Endocrine Reviews*, 31 (3), 343-363.

Rodriguez, M. (2012). The Role of Alpha-7 Nicotine Acetylcholine Receptors in Angiogenesis After In Vivo Nicotine Administration. (Undergraduate study Open Access Honors Thesis), Florida State University. Retrieved from Available from database.

Rosselli, M., Keller, R. J., & Dubey, R. K. (1998). Role of nitric oxide in the biology, physiology and pathophysiology of reproduction. *Human Reproduction Update*, 4 (1), 3-24.

Schwartz, S. M. (1978). Selection and characterization of bovine aortic endothelial cells. *In Vitro*, 14 (12), 966-980.

Shimizu, H., Hosokawa, H., Ninomiya, H., Miner, J. H., & Masaki, T. (1999). Adhesion of cultured bovine aortic endothelial cells to laminin-1 mediated by dystroglycan. *Journal of Biological Chemistry*, 274 (17), 11995-12000.

Shivakumar, E., Das, C. K., Pandey, K. N., Alam, S., & N. Mathur, G. (2005). Blends of silicone rubber and liquid crystalline polymer. *Macromolecular Research*, 13 (2), 81-87.

Shum, D., Radu, C., Kim, E., Cajuste, M., Shao, Y., Seshan, V. E., & Djaballah, H. (2008). A high density assay format for the detection of novel cytotoxic agents in large chemical libraries. *Journal of Enzyme Inhibition and Medicinal Chemistry*, 23 (6), 931-945.

Soucy, K. G., Ryoo, S., Benjo, A., Lim, H. K., Gupta, G., Sohi, J. S., Elser, J., Aon, M. A., Nyhan, D., Shoukas, A. A.*, et al.* (2006). Impaired shear stress-induced nitric oxide production through decreased NOS phosphorylation contributes to age-related vascular stiffness. *Journal of Applied Physiology*, 101 (6), 1751-1759.

Stegemann, J. P., Kaszuba, S. N., & Rowe, S. L. (2007). Review: advances in vascular tissue engineering using protein-based biomaterials. *Tissue engineering*, 13 (11), 2601-2613.

Steinman, D. A., & Ethier, C. R. (1994). The effect of wall distensibility on flow in a two-dimensional end-to-side anastomosis. *Journal of Biomechanical Engineering*, 116 (3), 3294-3301.

Steppan, J., Barodka, V., Berkowitz, D. E., & Nyhan, D. (2011). Vascular stiffness and increased pulse pressure in the aging cardiovascular system. *Cardiology Research and Practice*, 2011, 263-585.

Stewart, A. D., Millasseau, S. C., Kearney, M. T., Ritter, J. M., & Chowienczyk, P. J. (2003). Effects of inhibition of basal nitric oxide synthesis on carotid-femoral pulse wave velocity and augmentation index in humans. *Hypertension*, 42 (5), 915-918.

Su, X., & Li, J. (2011). Low temperature synthesis of single-crystal alpha alumina platelets by calcining bayerite and potassium sulfate. *Journal of Materials Science & Technology*, 27 (11), 1011-1015.

Sun, D., Huang, A., Yan, E. H., Wu, Z., Yan, C., Kaminski, P. M., Oury, T. D., Wolin, M. S., & Kaley, G. (2004). Reduced release of nitric oxide to shear stress in mesenteric arteries of aged rats. *American Journal of Physiology - Heart and Circulatory Physiology*, 286 (6), 2249-2256.

Sunyer, R., Jin, A. J., Nossal, R., & Sackett, D. L. (2012). Fabrication of hydrogels with steep stiffness gradients for studying cell mechanical response. *PLoS ONE*, 7 (10), e46107.

Takeda, H., Komori, K., Nishikimi, N., Nimura, Y., Sokabe, M., & Naruse, K. (2006). Bi-phasic activation of eNOS in response to uni-axial cyclic stretch is mediated by differential mechanisms in BAECs. *Life Sciences*, 79 (3), 233-239.

Tan, P. S., & Teoh, S. H. (2007). Effect of stiffness of polycaprolactone (PCL) membrane on cell proliferation. *Materials Science and Engineering: C*, 27 (2), 304-308.

Throm Quinlan, A. M., Sierad, L. N., Capulli, A. K., Firstenberg, L. E., & Billiar, K. L. (2011). Combining dynamic stretch and tunable stiffness to probe cell mechanobiology in vitro. *PLoS ONE*, 6 (8), e23272.

Van Beijnum, J. R., Rousch, M., Castermans, K., Linden, E. v. d., & Griffioen, A. W. (2008). Isolation of endothelial cells from fresh tissues. *Nature Protocols*, 3 (6), 1085-1091.

Vogel, V. (2006). Mechanotransduction involving multimodular proteins: converting force into biochemical signals. *Annual Review of Biophysics and Biomolecular Structure*, 35 (1), 459-488.

Wang, H., Long, C., Duan, Z., Shi, C., Jia, G., & Zhang, Y. (2007). A new ATP-sensitive potassium channel opener protects endothelial function in cultured aortic endothelial cells. *Cardiovascular Research*, 73 (3), 497-503.

Wells, R. G. (2008). The role of matrix stiffness in regulating cell behavior. *Hepatology*, 47 (4), 1394-1400.

Wilkinson, I. B., MacCallum, H., Cockcroft, J. R., & Webb, D. J. (2002). Inhibition of basal nitric oxide synthesis increases aortic augmentation index and pulse wave velocity in vivo. *British Journal of Clinical Pharmacology*, 53 (2), 189-192.

Yang, C. Y., Y., H. L., L, S. T., & A, Y. J. (2010). Cell adhesion, morphology and biochemistry on nano-topographic oxidized silicon surfaces. *European Cells & Materials*, 20, 415-430.

Yeh, Y.-T., Hur, S. S., Chang, J., Wang, K.-C., Chiu, J.-J., Li, Y.-S., & Chien, S. (2012). Matrix stiffness regulates endothelial cell proliferation through septin 9. *PLoS ONE*, 7 (10), e46889.

Yeung, T., Georges, P. C., Flanagan, L. A., Marg, B., Ortiz, M., Funaki, M., Zahir, N., Ming, W., Weaver, V., & Janmey, P. A. (2005). Effects of substrate stiffness on cell morphology, cytoskeletal structure, and adhesion. *Cell Motility and the Cytoskeleton*, 60 (1), 24-34.

Zeng, D., Juzkiw, T., Read, A. T., Chan, D. W. H., Glucksberg, M. R., Ethier, C. R., & Johnson, M. (2010). Young's modulus of elasticity of Schlemm's canal endothelial cells. *Biomechanics and Modeling in Mechanobiology*, 9 (1), 19-33.

Zhang, W., Choi, D. S., Nguyen, Y. H., Chang, J., & Qin, L. (2013). Studying cancer stem cell dynamics on PDMS surfaces for microfluidics device design. *Scientific Reports*, 3, 2332-2340.

Zhao, S., Suciu, A., Ziegler, T., Moore, J. E., Bürki, E., Meister, J.-J., & Brunner, H. R. (1995). Synergistic effects of fluid shear stress and cyclic circumferential

stretch on vascular endothelial cell morphology and cytoskeleton. *Arteriosclerosis, Thrombosis, and Vascular Biology*, 15 (10), 1781-1786.

Ziegler, T., Bouzourène, K., Harrison, V. J., Brunner, H. R., & Hayoz, D. (1998). Influence of oscillatory and unidirectional flow environments on the expression of endothelin and nitric oxide synthase in cultured endothelial cells. *Arteriosclerosis, Thrombosis, and Vascular Biology*, 18 (5), 686-692.

Zieman, S. J., Melenovsky, V., & Kass, D. A. (2005). Mechanisms, pathophysiology, and therapy of arterial stiffness. *Arteriosclerosis, Thrombosis, and Vascular Biology*, 25 (5), 932-943.

APPENDIX A

A LIST OF PUBLICATIONS

A. 1. Peer-reviewed publication

Forough Ataollahi, Belinda Pingguan- Murphy, Ali Moradi, Wan Abu Bakar Wan Abas, Kien Hui Chua, & Noor Azuan Abu Osman. (2014). A new method in the isolation of large vessels endothelial cells, *Cythotherapy*, 16, 1145-1152.

Forough Ataollahi, Sumit Pramanik, Ali Moradi, Adel Dalilottojari, Belinda Pingguan-Murphy, Wan Abu Bakar Wan Abas, & Noor Azuan Abu Osman. (2014). Endothelial cell responses in terms of adhesion, proliferation, and morphology to stiffness of polydimethylsiloxane elastomer substrates, *Journal of Biomedical Materials Research Part A*, DOI: 10.1002/jbm.a.35186 (In press).

A. 2. Conferences Presentation

Forough Ataollahi, Belinda Pingguan-Murphy, Wan Abu Bakar Wan Abas, & Noor Azuan Abu Osman (2014). *Effects of Stiffness on Endothelial Cells Behaviour,* Paper presented at the International Journal of Medical, Pharmaceutical Science and Engineering, 8(2) (supplementary): 82-84.

Cytotherapy, 2014; 16: 1145–1152

International Society for Cellular Therapy ISCT®

New method for the isolation of endothelial cells from large vessels

FOROUGH ATAOLLAHI[1], BELINDA PINGGUAN-MURPHY[1], ALI MORADI[1], WAN ABU BAKAR WAN ABAS[1], KIEN HUI CHUA[2] & NOOR AZUAN ABU OSMAN[1]

[1]*Department of Biomedical Engineering, Faculty of Engineering, University of Malaya, Kuala Lumpur, Malaysia, and* [2]*Biochemistry Department, Faculty of Medicine, University Kebangsaan Malaysia, Kuala Lumpur, Malaysia*

Abstract

Background aims. Numerous protocols for the isolation of bovine aortic endothelial cells have been described in the previous literature. However, these protocols prevent researchers from obtaining the pure population of endothelial cells. Thus, this study aimed to develop a new and economical method for the isolation of pure endothelial cells by introducing a new strategy to the enzymatic digestion method proposed by previous researchers. *Methods.* With the use of this method, the lumen of a bovine aorta was filled with wash medium and the outer surface of the sample was washed with alcohol for 30 seconds. Under a laminar flow hood, the inner surface of the sample was covered with filter paper. Collagenase type II was dripped onto the filter paper as a digestion enzyme. The digestion fluid was seeded in T25 flasks and fed with complete medium every 3 days. *Results.* The isolated cells were characterized by markers such as CD31, von Willebrand factor, 1,1′-dioctadecyl-1,3,3,3′,3′-tetramethylindocarbocyanine perchlorate acetylated low-density lipoprotein and angiogenesis behavior. The purity of endothelial cells was detected by flow cytometry to be of nearly 90% purity; these results were confirmed by immunostaining. Moreover, endothelial cells formed blood vessel–like tubes in a three-dimensional environment, which is specific dynamic behavior for endothelial cells. *Conclusions.* The new strategy presented in the current report enables isolation of a highly pure population of endothelial cells that can survive long-term culture without inducing an overgrowth of fibroblast cells.

Key Words: *bovine aortic endothelial cells, characterization, fibroblast contamination, filter paper, new strategy, pure population*

Introduction

Endothelial cells have historically been viewed as an inert membrane in the circulatory system (1). Harvey's description of the circulatory system and studies by Malphigi, Reckingausen and other researchers show the critical role of endothelial cells in physio-pathological processes (2,3). The entire vascular system is lined by a single layer of endothelial cells separated from outer tissues by connective tissue. Although the amount of connective tissue is generally dependent on the vessel diameter, endothelial cells are always present in all vessels (4). The vascular endothelium maintains the structure and integrity of vessels and acts as a barrier between the blood and parenchymal cells (2).

Physio-pathological events such as wound healing, inflammation and tumor generation can result in endothelial dysfunction, which is the primary cause of certain diseases such as sepsis (5), atherosclerosis (6), diabetes mellitus (7), vasculitis, hypertension and ischemic heart disease (8). Therefore, pure populations of endothelial cells provide opportunities to obtain specific and significant information about cell behavior in physiological and pathological situations *in vitro*. Significant progress in vascular biology has recently been achieved through the isolation of endothelial cells from vessel preparations (9–11).

Endothelial cells are commonly isolated from large elastic mammalian vessels such as rat (12), porcine (13), bovine aorta (14), bovine pulmonary artery and human umbilical cord (15). Several techniques have been reported in the literature for bovine aortic endothelial cell (BAEC) isolation such as physical removal, the outgrowth method, enzymatic digestion and the use of magnetic beads (6,14,16–18). Recently, these techniques are followed by methods such as manual weeding, the use of a specific growth medium, enzymatic detachment and size-defined filtration to improve the purity of endothelial cell populations. Although these methods are reportedly effective in endothelial cell purification, there are some drawbacks for these methods. Fibroblast contamination, particularly in

Correspondence: **Forough Ataollahi**, DVM, MSc, Department of Biomedical Engineering, Faculty of Engineering, University of Malaya, Kuala Lumpur–50603, Malaysia. E-mail: Forough_at@yahoo.com

(Received 25 August 2013; accepted 14 January 2014)

ISSN 1465-3249
http://dx.doi.org/10.1016/j.jcyt.2014.01.010

Society For Biomaterials

Endothelial cell responses in terms of adhesion, proliferation, and morphology to stiffness of polydimethylsiloxane elastomer substrates

Forough Ataollahi, Sumit Pramanik, Ali Moradi, Adel Dalilottojari, Belinda Pingguan-Murphy, Wan Abu Bakar Wan Abas, Noor Azuan Abu Osman

Department of Biomedical Engineering, Faculty of Engineering, University of Malaya, Kuala Lumpur 50603, Malaysia

Received 28 November 2013; revised 26 February 2014; accepted 31 March 2014
Published online 00 Month 2014 in Wiley Online Library (wileyonlinelibrary.com). DOI: 10.1002/jbm.a.35186

Abstract: Extracellular environments can regulate cell behavior because cells can actively sense their mechanical environments. This study evaluated the adhesion, proliferation and morphology of endothelial cells on polydimethylsiloxane (PDMS)/alumina (Al_2O_3) composites and pure PDMS. The substrates were prepared from pure PDMS and its composites with 2.5, 5, 7.5, and 10 wt % Al_2O_3 at a curing temperature of 50°C for 4 h. The substrates were then characterized by mechanical, structural, and morphological analyses. The cell adhesion, proliferation, and morphology of cultured bovine aortic endothelial (BAEC) cells on substrate materials were evaluated by using resazurin assay and 1,1′-dioctadecyl-1,3,3,3′,3′-tetramethylindocarbocyanine perchlorate-acetylated LDL (DiI-Ac-LDL) cell staining, respectively. The composites (PDMS/2.5, 5, 7.5, and 10 wt % Al_2O_3) exhibited higher stiffness than the pure PDMS substrate. The results also revealed that stiffer substrates promoted endothelial cell adhesion and proliferation and also induced spread morphology in the endothelial cells compared with lesser stiff substrates. Statistical analysis showed that the effect of time on cell proliferation depended on stiffness. Therefore, this study concludes that the addition of different Al_2O_3 percentages to PDMS elevated substrate stiffness which in turn increased endothelial cell adhesion and proliferation significantly and induced spindle shape morphology in endothelial cells. © 2014 Wiley Periodicals, Inc. J Biomed Mater Res Part A: 00A: 000–000, 2014.

Key Words: stiffness, proliferation, bovine aortic endothelial cells, extra cellular matrix, vessels

How to cite this article: Ataollahi F, Pramanik S, Moradi A, Dalilottojari A, Pingguan-Murphy B, Wan Abas WAB, Abu Osman NA. 2014. Endothelial cell responses in terms of adhesion, proliferation, and morphology to stiffness of polydimethylsiloxane elastomer substrates. J Biomed Mater Res Part A 2014:00A:000–000.

INTRODUCTION

Cells have been resided on mechanical environments in the form of tissues and organs. In the cellular concept, cells impose forces on their environment as extra cellular matrix (ECM); however, ECM applies forces like gravity and tissue-specific interactions to cells. Besides these imposed forces, local ECM stiffness has important mechanical effects on cell function. Tissue stiffness does not remain stable, and it changes during physiological responds like embryonic development, wound healing and pathological process such as tumorigenesis and atherosclerosis.

Live cells follow a pattern called "stiffness sensing" which denotes that cells can sense their outer environment as they adhere to and respond to mechanical resistivity of ECM. Cells can recognize substrate mechanical properties via receptors attached to the substrate.[1–4] As cells can sense the outer environment, they have the ability to convert mechanical cascades into complicated intracellular signaling inputs which regulate cell functions including adhesion, proliferation and spreading.

Therefore, the availability of proper stiffness profiles can elevate the feasibility of biophysical studies on cell-substrate interaction.[5]

Polydimethylsiloxane (PDMS) elastomeric materials have shown potential biocompatibility for vascular and nerve tissue applications.[6] PDMS is attracting research attention in the field of cell biology because of its biocompatibility, simple fabrication, tunable flexibility, gas permeability, high oxidative, and thermal stability and low cost.[7–9] PDMS can exhibit specific mechanical properties, such as high stiffness, in its native flexibility by adding a second phase material. Among the available second phase materials for controlling substrate-stiffness, α-alumina (Al_2O_3), which has a well-known biocompatibility, thermal and electrical resistivity, thermal and chemical stability and abundance availability[10] was chosen in this study. The stability of α-phase Al_2O_3

Correspondence to: F. Ataollahi; e-mail: forough_at@yahoo.com
Contract grant sponsor: Ministry of Higher Education (MOHE) of Malaysia; contract grant number: UM.C/HIR/MOHE/ENG/14 D000014–16001
Contract grant sponsor: University of Malaya Faculty of Engineering; contract grant number: UM-TNC2/IPPP/PPGP/638/PPP/PG0872013B

World Academy of Science, Engineering and Technology
International Journal of Medical, Pharmaceutical Science and Engineering Vol:8 No:2, 2014

Effects of Stiffness on Endothelial Cells Behavior

Forough Ataollahi, Belinda Pingguan-Murphy, Wan Abu Bakar Wan Abas, Noor Azuan Abu Osman

***Abstract*—**Endothelium proliferation is an important process in cardiovascular homeostasis and can be regulated by extracellular environment, as cells can actively sense mechanical environment. In this study, we evaluated endothelial cell proliferation on PDMS/alumina (Al_2O_3) composites and pure PDMS. The substrates were prepared from pure PDMS and its composites with 5% and 10% Al_2O_3 at curing temperature 50°C for 4h and then characterized by mechanical, structural and morphological analyses. Higher stiffness was found in the composites compared to the pure PDMS substrate. Cell proliferation of the cultured bovine aortic endothelial cells on substrate materials were evaluated via Resazurin assay and 1, 1'-Dioctadecyl-1, 3, 3, 3', 3'-Tetramethylindocarbocyanine Perchlorate-Acetylated LDL (Dil-Ac-LDL) cell staining, respectively. The results revealed that stiffer substrates promote more endothelial cells proliferation to the less stiff substrates. Therefore, this study firmly hypothesizes that the stiffness elevates endothelial cells proliferation.

***Keywords*—**Bovine aortic endothelial cells, extra cellular matrix, proliferation, stiffness.

I. Introduction

BLOOD vessels as a scaffold provide special extra cellular matrix for endothelial cells. The entire vascular system has been lined by a single layer of endothelial cells which is separated from the underlying layers by connective tissue [1]-[2]. Normally, endothelial cells sit on collagen which acts as a substrate. Collagen deposition, hyper-proliferation and mineralization by calcium and phosphorous induced by risk factors like aging, atherosclerosis, diabetes mellitus and renal disorders elevate vessel stiffening [3], [4]. Alive cells follow a fact called "stiffness sensing" which means they can sense their outer environment and respond to mechanical resistivity of extracellular matrix. Endothelial cell cytoskeleton can recognize substrate mechanical properties through receptors [5]-[8]. Therefore, availability of proper stiffness profiles can elevate the feasibility of the biophysical studies on cell-substrate interaction [9]. In addition to its biocompatibility, simple fabrication, optical transparency, tunable flexibility, gas permeability, high oxidative and thermal stability and inexpensiveness have made this material attractive in cell biology [10]-[12]. From the many available means of controlling substrate-stiffness α-alumina (Al2O3) as a well-known biocompatible and stable ceramic [13] was chosen to control the substrate stiffness in this present study. Hence, this study introduces an in vitro method to show the profound role of vascular stiffness on endothelium responds in terms of adhesion, proliferation and cell morphology.

F. A. is with the Department of Biomedical Engineering, Faculty of Engineering, University of Malaya, Kuala Lumpur - 50603, Malaysia (corresponding author to provide phone: 603-79674581; fax:603-79674581; e-mail: forough_at@ yahoo.com).

B. P. M., W. A. B. W. A., and N. A. A. O. are with the Department of Biomedical Engineering, Faculty of Engineering, University of Malaya, Kuala Lumpur - 50603, Malaysia (e-mail: bpingguan@gmail.com, drirwan1@um.edu.my, azuan@um.edu.my, respectively).

T. C. is with the Electrical Engineering Department, University of Colorado, Boulder, CO 80309 USA, on leave from the National Research Institute for Metals, Tsukuba, Japan (e-mail: author@nrim.go.jp).

II. Procedure

A. Preparation of Different Stiffness of PDMS Substrate

PDMS/Al2O3 composites were prepared first, by mixing PDMS gel (SYLGARD 184 Silicon Elastomer Base purchased from Dow Corning) with 5 and 10 percent of Al2O3 (supplied by Sigma) as a second phase ceramic particle using planetary ball mill (Retsch, PM200). Then a curing agent (supplied by Dow Corning along with SYLGARD 184 Silicon Elastomer) with proportion of 1:10 (v/v) (curing agent: PDMS gel) was added to PDMS/Al2O3 mixture at room temperature.

B. Stiffness Measurement

Mechanical properties of pure PDMS elastomer and its composites with different concentrations (5 and 10 wt%) of Al2O3 were characterized following the ASTM standard—ASTM D 412 test standard for vulcanized rubber and thermoplastic elastomers 16 using a universal testing machine, (Instron MicroTester, # 5848) at a constant crosshead speed of $1mm.min^{-1}$.

C. In vitro Assay

In vitro cell attachment and proliferation were determined by the Resazurin assay. This test was used to show cell metabolism. Isolated bovine aortic endothelial cells were grown in completed medium (M200) (Gibco#M200-500). Then, $1*10^4$ in passage 9 were used to seed on substrates with different stiffness which were coated on 100µl fibronectin (Sigma- Aldrich, # F1141).

Resazurin assay was performed at four time points, namely day 3, day 6, day 12, and day 18. 10% Resazurin solution were prepared at PBS. In the selected time points, medium was discarded and cells were washed with pre-warmed PBS and then incubated at 37°C for 4h.

After incubation time, 100µl of resazurin solution were taken for absorbance measurements at 570nm and 600nm to determine the metabolism and proliferation rate of endothelial cells using the following (1):

$$\frac{(\varepsilon_{OX})\lambda_2 A\lambda_1 - (\varepsilon_{OX})\lambda_1 A\lambda_2}{(\varepsilon_{RED})\lambda_1 A^o\lambda_2 - (\varepsilon_{RED})\lambda_2 A^o\lambda_1}\times 100$$

where,

ε_{OX} = molar extinction coefficient of Resazurin oxidized form (BLUE)